ISSN 2518-718X (Print)
ISSN 2663-4872 (Online)

№ 1(93)/2019

**ХИМИЯ сериясы**
**Серия ХИМИЯ**
**CHEMISTRY Series**

# ҚАРАҒАНДЫ УНИВЕРСИТЕТІНІҢ ХАБАРШЫСЫ

# ВЕСТНИК КАРАГАНДИНСКОГО УНИВЕРСИТЕТА

# BULLETIN OF THE KARAGANDA UNIVERSITY

**ISSN 2518-718X (Print)**
**ISSN 2663-4872 (Online)**
Индексі 74617
Индекс 74617

# ҚАРАҒАНДЫ УНИВЕРСИТЕТІНІҢ ХАБАРШЫСЫ

---

# ВЕСТНИК КАРАГАНДИНСКОГО УНИВЕРСИТЕТА

# BULLETIN OF THE KARAGANDA UNIVERSITY

---

## **ХИМИЯ** сериясы

## Серия **ХИМИЯ**

## **CHEMISTRY** Series

## № 1(93)/2019

Қаңтар–ақпан–наурыз
30 наурыз 2019 ж.
Январь–февраль–март
30 марта 2019 г.
January–February–March
March, 30, 2019

1996 жылдан бастап шығады
Издается с 1996 года
Founded in 1996

Жылына 4 рет шығады
Выходит 4 раза в год
Published 4 times a year

Қарағанды, 2019
Караганда, 2019
Karaganda, 2019

*Редакцияның мекенжайы:* 100024, Қазақстан, Қарағанды қ., Университет к-сі, 28
Тел.: (7212) 77-03-69 (ішкі 1026); факс: (7212) 77-03-84.
E-mail: vestnick_kargu@ksu.kz; yelenaminayeva@yandex.ru (*жауапты хатшы*)
Сайты: http://chemistry-vestnik.ksu.kz

*Редакторы*
Ж.Т. Нурмуханова

*Компьютерде беттеген*
В.В. Бутяйкин

**Қарағанды университетінің хабаршысы. Химия сериясы.**
**ISSN 2518-718X (Print). ISSN 2663-4872 (Online).**

Меншік иесі: «Академик Е.А. Бөкетов атындағы Қарағанды мемлекеттік университеті» РММ.

Қазақстан Республикасының Мәдениет және ақпарат министрлігімен тіркелген. 23.10.2012 ж. № 13110–Ж тіркеу куәлігі.

Басуға 29.03.2019 ж. қол қойылды. Пішімі 60×84 1/8. Қағазы офсеттік. Көлемі 12,75 б.т. Таралымы 300 дана. Бағасы келісім бойынша. Тапсырыс № 23.

Е.А. Бөкетов атындағы ҚарМУ баспасының баспаханасында басылып шықты.
100012, Қазақстан, Қарағанды қ., Гоголь к-сі, 38. Тел. 51-38-20. E-mail: izd_kargu@mail.ru

*Адрес редакции:* 100024, Казахстан, г. Караганда, ул. Университетская, 28
Тел.: (7212) 77-03-69 (внутр. 1026); факс: (7212) 77-03-84.
E-mail: vestnick_kargu@ksu.kz; yelenaminayeva@yandex.ru (*отв. секретарь*)
Сайт: http://chemistry-vestnik.ksu.kz

*Редактор*

Ж.Т. Нурмуханова

*Компьютерная верстка*

В.В. Бутяйкин

**Вестник Карагандинского университета. Серия Химия.**

**ISSN 2518-718X (Print). ISSN 2663-4872 (Online).**

Собственник: РГП «Карагандинский государственный университет имени академика Е.А. Букетова».

Зарегистрирован Министерством культуры и информации Республики Казахстан. Регистрационное свидетельство № 13110–Ж от 23.10.2012 г.

Подписано в печать 29.03.2019 г. Формат 60×84 1/8. Бумага офсетная. Объем 12,75 п.л. Тираж 300 экз. Цена договорная. Заказ № 23.

Отпечатано в типографии издательства КарГУ им. Е.А. Букетова.
100012, Казахстан, г. Караганда, ул. Гоголя, 38, тел.: (7212) 51-38-20. E-mail: izd_kargu@mail.ru

*Main Editor*

Doctor of chemical sciences, Professor, Corresponding member of NAS RK

**A.T. Yedrissov**

| | |
|---|---|
| *Deputy main Editor* | **Kh.B. Omarov**, Doctor of techn. sciences, Professor, Corresponding member of NAS RK |
| *Responsible secretary* | **G.Yu. Amanbayeva**, Doctor of phylol. sciences, Professor |

*Editorial board*

| | |
|---|---|
| **M.I. Baikenov,** | Science editor Doctor of chem. sciences (Kazakhstan); |
| **Z.M. Muldakhmetov**, | Academician of NAS RK, Doctor of chem. sciences (Kazakhstan); |
| **S.M. Adekenov,** | Academician of NAS RK, Doctor of chem. sciences (Kazakhstan); |
| **S.E. Kudaibergenov,** | Doctor of chem. sciences (Kazakhstan); |
| **V. Khutoryanskiy**, | Professor (United Kingdom); |
| **Fengyung Ma,** | Professor (PRC); |
| **Xintai Su**, | Professor (PRC); |
| **R.R. Rakhimov,** | Doctor of chem. sciences (USA); |
| **M.B. Batkibekova,** | Doctor of chem. sciences (Kyrgyzstan); |
| **S.A. Beznosyuk,** | Doctor of phys.-math. sciences (Russia); |
| **B.F. Minaev,** | Doctor of chem. sciences (Ukraine); |
| **N.U. Aliev,** | Doctor of chem. sciences (Kazakhstan); |
| **R.Sh. Erkasov,** | Doctor of chem. sciences (Kazakhstan); |
| **V.P. Malyshev,** | Doctor of techn. sciences (Kazakhstan); |
| **L.K. Salkeeva,** | Doctor of chem. sciences (Kazakhstan); |
| **E.M. Tazhbaev,** | Doctor of chem. sciences (Kazakhstan); |
| **A.K. Tashenov,** | Doctor of chem. sciences (Kazakhstan); |
| **Xian Li**, | Associated Professor (PRC); |
| **Ye.V. Minaeva,** | Secretary Candidate of chem. sciences (Kazakhstan) |

*Postal address*: 28, University Str., Karaganda, 100024, Kazakhstan
Tel.: (7212) 77-03-69 (add. 1026); fax: (7212) 77-03-84.
E-mail: vestnick_kargu@ksu.kz; yelenaminayeva@yandex.ru (*secretary*)
Web-site: http://chemistry-vestnik.ksu.kz

*Editor*

Zh.T. Nurmukhanova

*Computer layout*

V.V. Butyaikin

**Bulletin of the Karaganda University. Chemistry series.**

**ISSN 2518-718X (Print). ISSN 2663-4872 (Online).**

Proprietary: RSE «Academician Ye.A. Buketov Karaganda State University».

Registered by the Ministry of Culture and Information of the Republic of Kazakhstan. Registration certificate No. 13110–Zh from 23.10.2012.

Signed in print 29.03.2019. Format 60×84 1/8. Offset paper. Volume 12,75 p.sh. Circulation 300 copies. Price upon request. Order № 23.
Printed in the Ye.A. Buketov Karaganda State University Publishing house.
38, Gogol Str., Karaganda, 100012, Kazakhstan. Tel.: (7212) 51-38-20. E-mail: izd_kargu@mail.ru

**© Karaganda State University, 2019**

# МАЗМҰНЫ

## ОРГАНИКАЛЫҚ ХИМИЯ

## ФИЗИКАЛЫҚ ЖӘНЕ АНАЛИТИКАЛЫҚ ХИМИЯ

## БЕЙОРГАНИКАЛЫҚ ХИМИЯ

## ХИМИЯЛЫҚ ТЕХНОЛОГИЯ

# СОДЕРЖАНИЕ

## ОРГАНИЧЕСКАЯ ХИМИЯ

## ФИЗИЧЕСКАЯ И АНАЛИТИЧЕСКАЯ ХИМИЯ

## НЕОРГАНИЧЕСКАЯ ХИМИЯ

## ХИМИЧЕСКАЯ ТЕХНОЛОГИЯ

# CONTENTS

## ORGANIC CHEMISTRY

## PHYSICAL AND ANALYTICAL CHEMISTRY

## INORGANIC CHEMISTRY

## CHEMICAL TECHNOLOGY

# ОРГАНИКАЛЫҚ ХИМИЯ
# ОРГАНИЧЕСКАЯ ХИМИЯ
# ORGANIC CHEMISTRY

DOI: 10.31489/2019Ch1/8-16

UDC 661.746.2:544.56

G.Ya. Guba[1], A.O. Gusar[1], A.A. Bakibayev[2], Ye.M. Tazhbayev[3], Ye.V. Minayeva[3]

*[1]Tomsk Polytechnic University, Russia;*
*[2]Tomsk State University, Russia;*
*[3]Ye.A. Buketov Karaganda State University, Kazakhstan*
*(E-mail: anngsa@mail.ru)*

## Dehydration/polycondensation of lactic acid under microwave irradiation

In this paper the effect of microwave irradiation power (MW) on the processes of polycondensation of lactic disturbed total internal reflection acid (LA) was studied for the first time. LA polycondensation was carried out in a multimodal reactor in a vacuum while bubbling with nitrogen at powers of 80, 130, 280, 360 and 500 watts. The change in the temperature of the LA sample under conditions of MW as a function of time and irradiation power was determined. Based on the data of 1H NMR and IR spectroscopy, it was suggested that at 80 W the molecules of physically bound water are mainly removed. The formation of lactic acid oligomers (LAO) occurs at a power of 130–280 W along with the removal of water and LA. Complete removal of water from LAO occurs at 360 watts. When LA is heated at MW power of 430 W, the formation and isolation of colorless crystals is observed, which can be classified by the IR spectra as lactide molecules (νC=O is 1770 $cm^{-1}$, νC–O–C is 1240 $cm^{-1}$). The molecular weight of LAO decreases at a power of 430 W and above. The kinetic curves of LA polycondensation at 130, 280 and 360 W are presented. The process of LA polycondensation at 360 watts is optimal. It was established that the rate of LA dehydration under MW conditions increases by 15–20 times as compared with carrying out the process under normal heating conditions.

*Keywords*: microwave irradiation, lactic acid, polylactic acid, lactic acid oligomers, NMR spectroscopy, IR spectroscopy, specific optical rotation, molecular weight.

### *Introduction*

Polylactic acid (PLA) occupies the most significant market share of biodegradable polymers. PLA preference is due to the fact that it is made from renewable raw materials and has the ability to decompose in the natural environment under the action of bacteria, first to lactic acid and then to $H_2O$ and $CO_2$, ultimately without damaging the biosphere [1–7]. PLA is widely used in the biomedical and pharmaceutical industries as an agent for controlled drug delivery and wound healing, tissue engineering etc. The use of PLA in medicine is primarily due to the fact that it does not cause allergic, inflammatory and other harmful reactions in living organisms and is completely decomposed into non-toxic metabolizing products [2–4, 7]. Lactic acid (LA) is used as a raw material for the synthesis of PLA. Due to the high hygroscopicity of LA, its concentrated aqueous solutions, namely, syrupy colorless odorless liquids with different percentages are usually used. In general, lactic acid polymers are obtained under conditions of ordinary heating in two ways, namely, by polymerization of lactic acid dimers (lactides) with ring opening [1–3, 5] and direct LA polycondensation [1, 5].

During the last decade, significant progress has been made in the field of polymer synthesis under MW conditions, including biologically active substances [8–17]. The use of MW can significantly reduce the time of reactions from hours to minutes, increase the yield and molecular weight of the product, and develop resource-efficient and environmentally friendly methods for the synthesis of biologically active compounds [8–14, 18, 19].

At the initial stage in all methods, dehydration / polycondensation of aqueous solutions of LA is carried out. This process is energy-intensive under normal conditions, the time for removal of water is up to 5–7 hours, and complete removal of water is difficult [18]. Microwave reactors are divided into multimode and monomode depending on the type of energy distribution in the reaction space. Some chemical reactions are sensitive to the type of irradiation and occur at different rates in multimode and monomode microwave reactors [8–9, 11, 13, 18–20]. LA and its LAO are polar molecules and can absorb microwave energy [21–23]. In this regard, much attention is paid to the synthesis of PLA polymers in the MW conditions [2–3, 8–10, 21, 24–27].

The processes of direct LA polymerization in MW conditions are attractive as energy-saving processes, since they make it possible to avoid the labor-intensive and energy-intensive stage of lactide synthesis [9, 17, 18, 26, 28]. The rate of LA polycondensation processes in the MW conditions depends on the volume of the reacting substances [26] and pressure [6].

The process of water removal and the subsequent lactic acid polycondensation under microwave irradiation takes place 10–15 times faster than at conventional thermal heating [18, 28, 29]. Direct LA condensation is carried out in three stages, namely, removal of free water, polycondensation of oligomers and condensation of high molecular weight polymers in the melt. In the first and third stages, the removal of water is decisive for the reaction rate. For the second stage, the rate is determined by chemical reaction [17, 12, 24].

LAO of high-purity without impurities of metals and solvents were obtained under MW conditions [18]. The reaction was carried out in a monomode reactor at 100–250 ºC at a power of 300 W. This high-purity oligomer of LA can be used as a safe and high-purity intermediate for the synthesis of PLA for use in medicine and pharmaceuticals. In Japan [10], an industrial installation of microwave synthesis of highly pure lactic acid oligomers under MW conditions for medical purposes was created.

In [10, 26], LAO was synthesized from aqueous solutions of LA in the presence of catalysts in monomode reactors under irradiation with 300 W [10, 26, 18]. When comparing the conduct of the polycondensation reaction of LA under MW conditions at 250–300 W in multi- and monomode reactors [30], the formation of high molecular weight PLAs in the case of multimode irradiation was noted. Thus, despite the large number of publications on the synthesis of PLA under MW conditions, the data obtained are scattered, performed under unequal conditions and in different microwave reactors. Although it is definitely possible to say that the time of PLA synthesis decreases by 10–15 times under MW conditions. Systematic studies on the effect of irradiation power and time on the process of dehydration / polycondensation of LA in the literature are missing. In this work, we investigated the effect of the MW power and the time on the LA polycondensation process under MW conditions in a multimode reactor.

## *Experimental*

80 % Aqueous solution of D(+)lactic acid of brand «PURAK 80», manufacturer the Netherlands, was used as an object of the study. Chloroform was used as a solvent to determine the molecular weight. IR spectra of starting compounds and reaction products were recorded on an Agilent Resolutions Pro IR spectrometer. $^1$H NMR spectra of LAO and PLA synthesized were recorded using a Fourier spectrometer AVANCE AV 300 from Bruker (Germany), the operating frequency was 300 MHz, and the solvent was deuterated chloroform. The molecular weight of the samples obtained was determined by the viscometric method using an Ubbelohde viscometer. To determine the molecular weight M, a non-linear Mark — Huvink equation is used, expressing the dependence of the characteristic viscosity on the molecular weight:

$$[\eta] = KM^a ,$$

where $K$ — is the Huggins constant; α is a constant for this polymer-solvent system. Usually, depending on the nature of the solvent, the value of α, which determines the degree of curliness of the macromolecule, ranges from 0.5 to 0.8. In this work, $K = 4.7\times10^{-4}$, $\alpha = 0.67$ for LAO and PLA solutions in chloroform. The molecular weights of the PLA samples obtained were also determined by gel permeation chromatography on an Agilent 1200 instrument. Chloroform was used as a solvent; the eluent rate was 1 ml/s. To determine the angle of optical rotation (degrees×ml/dm×g), an AP-300 polarimeter was used, a tube length of 1 dm, solvent — chloroform, $\lambda = 589$ nm.

Dehydration/polycondensation of LA was carried out in a multimode microwave reactor in a vacuum while bubbling with nitrogen at powers of 80, 130, 280, 360 and 500 watts. The microwave reactor was created using a Daewoo Kor-5A17W microwave oven. The temperature was measured with a thermometer through the side opening of the microwave oven.

20 g of LA were loaded into a 100 ml glass heat-resistant flask, placed in a microwave reactor and sparged with nitrogen at a pressure of 200 mmHg at various capacities.

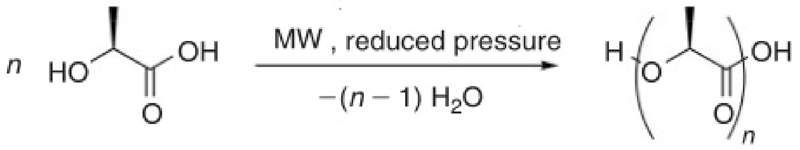

*Results and discussion*

*Dehydration of LA in the MW conditions.* Figure 1 shows the change in the temperature of the LA sample under MW conditions as a function of time and irradiation power. As MW power is increased from 130 (478 K) to 280 W, the temperature is increased only by 283 K. The temperature of LA samples in the MW conditions at a power of 280, 360, 500 W is the same and is 488 K.

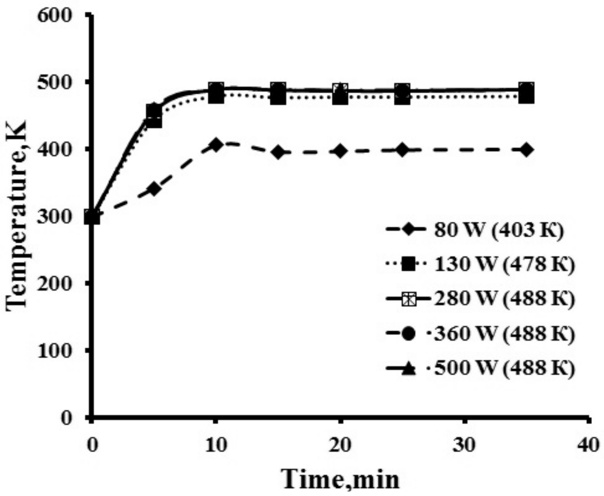

*1* — 80 watts; *2* — 130 watts; *3* — 280 watts; *4* — 360 watts; *5* — 500 watts

Figure 1. Dependence of the temperature of a sample of lactic acid on time under MW conditions

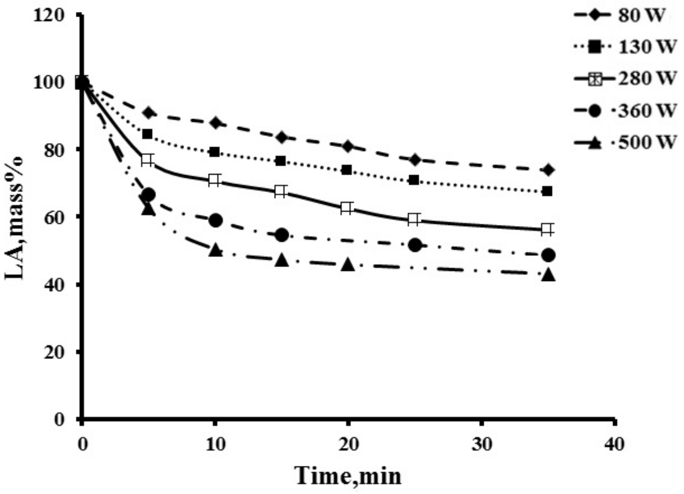

*1* — 80 W; *2* — 130 W; *3* — 280 W; *4* — 360 W; *5* — 500 W

Figure 2. Weight reduction of 80 % LA solution after vacuuming under MW conditions

Figure 2 shows the decrease in the LA weight after vacuuming under MW conditions. In the first 5 minutes of LA dehydration the maximum amount of water and LA were obtained. With increasing vacuum time, the process of water removal slows down. At 80 and 130 W, LA samples approximately lose 30 % of their weight.

The course of the dehydration/polycondensation reaction was evaluated by the change in the intensity of the absorption bands in the IR spectra (Fig. 3). The values of the troughs of the PLA IR spectra are given below (wavenumber, cm$^{-1}$ (group): 3500–3300 (υOH), 2997 (υ$_{as}$CH$_3$), 2947 (υ$_s$CH$_3$), 2882 (υCH), 1760–1727 (υC=O), 1452 (δ$_{as}$CH$_3$), 1388–1348 (δ$_s$CH$_3$), 1368–1360 (δ1CH+δ$_s$CH$_3$), 1315–1300 (δ2CH), 1270 (υCOC), 1215–1185 (υ$_{as}$COC), 1130 (r$_{as}$CH$_3$), 1100–1090 (υ$_s$COC), 1045 (υC-CH$_3$), 960–950 (rCH$_3$ + + υCC), 875–860 (υC–COO).

In the IR spectrum of 80 % LA, a broad intense band with a maximum at 3400 cm$^{-1}$ is observed, which can be attributed to the stretching vibrations of OH groups belonging to the associated water molecules. The intense band at 1727 cm$^{-1}$ refers to the stretching vibrations of the C=O groups. The absorption band at 1650 cm$^{-1}$ characterizes the deformation vibrations of O–H groups of water molecules. Also on this spectrum there is an intense band of 1240 cm$^{-1}$, which refers to the stretching vibrations of the C–O group.

After microwave irradiation at 80 W, an absorption band at 1727 cm$^{-1}$ is observed in the IR spectra of LA, which relates to stretching vibrations of the C=O groups of LA, and a shift of the band at 1240 cm$^{-1}$ to the low frequency region (1211 cm$^{-1}$) (Fig. 3, spectrum 1). It can be assumed that the molecules of physically bound water are mainly removed at 80 W.

As the MW power increases to 130 and 280 W (Fig. 3, spectra 2 and 3), the absorption bands of carbonyl groups at 1744 cm$^{-1}$ are observed in the LA IR spectra, and the vibrations of the C–O bond shift to the low-frequency region (1188 cm$^{-1}$). The data obtained suggest that,, the polycondensation processes of LA and the rearrangement of the LAO obtained occur at a power of 130–280 W along with the removal of water.

The absorption band with a maximum of 1650 cm$^{-1}$, which characterizes the bending vibrations of water molecules, is absent in the IR spectra of LAO synthesized at MW power of 360–500 W (Fig. 3, curves 4 and 5). Consequently, the process of removing water from LA is complete.

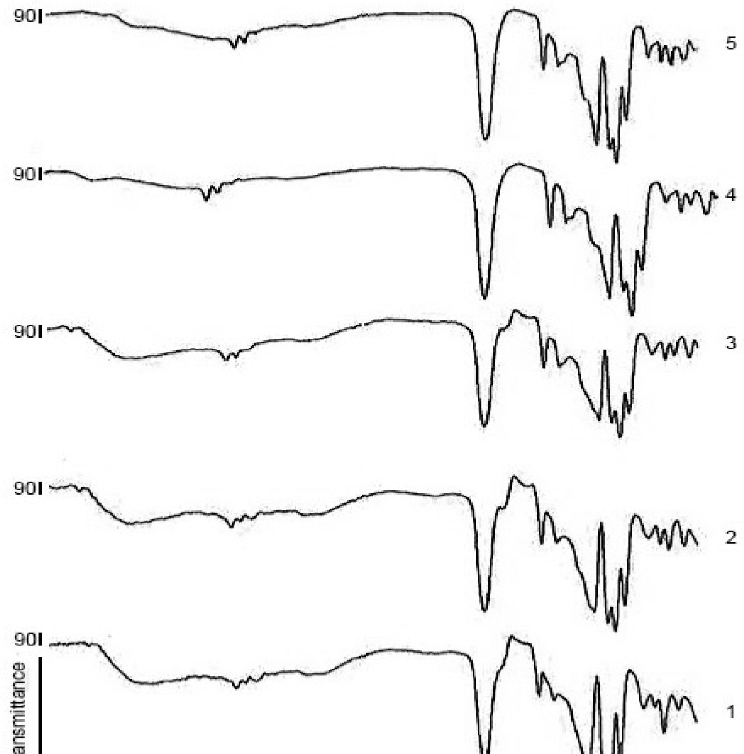

1 — 80 W; *2* —130 W; 3 — 280 W; 4 — 360 W; *5* — 500 W

Figure 3. The Disturbed Total Internal Reflection IR-spectrum of LA after vacuuming in the MW conditions for 35 minutes at a power

At MW power of 430 W and above, the formation and release of colorless crystals is observed, which can be classified by IR spectra as lactide molecules (νC=O is 1770 $cm^{-1}$, νC-O-C is 1240 $cm^{-1}$). The assumption of the process of dehydration/polycondensation of LA is confirmed by $^1$H NMR data. The $^1$H NMR chemical shifts are presented below.

The multiplet of the methylene group of LA is observed at 4.4 ppm, the chemical shift of the proton of the LAO methylene group multiplet is observed at 5.2 ppm. By changing the chemical shifts of the methylene groups of LA and LAO, one can judge the course of the process of oligomerization of lactic acid. The results of the $^1$H NMR studies are presented in Figure 4 and Table.

| **Chemical shift, ppm** | **Structural fragments** |
|---|---|
| 5.2 | 1H, m, -C**H**($CH_3$)-) |
| 4.4 | 1H, m, -C**H**($CH_3$)OH, end group) |
| 1.6 | (3H, d, -C**H₃**) |

In the $^1$NMR spectrum of an LAO sample obtained by vacuuming LA under MW conditions at 130 W (Fig. 4), there are quite intense chemical shifts of 4.4 and 5.2 ppm, characterizing the C–H group of LA and LAO, respectively. With an increase in power, the chemical shift at 5.2 ppm increases and 4.4 ppm decreases, that is, the formation of LAO.

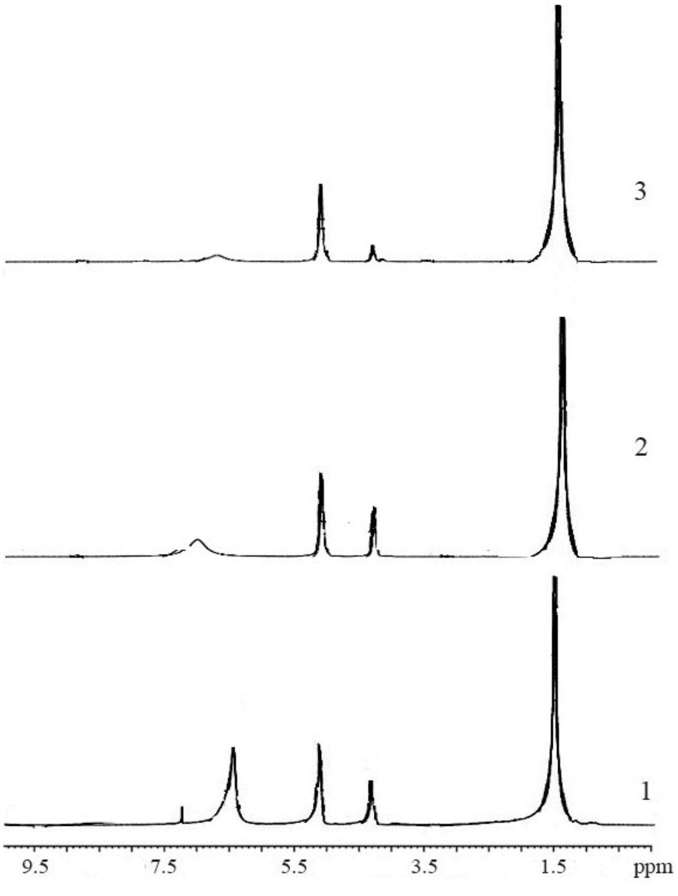

*1* — 130 W; *2* — 280 W; *3* — 360 W

Figure 4. $^1$H NMR spectrum of LA after vacuuming in MW conditions for 35 minutes

Table

**$^1$H NMR chemical shifts and physico-chemical properties of the LAO samples synthesized**

| Power (heating time) W/(min) | Chemical shifts, ppm (intensity) | | The degree of conversion, % | M [Da] |
|---|---|---|---|---|
| | LA,δ, m(C–H) | LAO, δ, m(C–H) | | |
| 80(35) | 4.3(1.18) | 5.1(1) | 46 | - |
| 130(35) | 4.40(0.55) | 5.2(1) | 64 | 290 |
| 280(35) | 4.4(0.49) | 5.2(1) | 67 | 440 |
| 360(35) | 4.4(0.22) | 5.2(1) | 85 | 758 |
| 500(15) | 4.3(0.51) | 5.1(1) | 66 | 420 |

The degree of conversion of LA into LAO was determined by the formula:

$$\frac{I(CH)_{LAO}}{I(CH)_{LA}+I(CH)_{LAO}}\times 100\,\%.$$

Based on the $^1$H NMR data presented in Table, it can be assumed that the molecules of physically bound water are mainly removed at 80 W and the formation of LAO does not occur. When dehydrating LA under MW conditions at 130 W, an increase in the molecular weight and an increase in the intensity of the chemical shift of 5.2 ppm, characterizing the C–H bond of the LAO, are observed. It can be assumed that, at a given power, the formation of LAO begins. In the range of 130–280 W, it appears that polycondensation of LA and LAO occurs, while in this power range the molecular weight changes slightly (Fig. 5).

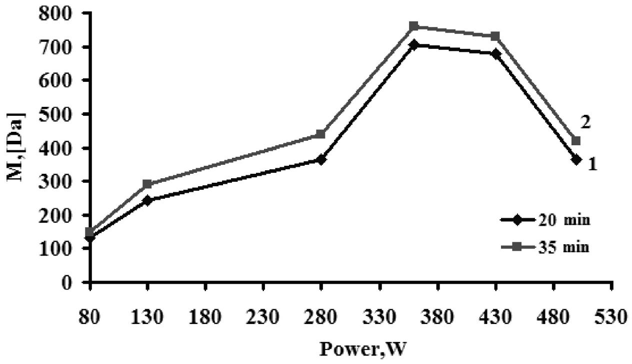

*1* — 20 minutes; *2* — 35 minutes

Figure 5. Dependence of the molecular weight of LAO on the MW power

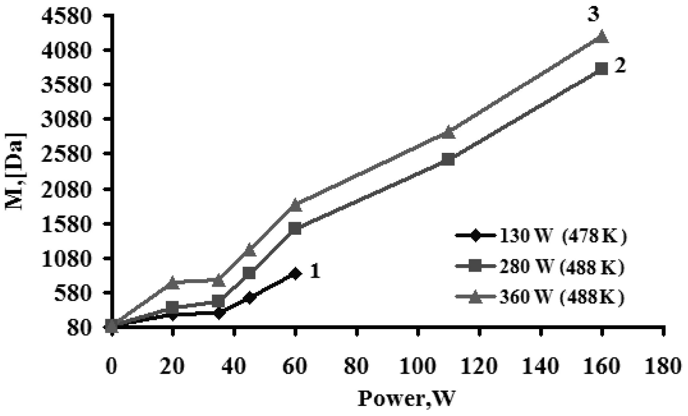

*1* — 130 W (478 K); *2* — 280 W (488 K); *3* — 360 W (488 K)

Figure 6. Dependence of the molecular weight of LAO on the time of LA dehydration

When LA is heated at MW power above 360 W, the formation and release of colorless crystals is observed, which can be classified by IR spectra as lactide molecules (νC=O is 1770 $cm^{-1}$, νC–O–C is 1240 $cm^{-1}$).

With a power of 360 W, a significant increase in molecular weight occurs (Fig. 5). With an increase in the MW monosity up to 430 W and higher, the molecular weight of LAO decreases. The destruction of LAO apparently occurs with the formation of lactide.

The kinetic curves of LA polycondensation are shown in Figure 6. On the kinetic curves for up to 35 minutes, there is a slight increase in the molecular weight of LAO. Apparently, in this interval, the limiting stage is the removal of water molecules. In the range from 35 to 60 minutes, there is a sharp increase in the molecular weight of the polymer. Then the chain slows down, which may be due to the fact that the limiting stage is the release of water during the polymerization of higher molecular weight LAOs. The process of LA polycondensation at 360 watts is optimal.

## *Conclusions*

It is established that when the MW power is increased from 130 to 280 W, the LA temperature is increased by 283 K, and at 280, 360, 500 W, the temperature of LAO samples is the same and is 488 K. Based on $^1$H NMR and IR spectroscopy, it has been suggested that at 80 W physically bound water molecules are mainly removed. The formation of low molecular weight oligomers of lactic acid (LAO) occurs at a power of 130–280 W along with the removal of water and LA. LA polycondensation in the absence of a catalyst proceeds most effectively at 360 watts. That is, the process of polycondensation is determined not only by temperature, but primarily by the MW power. When LA is heated at MW power of 430 W, the formation and release of colorless crystals is observed, which can be classified by the IR spectra as lactide molecules (νC=O is 1770 $cm^{-1}$, ν C–O–C is 1240 $cm^{-1}$). The molecular weight of LAO decreases at a power of 430 W and above. The kinetic curves of LA polycondensation at 130, 280 and 360 W are presented. The process of LA polycondensation at 360 watts is optimal. It is established that the rate of LA dehydration under MW conditions is increased by 15–20 times as compared with carrying out the process under normal heating conditions.

## References

1 Masutani, K., & Kimura, Y. (2014). PLA Synthesis. From the Monomer to the Polymer, in Poly (lactic acid) Science and Technology: Processing, Properties, Additives and Applications. *Polymer Chemistry Series*, *12*, 1–36.

2 Madhavan, K. Nampoothiri, Nimisha, Rajendran Nair, & Rojan, Pappy John. (2010). An overview of the recent developments in polylactide (PLA) research, *Bioresource Technology*, *101*(22), 8493–8501.

3 Nakatsuka, T. (2011). Polylactic acid-coated cable. *Fujikura Technical Review*, *40*, 39–45.

4 Lasprilla, Astrid J.R., Martinez, Guillermo A.R., Lunelli, Betânia H., & Jardini, André L. (2012). Polylactic acid synthesis for application in biomedical devices — A review. *Biotechnology Advances*, *30*(1), 321–328.

5 Gupta, A., & Kumar, V. (2007). New emerging trends in synthetic biodegradable polymers. *European Polymer Journal*, 43, 4053–4074.

6 Fangchao Song, & Linbo Wu. (2011). Synthesis of high molecular weight poly (L-lactic acid) via melt/solid polycondensation: intensification of dehydration and oligomerization during melt polycondensation. *Applied Polymer Science*, *120*(5), 2780–2785.

7 Janusz, J., & Kasperczyk, K. (2013). Polyesters and polyestercarbonates for controlled drug delivery. *Polymer*, *58*(9), 654–662.

8 Giachi, G., Frediani, M., Rosi, L., & Frediani, P. (2011). Synthesis and Processing of Biodegradable and Bio-Based Polymers by Microwave Irradiation. Microwave Heating ed. by Dr. Usha Chandra, Florence, 181–206. DOI: 10.5772/23692

9 Komorowska-Durka, M., Dimitrakis, G., Bogdał, D., Stankiewicz, A.I., & Stefanidis, G. (2015). A concise review on microwave-assisted polycondensation reactions and curing of polycondensation polymers with focus on the effect of process conditions. *Chemical Engineering Journal*, *264*, 633–644.

10 Sosnika, A., Gotelli, G, & Abrahamb, G. (2011). Microwave-assisted polymer synthesis (MAPS) as a tool in biomaterials science, How new and how powerful. *Progress in Polymer Science*, *36*(8), 1050–1078.

11 Fimberger, M., & Wiesbrock, F. (2016). Microwave-assisted synthesis of polyesters and polyamides by ring-opening polymerization. *Advances in Polymer Science, 274*, 149–182.

12 Kempe, K., Becer, R., & Schubert, U.S. (2011). Microwave-Assisted Polymerizations: Recent Status and Future Perspectives. *Macromolecules*, *44*(15), 5825–5842.

13 Wiesbrock, F., Hoogenboom, R., & Schubert, U.S. (2004). Microwave-Assisted Polymer Synthesis: State-of-the-Art and Future Perspectives. *Macromolecular Rapid Communications, 25*(20), 1739–1764.

14 Zhang, C., Liao, L., & Gong, S. (2007). Recent developments in microwave-assisted polymerization with a focus on ring-opening polymerization. *Green Chemistry, 9*(4), 303–314.

15 Gawande, M.B., Shelke, Sh.N., Zboril, R., & Varma, R.S. (2014). Microwave-Assisted Chemistry: Synthetic applications for rapid assembly of nanomaterials and organics. *Accounts of Chemical Research*, *47*(4), 1338−1348.

16 Mallakpour, S., & Rafiee, Z. (2008). Application of microwave-assisted reactions in step-growth polymerization: a review. *Iran Polymer Journal,* 12, 907–935.

17 Nagahata, R., Sano, D., Suzuki, H., & Takeuchi, K. (2007). Microwave-assisted single-step synthesis of poly(lactic acid) by direct polycondensation of lactic acid. *Macromolecular Rapid Communications, 28*(4), 437–442.

18 Nagahata, R., Momotake, M., Takeuchi, K., & Nakamura, T. (2012). US Patent 8,242,186 B2.

19 Pandey, A., & Aswath, P.B. (2009). Microwave Synthesis of Poly (L-lactic acid). *Journal of Biomaterials Science, 20*(1), 33–48.

20 Li, H., Liao, L., & Liu, L. (2007). Kinetic Investigation into the Non-Thermal Microwave Effect on the Ring-Opening Polymerization of ε-Caprolactone. *Macromol. Rapid Communications, 28*(4), 411–416.

21 Nikolic, L., Ristic, I., Adnadjevic, B., Nikolic, V., Jovanovic, J., & Stankovic, M. (2010). Novel microwave-assisted synthesis of poly (D, L-lactide): The influence of monomer/initiator molar ratio on the product properties, *Sensors, 10*(5), 5063–5073.

22 Nakamura, T., Nagahata, R., Suemitsu, S., & Takeuchi, K. (2010). In-situ measurement of microwave absorption properties at 2.45 GHz for the polycondensation of lactic acid. *Polymer, 51*(2), 329–333.

23 Hirao, K., Nakatsuchi, Y., & Ohara, H. (2010). Alcoholysis of poly (L-lactic acid) under microwave irradiation. *Polymer Degradation and Stability*, *95*(6), 925–928.

24 Lei, H., Wang, P., & Yuan, W. (2009). Microwave-assisted synthesis of poly (L-Lactic Acid) via direct melt polycondensation using solid super acids. *Macromolecular Chemistry and Physics, 210*(23), 2058–2062.

25 Ramier, J., Renard, E., & Grande, D. (2012). Microwave-assisted ring-opening polymerization of d,l-lactide: A probe for the nonexistence of nonthermal microwave effects. *Macromolecular Chemistry and Physics, 213*(7), 784–788.

26 Nagahata, R., Kunii, K., Soga, H., Sugimoto, S., & Takeuchi, K. (2010). Large-scale polycondensation of lactic acid using microwave batch reactors. *Organic Process Research Development, 14*(4), 781–786.

27 Gawande, M.B., Shelke, Sh.N., Zboril, R., & Varma, R.S. (2014). Microwave-assisted chemistry: synthetic applications for rapid assembly of nanomaterials and organics. *Accounts of Chemical Research, 47*(4), 1338−1348.

28 Bakibaev, A.A., & Guba, G.Ya. (2015). Polymerization of lactic acid using microwave and conventional heating. *Procedia Chemistry, 15*, 97–102.

29 Tanga, X., Huanga, J., & Xub L. (2014). Microwave-assisted rapid synthesis, characterization and application of poly (D,L-lactide)-graft-pullulan. *Carbohydrate Polymers,* 107, 7–15.

30 Yamada, S., Takasu, A., Takayama, S., & Kawamura, K. (2014). Microwave-assisted solution polycondensation of L-lactic asid using a Dean-Stark apparatus for a non-thermal microwave polymerization effect induced by the electric field. *Polymer Chemistry*, *5*(18), 5283–5288.

---

Г.Я. Губа, А.О. Гусар, А.А. Бакибаев, Е.М. Тажбаев, Е.В. Минаева

# Сүт қышқылының микротолқынды сәулелендіру жағдайларында дегидратациялануы/поликонденсациялануы

Мақалада алғаш рет микротолқынды сәулелендірудің (МТС) сүт қышқылының (СҚ) поликонденсациялану үрдістеріне әсері зерттелді. СҚ поликонденсациялануын мультимодалды реакторда вакуумда азотты 80, 130, 280, 360 және 500 Вт қуатында өткізу арқылы жүргізілді. СҚ үлгісінің температурасы МТС жағдайларында уақытқа және сәулелендіру қуатына байланысты өзгеретіні анықталды. $^1$Н ЯМР және ИҚ-спектроскопия мәліметтері негізінде қуат 80 Вт болғанда негізінен физикалық байланысқан су молекулалары кететіні туралы болжам ұсынылды. Қуат мөлшері 130–280 Вт болғанда, судың және СҚ бөлінуінен басқа, сүт қышқылының олигомерлері (СҚО) түзілетіні байқалды. Судың СҚО толық бөлінуі 360 Вт қуатында жүреді. СҚ МТС 430 Вт қуатында қыздырғанда түссіз кристалдардың түзілуі және бөлінуі байқалады. Оларды ИҚ-спектрлері бойынша лактид (ν С=О 1770 см$^{-1}$, ν С–О–С 1240 см$^{-1}$ құрады) молекулалары деп жіктеуге болады. СҚО молекулалық салмағы қуаты 430 Вт және оданда жоғары болғанда төмендейді. Қуат мөлшерлері 130, 280 және 360 Вт болғанда СҚ поликонденсациялануының кинетикалық қисықтары көрсетілген. Оңтайлы болып СҚ поликонденсациялануы 360 Вт қуатында табылады. СҚ дегидратациялану жылдамдығы МТС жағдайларында үрдісті әдеттегі қыздыру жағдайында өткізгенмен, салыстырғанда 15–20 есе артатыны анықталды.

*Кілт сөздер:* микротолқынды сәулелендіру, сүт қышқылы, полисүт қышқылы, сүт қышқылының олигомерлері, ЯМР-спектроскопия, ИҚ-спектроскопия, меншікті оптикалық айналу, молекулалық салмақ.

Г.Я. Губа, А.О. Гусар, А.А. Бакибаев, Е.М. Тажбаев, Е.В. Минаева

# Дегидратация/поликонденсация молочной кислоты в условиях микроволнового облучения

В статье впервые изучено влияние мощности микроволнового облучения (МВО) на процессы поликонденсации молочной кислоты (МК). Поликонденсацию МК проводили в мультимодальном реакторе в вакууме при барботировании азотом при мощностях 80, 130, 280, 360 и 500 Вт. Определено изменение температуры образца МК в условиях МВО в зависимости от времени и мощности излучения. На основании данных $^1$H ЯМР и ИК-спектроскопии высказано предположение, что при 80 Вт в основном удаляются молекулы физически связанной воды. При мощности 130–280 Вт, наряду с удалением воды и МК, происходит образование олигомеров молочной кислоты (ОМК). Полное удаление воды из ОМК происходит при 360 Вт. При нагревании МК при мощности МВО 430 Вт наблюдается образование и выделение бесцветных кристаллов, которые можно классифицировать по ИК-спектрам как молекулы лактида (ν C=O составляет 1770 см$^{-1}$, ν C–O–C — 1240 см$^{-1}$). Молекулярный вес ОМК при мощности 430 Вт и выше уменьшается. Представлены кинетические кривые поликонденсации МК при 130, 280 и 360 Вт. Оптимальным является процесс поликонденсации МК при 360 Вт. Установлено, что скорость дегидратации МК в условиях МВО увеличивается в 15–20 раз по сравнению с проведением процесса в условиях обычного нагрева.

*Ключевые слова:* микроволновое облучение, молочная кислота, полимолочная кислота, олигомеры молочной кислоты, ЯМР-спектроскопия, ИК-спектроскопия, удельное оптическое вращение, молекулярный вес.

DOI: 10.31489/2019Ch1/17-24

UDC 541.6:547.39:636.597

Zh.S. Kassymova, L.K. Orazzhanova, B.B. Bayakhmetova,
B.S. Gaisina, N.B. Kassenova, G.T. Yelemessova

*Shakarim State University of Semey, Kazakhstan*
*(E-mail: bulbul.bayahmetova@mail.ru)*

# Preparation of interpolymer complexes of chitosan and sodium alginate

The method of synthesis of new cheap and biodegradable soil former — an interpolymer complex (IPC) based on natural polymers has been developed for the first time. To solve environmental problems biocompatible with living tissues, bioinert natural polymers — polysaccharides chitosan (CS) and sodium alginate (AL) were used as structural components of the IPC. The chitosan-sodium alginate IPC was prepared by mixing equimolar solutions of polymers in a given proportion. The composition and properties of the prepared polymer complexes — mass, electrical conductivity, mechanical properties, rheological properties, size and particle charge, structure were determined by physicochemical methods (reoviscosimetry, mechanical analysis, gravimetry, potentiometric and conductometric titration, dynamic light scattering and Fourier-transform infrared spectroscopy). The composition of the chitosan — sodium alginate complex CS: AL is 1:4. It is established that the formation of an interpolymer non-stoichiometric complex occurs as a result of ion-ion interactions. Films based on IPC of CS and AL were prepared and mechanical properties of this films were detected. Films based on interpolymer complex have higher mechanical strength than films of individual polymers. Therefore, this polymer system is a promising material for the use it in preventing wind and water migration of lands.

*Keywords:* complexation, biopolymers, chitosan, sodium alginate, composition, nonstoichiometric complex, films, polyionic complexes.

## *Introduction*

The production of new functional materials with a wide range of practical application is one of the main challenges of modern science. From a scientific and practical point of view there is a special interest to interpolymer complexes. IPCs possess a complex of unique physicochemical, colloidal and mechanical properties which are promising for the use in various fields of science, engineering, medicine and agriculture [1–3].

As known, IPCs are the products of the interaction between chemically complementary polymers which form a large number of intermolecular bonds such as hydrogen, electrostatic, ion-dipole, Van der Waals, and hydrophobic interactions [4].

The formation of IPC occurs in aqueous solutions through the binding of counter-ions with the ionization of their reactive functional groups. The initial complexing polyelectrolytes contain ionic functional groups, amount and relative position of which affect the thermodynamics of complexation and control stability, define the structure and properties of IPC [5].

Interpolymer complexes based on natural polymers represent an extensive class of polymer compounds, which due to their biodegradability, biocompatibility and non-toxicity find practical application as structure-builders for disperse systems, materials for medical and biotechnological purposes, medicines, etc. [6–11]. Biopolymers like chitosan (polycation) and sodium alginate (polyanion) arouse interest among natural polymers capable of forming polymer-polymer complexes.

Chitosan (poly β-1,4–2-deoxy-2-amino-D-glucopyranose) is the product of deacetylation of natural chitin polysaccharide (Fig. 1).

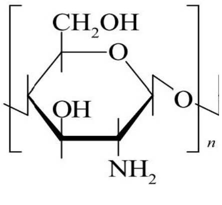

Figure 1. The structural formula of chitosan

It is known [12, 13] that the presence of amino groups defines the behavior of chitosan in solution as a weak cationic polyelectrolyte and it has pH-dependent solubility (it is easy to dissolve in acidic environments and not to dissolve in neutral and alkaline environments).

Sodium alginate is an ionic polysaccharide obtained by alkaline extraction of brown algae, due to the complex of very valuable properties in practical terms (water solubility, non-toxicity, high thickening ability) holds one of the leading positions among water-soluble polymers of natural origin (Fig. 2).

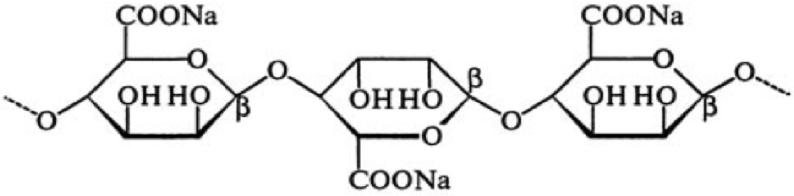

Figure 2. The structural formula of sodium alginate

Sodium alginate belongs to the family of unbranched double copolymers: residues of β-D-mannuric acid and α-L-guluronic acid, connected by 1 → 4 glycosidic bonds. Due to its good water-holding capacity and water solubility its main use is related to the ability to form gel [14].

The presence of ionogenic groups in chitosan and sodium alginate which are capable to form intermolecular ion-ion and ion-dipole bonds creates a prerequisite for their use as components of the interpolymer complex.

The purpose of this work is to establish the patterns of formation and structure of the interpolymer complex based on natural polymers — chitosan (CS) and sodium alginate (AL).

## *Experimental*

Chitosan is a commercial sample of Sigma-Aldrich (USA) with a medium viscosity molecular weight (MW = 500 kDa), degree of deacetylation (DD 80 %).

Sodium alginate is a commercial sample with a molecular weight (440 kDa) (produced by Sigma-Aldrich (China)).

The synthesis of IPCs was carried out by mixing the solutions of 0.01 M chitosan in 0.1 M hydrochloric acid solution with 0.01 M aqueous solution of sodium alginate in molar ratios of [CS]:[AL] = [100:0], [90:10], [80:20], [70:30], [60:40], [50:50], [40:60], [30:70], [20:80], [10:90], [0:100] (mol.%) at a temperature range 293–298 K. The obtained mixture was vigorously stirred on a shaker (model LS 110, LOIP, Russia) for 0.5–1 hours and kept for 1 day at room temperature, then it was centrifuged for 15 minutes at 3500 rpm and precipitate of IPC was filtrated. After washing the IPC with distilled water, the final product was lyophilized (FreeZone, Labconco, USA).

Conductometric study of the CS-AL interpolymer complex formation was carried out using the S230 Seven Compact Mettler Toledo (Switzerland).

The structure of the IPCs was established by IR spectroscopy. IR spectra were recorded on a Fourier-transform infrared spectrometer (FTIR) Carry 660 Agilent (USA) equipped with an ATR attachment in the range from 400 to 4000 cm$^{-1}$.

The charge of IPCs particles was determined by dynamic light scattering (DLS) on a Zetasizer Nano ZS 90 (Malvern, UK) instrument.

Studies of the rheological properties (structural viscosity) of synthesized IPCs solutions were performed on a rotational viscometer RheolabQC, «Anton Paar» (Austria) with a working cylinder-cylinder unit in the range of shear stresses 3–600 Pa at room temperature.

Study of the mechanical characteristics of films from individual polymers, IPC-systems based on them was carried out at room temperature on the TAXT plus Texture analyzer (Stable MicroSystems, UK) instrument in compression mode using P/5S at a speed of 0.1 mm/s. For obtaining films the initial polymers and IPCs mixtures were poured onto the polymer substrate and evaporated at room temperature and normal atmospheric pressure till an air-dry state [15].

## *Results and discussion*

Complexation in the system chitosan-sodium alginate was detected by a combination of physical and chemical methods.

The results of conductometric determination of electrical conductivity in the system chitosan — sodium alginate are presented in Figure 3.

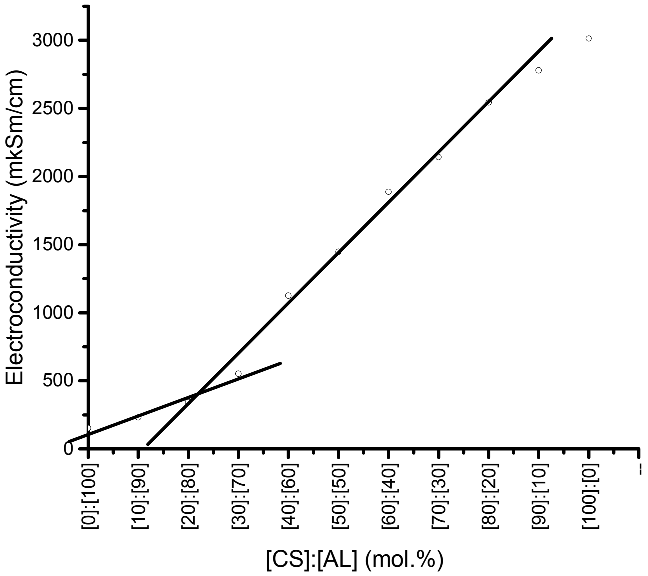

Figure 3. Conductometric titration curve in the CS-AL system

Figure 3 shows the conductometric titration curve of the chitosan-sodium alginate system at the molar ratios [CS]:[AL] = [100:0], [90:10], [80:20], [70:30], [60:40], [50:50], [40:60], [30:70], [20:80], [10:90], [0:100] and at the ratio [CS]:[AL] = [20]:[80] it has a pronounced bend, which according to the fundamentals of the physical and chemical analysis indicates on the formation of an individual compound — IPC with the composition [CS]:[AL] = [1]:[4].

Evidence of the CS and AL complexation is the formation of a precipitate which is insoluble in water and acidic solutions. The formed precipitation of IPC was a white, odorless gel-like mass, stable during centrifugation; the maximum mass of the precipitate was determined by IPC with the [20]:[80] mol.% ratio.

The masses of precipitates of IPCs after centrifugation are given in Table 1.

Table 1

**The masses of IPC precipitates after centrifugation**

| [CS]:[AL], mol.% | The mass of wet IPC precipitates, g |
|---|---|
| [10]:[90] | 0.0562 |
| [20]:[80] | 1.1825 |
| [30]:[70] | 1.1681 |
| [40]:[60] | 0.7730 |
| [50]:[50] | 0.5989 |
| [60]:[40] | 0.6537 |
| [70]:[30] | 0.5028 |
| [80]:[20] | 0.4215 |
| [90]:[10] | 0.3114 |

Maximum mass of the IPC precipitates is observed for the molar ratio [CS]:[AL] = [20]:[80] mol.%, according to Table 1.

The complexation in the chitosan — sodium alginate system was also confirmed by the dynamic light scattering (DLS) method. Dependence of the ζ-potential of particles on the ratio in the system of CS–AL is shown in Figure 4.

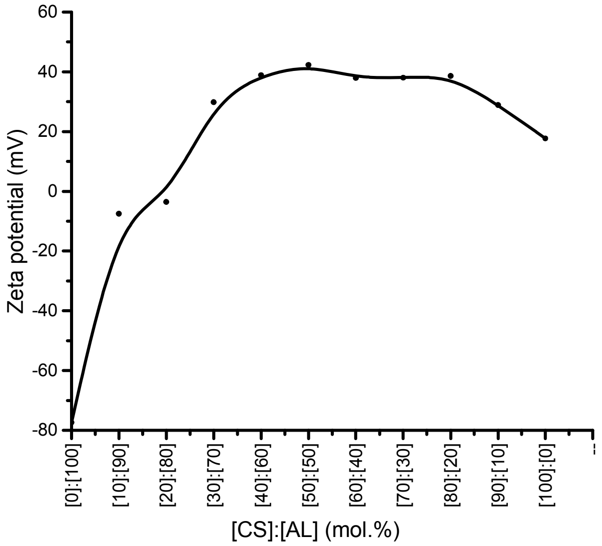

Figure 4. Dependence of the ζ-potential of the IPC particles on the composition of [CS]: [AL]

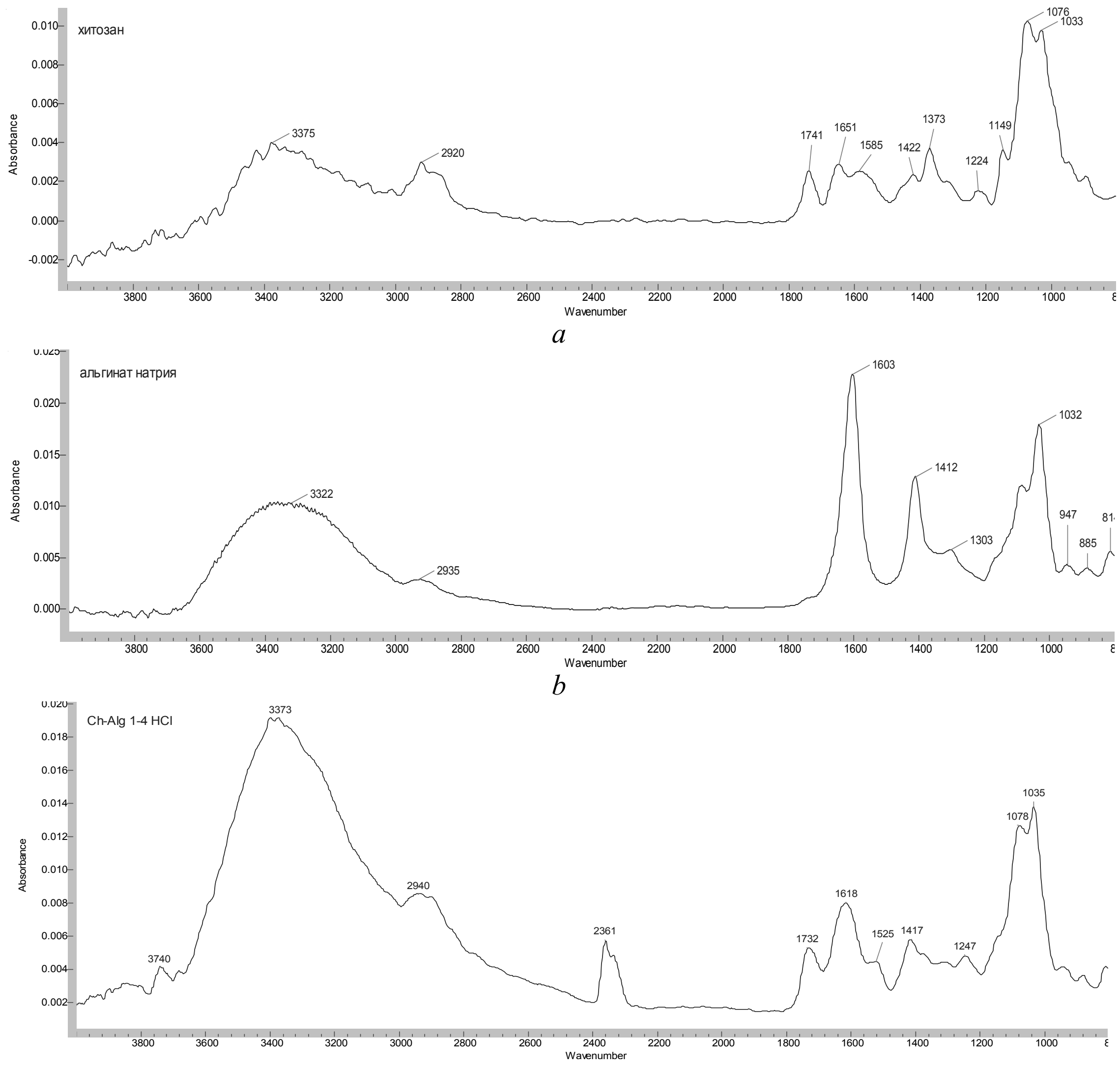

*a*

*b*

*c*

*a* — CS; *b* — AL; *c* — IPC of CS/AL

Figure 5. IR spectra

At the molar ratio [CS]:[AL] = [20]: [80] ζ-potential reaches zero value, as shown in Figure 4. It indicates the neutralization of the positive charge of chitosan by the negative charge of the carboxylic group of sodium alginate. This indicates the electrostatic interaction between the molecules of the polycation and the polyanion and the cooperative nature of complexation.

Data obtained using DLS correspond well with data of the IR Fourier spectroscopic investigation of complexation in the chitosan — sodium alginate system. IR spectra of CS, AL and IPCs based on them were obtained (Fig. 5 *a, b, c*).

IR spectra of chitosan and alginate contain absorption bands that characterize all polysaccharides — 3000–3500 cm$^{-1}$ (vibrations of OH-groups), 2900–2950 cm$^{-1}$ (vibrations of $CH_2$-groups), 1010–1050 cm$^{-1}$ (vibrations of C–O–C sugar groups). IR spectra of chitosan (Fig. 5, *a*) contains absorption bands in the 1651 cm$^{-1}$ region ($\delta NH_2$), this is characteristic of amino groups. Absorption bands are observed in the 1603 and 1412 cm$^{-1}$ region in IR spectra of alginate, it's due to the presence of carboxylate — ionic groups.

The main changes occur in the spectra of the absorption bands of $NH_2$-groups and carboxyl groups in IR spectra of IPCs, which to point on their electrostatic interaction [16]. Main changes occur in the region of the spectrum of stretching vibrations of carboxyl groups (1603 and 1412 cm$^{-1}$) and deformation vibrations of the amino group (1651 cm$^{-1}$), which during the formation of IPC lose their intensity and shift ($\nu^{sym}_{C=O}$ 1618 cm$^{-1}$, $\nu^{asym}_{C=O}$ 1417 cm$^{-1}$).

Rheological properties of [CS]:[AL] IPCs mixtures were investigated. The rheological behavior of polymer systems is determined by the mechanism of their formation, for which the nature, location and interaction of the functional groups of the polymer matrix are particular importance [17].

Figure 6 shows the curve of shear stress dependence on the [CS]:[AL] molar ratio.

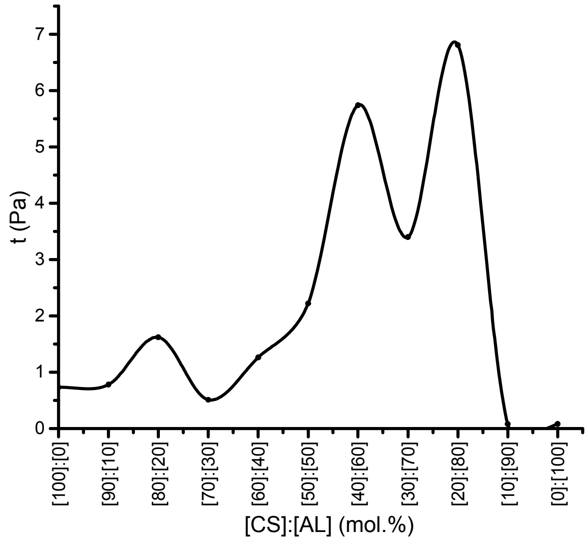

Figure 6. Dependence of the shear stress on the ratio [CS]: [AL]

As shown in Figure 6, the highest shear stress was in the complex solution with the molar ratio [CS]: [AL] = [20]: [80]. It's due to the high degree of adhesion of branched structures and the intensity of intermolecular interactions of the initial polymers [18] and leads to a decrease of IPCs associates size and their strength.

The films based on IPCs of chitosan – alginate were prepared and their mechanical properties were studied. The period of film formation on the polymer substrate IPC [CS]:[AL] was 3 days. The mechanical characteristics of the molded films are shown in Table 2.

Table 2

**Mechanical characteristics of films from chitosan, sodium alginate and IPCs based on them**

| Film composition | Elastic modulus, Pa |
|---|---|
| AL | 3.52±0.05 |
| CS | 0.26±0.08 |
| IPC [CS]:[AL]= [20]:[80] mol.% | 2.27±0.06 |

The value of elastic modulus of the IPC (2.27 ± 0.06 Pa) with the molar ratio [CS]:[AL] = [20]:[80] prevails over the value of the chitosan modulus (0.26±0.08 Pa) and comparable with the elastic modulus of sodium alginate (3.52±0.05 Pa), as shown in Table 2. Mechanical strength is an important characteristic of the IPCs, because it is further intended to be used as a former of the soil. Therefore, they must be resistant to various loads and preserve the integrity of the structure.

## *Conclusion*

Thus, as a result of complex physico-chemical studies, complexation was found in chitosan — sodium alginate system with the optimal composition of IPC [CS]:[AL] = [1]:[4]. This ratio for an interacting pair of polyelectrolytes characterizes the formation of non-stoichiometric IPCs. Alginate-chitosan polyionic complexes are formed due to the ion-ion interaction between the carboxyl groups of alginate and the amino groups of chitosan.

*The work was carried out with the financial support of the Ministry of Education and Science of the Republic of Kazakhstan, grant AP05134681.*

## References

1 Mukhamedov G.I. Interpolymer complexes: structure, properties, application: monograph / G.I. Mukhamedov, S.Ya. Inagamov, M.M. Hafizov. — LAP Lambert Academic Publishing, 2017. — 295 p.

2 Kabanov V.A. Polyelectrolytes in the solution of ecological problems / V.A. Kabanov, A.B. Zezin, V.A. Kasaikin, A.A. Yaroslavov, D.A. Topchiyev // Russian Chem. Reviews. — 1991. — Vol. 60, No. 3. — P. 288–297.

3 Ахмеджонов Д.Г. Эффективное использование интерполимерных комплексов при минерализации почв / Д.Г. Ахмеджонов, Х.Э. Туркменов, Х.Т. Бекмуродов // Молодой ученый. — 2016. — № 27. — С. 207, 208.

4 Абдиев К.Ж. Интерполимерное комплексообразование с участием полимеров, полученных на основе простых виниловых эфиров / К.Ж. Абдиев // Известия Национальной академии наук Республики Казахстан. Сер. хим. — 2008. — № 2. — С. 31–38.

5 Бовальдинова К.А. Получение и свойства «умных» чувствительных к давлению адгезивов на основе интерполимерных комплексов: дис. … канд. хим. наук: 02.00.06 — Высокомолекулярные соединения / К.А. Бовальдинова. — М., 2018. — 165 с.

6 Rhazi M. Influence of the nature of the metal ions on the complexation with chitosan. Application to the treatment of liquid waste / M. Rhazi, J. Tolaimate, M. Rinaudo, P. Vottero, A. Alagui, M. Meray // European Polymer Journal. — 2002. — Vol. 38, No. 8. — P. 1523–1530.

7 Riccardo A.A. Genipin — crosslinked chitosan hydrogels as biomedical and pharmaceutical aids / A.A. Riccardo // Carbohydrate Polymers. — 2009. — No. 77. — P. 1–9.

8 Kumari R. Physico-chemical and biological activity study of genipin cross linked chitosan scaffolds prepared by using supercritical carbon dioxide for tissue engineering applications / R. Kumari, P.K. Dutta // International J. Biological Macromolecules. — 2010. — No. 46. — P. 261–266.

9 Muzzarelli Riccardo A.A. Chitins and chitosans for the repair of wounded skin, nerve, cartilage and bone / Riccardo A.A. Muzzarelli // Carbohydrate Polymers. — 2009. — No. 76. — P. 167–182.

10 Хитин и хитозан: получение, свойства и применение / под ред. К.Г. Скрябина, Г.А. Вихоревой, В.П. Варламова. — М.: Наука, 2002. — 368 с.

11 Krayukhina M.A. Polyelectrolyte complexes of chitosan: formation, properties and applications / M.A. Krayukhina, N.A. Samoilova, I.A. Yamskov // Russian Chemical Reviews. — 2008. — Vol. 77, No. 9. — P. 799–813.

12 Berkovich L.A. Hydrodynamic and conformational parameters of chitosane / L.A. Berkovich, G.I. Timofeyeva, M.P. Tsyurupa, V.A. Davankov // Polymer Science U.S.S.R. — 1980. — Vol. 22, No. 8. — P. 2009–2018.

13 Gamzazade A.I. On the viscosity properties of chitosan solutions / A.I. Gamzazade, A.M. Sklyar, S.-S.A. Pavlova, S.V. Rogozhin // Polymer Science U.S.S.R. — 1981. — Vol. 23, No. 3. — P. 665–669.

14 Usov A.I. Alginic acids and alginates: analytical methods used for their estimation and characterisation of composition and primary structure / A.I. Usov // Russian Chemical Reviews. — 1999. — Vol. 68, No. 11. — P. 957–966.

15 Инагамов С.Я. Интерполимерные комплексы на основе натрийкарбоксиметилцеллюлозы — носители наночастиц / С.Я. Инагамов, Ф.С. Каюмходжаев, А.А. Абзалов // Научное обозрение. Биологические науки. — 2017. — № 2. — С. 71–74.

16 Петропавловский Г.А. Гидрофильные частично замещенные эфиры целлюлозы и их модификация путем сшивания / Г.А. Петропавловский. — Л.: Наука, 1988. — 295 с.

17 Юсова А.А. Свойства гидрогелей на основе смесей альгината натрия с другими полисахаридами природного происхождения / А.А. Юсова, И.В. Гусев, И.М. Липатова // Химия растительного сырья. — 2014. — № 4. — С. 59–66.

18 Kabanov V.A. Polyelectrolyte complexes in solution and in bulk / V.A. Kabanov // Russian Chem. Reviews. — 2005. — Vol. 74, No. 1. — P. 3–20.

Ж.С. Қасымова, Л.К. Оразжанова, Б.Б. Баяхметова,
Б.С. Гайсина, Н.Б. Қасенова, Г.Т. Елемесова

## Хитозан мен натрий альгинаты негізінде интерполимерлік комплекстерді алу

Алғаш рет жаңа арзан және биоыдырайтын топырақ құрылымтүзгіштер — табиғи полимерлер негізіндегі интерполимерлік комплекстерді (ИПК) синтездеу әдісі әзірленді. Экологиялық мәселелерді шешу мақсатында интерполимерлік комплекстің құрылымдық компоненттері ретінде тірі ұлпалармен биоүйлесімді, биоинертті табиғи полимерлер — хитозан (ХТЗ) мен натрий альгинаты (АЛNa) полисахаридтері қолданылды. Хитозан – натрий альгинаты интерполимерлік комплексі берілген қатынаста полимерлердің эквимолярлы ерітінділерін қосу әдісімен алынды. Алынған интерполимерлік комплекстердің құрамы мен қасиеттері — масса, электрөткізгіштік, механикалық және реологиялық қасиеттері, бөлшектердің өлшемі мен заряды, құрылымы физика-химиялық талдау әдістермен (реовискозиметрия, механикалық талдау, гравиметрия, потенциометрлік және кондуктометрлік титрлеу, динамикалық жарық шашырау (ДЖШ) және ИҚ-Фурье спектроскопия) анықталды. Интерполимерлік комплекс құрамы ХТЗ – АЛNa = 1:4. Стехиометриялық емес интерполимерлік комплекс ион-иондық өзара әрекеттесу нәтижесінде пайда болатыны байқалды. ХТЗ-АЛNa ИПК негізінде полимерлік жабындар алындып, олардың механикалық қасиеттері анықталды. Интерполимерлі комплекс негізіндегі жабындардың механикалық беріктілігі жеке полимерлердің жабындармен салыстырғанда жоғары; бұл алынған полимерлі жүйені топырақтың жел мен судың әсерінен миграциясына жол бермеу үшін қолдануға болатын перспективті материалдар жасауға мүмкіндік береді.

*Кілт сөздер*: комплекс түзу, биополимерлер, хитозан, натрий альгинаты, құрам, стехиометриялық емес комплекс, жабындар, полиионды комплекс.

Ж.С. Касымова, Л.К. Оразжанова, Б.Б. Баяхметова,
Б.С. Гайсина, Н.Б. Касенова, Г.Т. Елемесова

## Получение интерполимерных комплексов на основе хитозана и альгината натрия

Впервые разработана методика синтеза новых дешевых и биоразлагаемых структурообразователей почв — интерполимерного комплекса (ИПК) на основе природных полимеров. В качестве структурных компонентов интерполимерного комплекса для решения экологических проблем были использованы биосовместимые с живыми тканями биоинертные природные полимеры — полисахариды хитозан (ХТЗ) и альгинат натрия (АЛNa). Интерполимерный комплекс хитозан – альгинат натрия был получен методом смешения эквимолярных растворов полимеров в заданной пропорции. Методами физико-химического анализа (реовискозиметрии, механического анализа, гравиметрии, потенциометрического и кондуктометрического титрований, динамического лазерного светорассеяния (ДЛС) и ИК-Фурье спектроскопии) определены состав и свойства полученных полимерных комплексов — масса, электропроводность, механические свойства, реологические свойства, размеры и заряд частиц, структура. Состав интерполимерного комплекса [ХТЗ]:[АЛNa] = 1:4. Обнаружено, что формирование интерполимерного нестехиометрического комплекса происходит в результате ион-ионных взаимодействий. Получены полимерные пленки на основе ИПК ХТЗ–АЛNa, и определены их механические свойства. Установлено, что механическая прочность пленок на основе интерполимерного комплекса выше в сравнении с пленками отдельных полимеров, что делает данную полимерную систему перспективным материалом в целях использования для предотвращения ветровой и водной миграции земель.

*Ключевые слова*: комплексообразование, биополимеры, хитозан, альгинат натрия, состав, нестехиометрический комплекс, пленки, полиионные комплексы.

## References

1 Mukhamedov, G.I. (2017). *Interpolymer complexes: structure, properties, application.* LAP Lambert Academic Publishing.

2 Kabanov, V.A., Zezin, A.B., Kasaikin, V.A., Yaroslavov, A.A. & Topchiyev, D.A. (1991). Polyelectrolytes in the solution of ecological problems. *Russian Chem. Reviews*, *60*(3), 288–297.

3 Ahmedzhonov, D.G., Turkmenov, H.E., & Bekmurodov, H.T. (2016). Effektivnoe ispolzovanie interpolimernykh kompleksov pri mineralizatsii pochv [Efficient use of interpolymer complexes during soil mineralization]. *Molodoi uchenyi — Young scientist*, *27*, 207–208 [in Russian].

4 Abdiev, K.Zh. (2008). Interpolimernoe kompleksoobrazovanie s uchastiiem polimerov, poluchennykh na osnove prostykh vinilovykh efirov [Interpolymer complexation involving polymers derived from vinyl ethers]. *Izvestiia Natsionalnoi akademii nauk*

*Respubliki Kazakhstan. Seriia khimicheskaia, — News of the National Academy of Sciences of the Republic of Kazakhstan. Chemical series*, *2*, 31–38 [in Russian].

5 Bovaldinova, K.A. (2018). Poluchenie i svoistva «umnykh» chuvstvitelnykh k davleniiu adhezivov na osnove interpolimernykh kompleksov [Obtaining and properties of «smart» pressure-sensitive adhesives based on interpolymer complexes]. *Candidate's thesis*. Moscow [in Russian].

6 Rhazi, M., Tolaimate, J., Rinaudo, M., Vottero, P., Alagui, A., & Meray, M. (2002). Influence of the nature of the metal ions on the complexation with chitosan. Application to the treatment of liquid waste. *European Polymer Journal*, *38*(8), 1523–1530.

7 Riccardo, A.A. (2009). Genipin — crosslinked chitosan hydrogels as biomedical and pharmaceutical aids. *Carbohydrate Polymers*, *77*, 1–9.

8 Kumari, R., & Dutta, P.K. (2010). Physico-chemical and biological activity study of genipin cross linked chitosan scaffolds prepared by using supercritical carbon dioxide for tissue engineering applications. *International J. Biological Macromolecules*, *46*, 261–266.

9 Muzzarelli, Riccardo A.A. (2009). Chitins and chitosans for the repair of wounded skin, nerve, cartilage and bone. *Carbohydrate Polymers*, *76*, 167–182.

10 Skriabin, K.G., Vihoreva, G.A., & Varlamov, V.P. (2002). *Khitin i khitozan: poluchenie, svoistva i primenenie [Chitin and chitosan: preparation, properties and application]*. Moscow: Nauka [in Russian].

11 Krayukhina, M.A., Samoilova, N.A., & Yamskov, I.A. (2008). Polyelectrolyte complexes of chitosan: formation, properties and applications. *Russian Chemical Reviews, 77*(9), 799–813.

12 Berkovich, L.A., Timofeyeva, G.I., Tsyurupa, M.P., & Davankov, V.A. (1980). Hydrodynamic and conformational parameters of chitosane. *Polymer Science U.S.S.R., 22*(8), 2009–2018.

13 Gamzazade, A.I., Sklyar, A.M., Pavlova, S.-S.A., & Rogozhin, S.V. (1981). On the viscosity properties of chitosan solutions. *Polymer Science U.S.S.R., 23*(3), 665–669.

14 Usov, A.I. (1999). Alginic acids and alginates: analytical methods used for their estimation and characterization of composition and primary structure. *Russian Chemical Reviews*, 68*(11)*, 957–966.

15 Inagamov, S.Ya., Kaiumhodiaiev, F.S., & Abzalov, A.A. (2017). Interpolimernye kompleksy na osnove natriikarboksimetiltselliulozy — nositeli nanochastits [Sodium carboxymethylcellulose based interpolymer complexes are carriers of nanoparticles]. *Nauchnoe obozrenie. Biolohicheskie nauki — Scientific Review. Biological Sciences*, *2*, 71–74 [in Russian].

16 Petropavlovskii, G.A. (1988). *Hidrofilnye chastichno zameshchennye efiry tselliulozy i ikh modifikatsiia putem sshivaniia [Hydrophilic partially substituted cellulose ethers and their modification by crosslinking]*. Leningrad: Nauka [in Russian].

17 Iysova, A.A., Gusev, I.V., & Lipatova, I.M. (2014). Svoistva hidrohelei na osnove smesei alhinata natriia s druhimi polisakharidami prirodnoho proiskhozhdeniia [Properties of hydrogels based on mixtures of sodium alginate with other polysaccharides of natural origin]. *Khimiia rastitelnoho syria. — Chemistry of plant materials, 4*, 59–66 [in Russian].

18 Kabanov, V.A. (2005). Polyelectrolyte complexes in solution and in bulk. *Russian Chem. Reviews, 74*(1), 3–20.

DOI: 10.31489/2019Ch1/25-31

UDC 547.37

M.Zh. Burkeev[1], G.K. Kudaibergen[1], Ye.M. Tazhbayev[1], G.K. Burkeyeva[1],
A.Zh. Sarsenbekova[1], J. Hranicek[2], N.A. Yesentayeva[1], A.N. Bolatbay[1], S.B. Aukadieva[1]

*[1]Ye.A. Buketov Karaganda State University, Kazakhstan;*
*[2]Charles University, Czech Republic*
*(E-mail: gulshahar90@mail.ru)*

# Constants and parameters of radical copolymerization of poly(propylene glycol)fumarate with acrylic acid

In the present work, the binary radical copolymerization of poly(propylene glycol)fumarate with acrylic acid in a dioxane medium was investigated for the first time at various mole ratios of the initial monomer mixture. The kinetics of the copolymerization reaction was studied. Kinetic curves show that with increasing mole fraction of acrylic acid in solution, the reaction rate and sorption capacity of copolymers also increase. The synthesized copolymers composition was determined by chromatography-mass spectrometry. The constants and parameters of radical copolymerization were calculated using the integral methods of Mayo-Lewis, Fineman-Ross and Kelen-Tüdos. The Q-e parameters were calculated by the Alfray-Price equation on the basis of copolymerization constants. A lower reactivity characterization of poly(propylene glycol)fumarate was found at copolymerization of it with acrylic acid. The relative activity $r_1$ in the p-PGF-AA system is less than one. This suggests that the p-PGF ability to copolymerize with other monomers is higher than homopolymerization. Direct proportionality of the unsaturation degree of copolymers to the content of poly(propylene glycol)fumarate in the composition of the initial monomer mixture was shown. Thus, the results of this study show that the synthesized polymers based on PGPP have good characteristics and can be used in various fields of science.

*Keywords:* unsaturated polyester resins, poly(propylene glycol)fumarate, acrylic acid, copolymerization constants, monomer activity, kinetics, sorption, copolymerization.

## *Introduction*

Unsaturated polyester (UPE) resins are prepared from the polyesterification reaction of diols, unsaturated dibasic acids/acid anhydrides, and saturated dibasic acids/acid anhydrides. UPE resins, the most common thermoset resins for fiber-reinforced thermoset composites account for over 80 % of all of thermoset resins used. On the other hand, unsaturated polyesters provide the widest opportunity for directional modification due to polymerization reactions with various ionic monomers and, consequently, open the way to obtaining materials including composite ones with a predetermined valuable complex of properties [1, 2].

The interaction of polyesters with unsaturated compounds was firstly called the copolymerization reaction by Benig [3], so copolymerization with vinyl acetate, styrene and methyl methacrylate, simple and complex allyl ethers, vinyl formates was investigated. As a result of the studies carried out, the role of unsaturated polyesters macromolecule as a «skeleton» at large formations was shown. From the literature analysis, only comonomers of hydrophobic nature were involved in the copolymerization with unsaturated polyester resins [3–5], when the matter of hydrophilic monomers lay over until recently, which opens up prospects for new «intelligent» polymers.

Poly(propylene glycol)fumarate (p-PGF), an amorphous unsaturated polyesters resin, has been extensively studied as an injectable biomaterial for bone tissue engineering utilizing particulate leaching to achieve a porous scaffold. p-PGF is biodegraded through hydrolysis of its ester bonds into its original propylene glycol and fumaric acid sub units, both of which are nontoxic. Propylene glycol is used as a food additive in the food industry and it can be metabolized or excreted by the body [6–9].

The preparation of polymers based on unsaturated polyesters with the required combination of properties is possible only on the knowledge basis of the processes kinetics and mechanism of their radical copolymerization with ionic monomers. It seemed interesting and expedient to fill in the marked gap since the study of the kinetics, constants, and parameters of unsaturated polyesters copolymerization with ionic monomers remains undetermined and actual.

We have previously synthesized a number of copolymers based on unsaturated polyester resins with some unsaturated carboxylic acids [10–12]. This paper demonstrates the first studies on the reactions of radical copolymerization of poly(propylene glycol)fumarate (p-PGF) with acrylic acid (AA).

### *Method*

The initial p-PGF was obtained by the polycondensation reaction of fumaric acid and propylene glycol at a temperature of 403–453 K [13]. The course of the reaction was monitored by determining the acid number and the volume of water released. The synthesized polyester is a light-yellow, resinous, fusible substance, soluble in chloroform and dioxane. The resulting resin was purified from the initial monomers by repeated washing with acetone.

The molecular weight of the p-PGF was determined by light-scattering methods on the nephelometer 2100 AN by NACH and by the method of determining the end group fraction, which is 1488 amu.

Radical copolymerization of p-PGF with AA was carried out in the dioxane solution at various initial molar ratios of comonomers in the presence of an initiator — benzoyl peroxide (BP) at a temperature of 333 K. The polymers synthesized were repeatedly washed with dioxane and dried under vacuum until constant mass for purifying them from unreacted monomer residues.

The compositions of the copolymers obtained were determined by potentiometric titration and by the residual amount of monomers by chromatography- mass spectrometry on Agilent 7890A using the Agilent 5975C mass selective detector.

The kinetics of radical copolymerization of p-PGF with AA was studied by dilatometric method in the dioxane solution. The copolymerization constants $r_1$ and $r_2$ were determined on the basis of the copolymer compositions obtained at deep conversion ratios using the Mayo-Lewis integral equation [14], as well as the standard methods of Fineman-Ross and Kelen-Tüdos [15, 16].

### *Results and discussion*

The intensive development of fundamental research in the field of radical copolymerization, which allows regulating the properties, structure and molecular mass of polymers, the velocity of the process, opens up new ways of obtaining polymers with properties given. Products based on unsaturated polyesters cured with vinyl monomers possessing specific physical-chemical and physical-mechanical properties are of considerable interest. The presence of unsaturated double bonds in the p-PGF molecule provides an opportunity to use it as a polymer matrix for the preparation of spatially cross-linked polymers by copolymerization with reactive acrylic acid.

p-PGF is obtained by the polycondensation reaction of fumaric acid and propylene glycol. As a result of radical copolymerization of the oligomeric molecule of p-PGF with AA in the presence of the initiator — BP the formation of the spatially cross-linked copolymer can be represented by the following scheme:

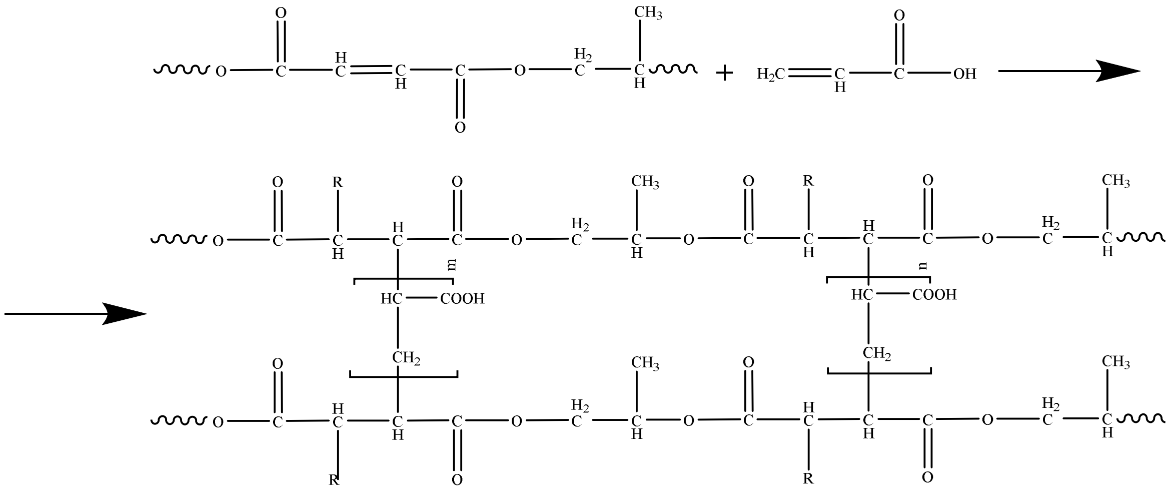

The values of constants and copolymerization parameters are important characteristics when considering the relative reactivity of the monomers depending on their structure. However, more complete information on the relative reactivity of the monomers during copolymerization can be obtained on the basis of kinetic data (Fig. 1).

However, more complete information on the relative reactivity of the monomers during copolymerization can be obtained on the basis of kinetic data (Fig. 1).

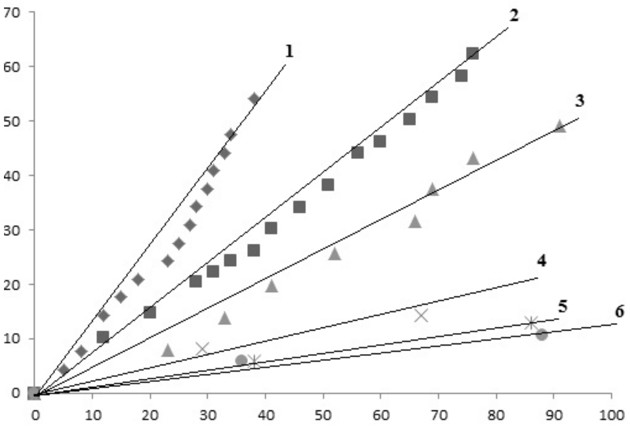

*1* — 9.98:90.02; *2* — 15.04:84.96; *3* — 24.92:75.08; *4* —50.06:49.94; *5* — 75.25:24.75; *6* — 90.13:9.87 mol.%

Figure 1. Kinetic curve of the copolymerization of p-PGF:AA

The kinetics of radical copolymerization of p-PGF with AA at various initial molar ratios was studied in detail to assess the relative activity of the monomers (Fig. 1). Increase of the reaction rate and yields of the copolymers was found with the growth in the content of AA in the initial monomer mixture, also these parameters decrease with the increase of the p-PGF content in the reaction mixture. This is apparently due to the presence of a functional –COOH carboxyl group in the AA chain that capable of participating in elementary polymer transfer reactions accompanied by an increase in the molecular weight due to branching processes. Figure 1 shows the kinetic data of radical copolymerization indicating a regular acceleration of the process with increasing molar fraction of AA in the initial monomer mixture. The radical copolymerization of p-PGF with AA forms insoluble polymers of the network structure in the entire range of the studied comonomer ratios. The experimental data obtained as a result of studying the processes of radical copolymerization in p-PGF-AA systems are presented in Table 1. The yield of the copolymers was 83–74 %.

Table 1

**Composition dependence of the copolymers on the initial mixture composition in the copolymerization of p-PGF ($M_1$) with AA ($M_2$) [BP] = 8 mol/m$^3$, T = 333 K**

| The initial ratio of monomers, mass. % | | Copolymer composition, mass. % | | Yield, % |
|---|---|---|---|---|
| $M_1$ | $M_2$ | $m_1$ | $m_2$ | |
| 9.98 | 90.02 | 7.23 | 92.77 | 84.23 |
| 15.04 | 84.96 | 10.85 | 89.15 | 82.84 |
| 24.92 | 75.08 | 20.45 | 79.55 | 78.41 |
| 50.06 | 49.94 | 46.89 | 53.11 | 74.98 |
| 75.25 | 24.75 | 72.36 | 27.67 | 69.55 |
| 90.13 | 9.87 | 89.05 | 10.95 | 65.45 |

Enrichment of the p-PGF-AA copolymers with AA units throughout the investigated range of the initial mixtures was seen from Table 1, while the content of the AA units in the copolymer composition increases sympathetically its amount in the initial monomer mixture. The copolymer yield and the swelling degree increase with increasing concentration in the initial AA mixture, which is apparently due to a sufficient degree of branching and cross-linking. Since the fumarate groups are not capable of homopolymerization reactions, the branching and cross-linking reactions diminish with a decrease in the molar AA concentration, respectively, while the unsaturation degree of the copolymer increases. Also, the above reactions are difficult with the increase of the p-PGF concentration in the initial monomer mixture, which in turn leads to the viscosity growth. The composition diagram demonstrates more clearly the dependence of the copolymer composition on the initial mixture composition (Fig. 2).

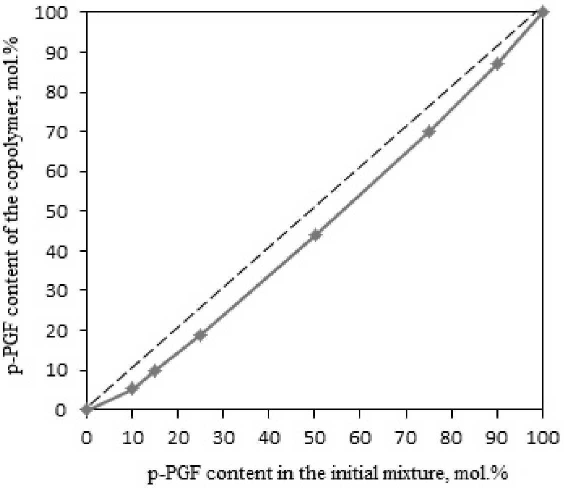

Figure 2. The dependence of the p-PGF-AA copolymers composition
on the composition of the initial monomer mixture

The relative activities of the comonomers were calculated using the integral Mayo-Lewis equation [9], the standard Fineman-Ross and Kelen-Tüdos methods on the basis of the copolymer and the initial monomer mixture compositions data. Table 2 shows the results of calculations. There was an assumption that p-EGF had a lower reactivity in radical copolymerization compared to AA. The obtained values of the relative activities of the copolymers confirm this assumption. The calculated values of the copolymerization constants indicate a greater AA activity in radical copolymerization. The data from Table 2 demonstrate the relative activity $r_1$ in the p-PGF-AA system that is less than one. It may indicate more activity of macroradical ending in the p-PGF unit towards the «foreign» monomer or radical, while the macroradical ending in the second comonomer AA ($r_2$>1) unit reacts much more easily with its «own» monomer. The product of copolymerization constants ($r_1 \cdot r_2$) close to unity indicates the possibility of copolymers to the formation of statistical structures.

Table 2

**Constants and parameters of radical copolymerization of p-PGF-AA binary systems**

| Method | $r_1$ | $r_2$ | $r_1 \cdot r_2$ | $1/r_1$ | $1/r_2$ | $e_1$ | $Q_1$ | $e_2$ | $Q_2$ |
|---|---|---|---|---|---|---|---|---|---|
| Mayo-Lewis | 0.75 | 1.18 | 0.89 | 1.33 | 0.85 | 0.42 | 0.74 | 0.77 | 1.15 |
| Fineman-Ross | 0.82 | 1.21 | 0.99 | 1.22 | 0.83 | 0.68 | 0.89 | 0.77 | 1.15 |
| Kelen-Tüdos | 0.78 | 1.28 | 1.00 | 1.28 | 0.78 | 0.73 | 0.87 | 0.77 | 1.15 |
| Average | 0.78 | 1.22 | 0.96 | 1.28 | 0.82 | 0.61 | 0.83 | 0.77 | 1.15 |

Various internal factors as conjugation, steric hindrance, polarity of the monomer and radical, influence on the monomers reactivity. The *Q-e* parameters were calculated by the Alfray and Price equations based on the values of copolymerization constants. Both p-PGF and AA monomers have different polarities of the double bond (Table 2). The *Q* values for these monomers are significantly different. The degree of conjugation in the double bond with the substituents is also different due to the less value of *Q* for p-PGF. This determines the high propensity of monomers and radicals ending in the p-PGF units to attach more «foreign» monomers under the polymerization conditions.

## *Conclusions*

Thus, a brief review of the studies in the paper shows a possibility to obtain new polymers of the spatially cross-linked structure as a result of radical copolymerization of poly(propylene glycol)fumarate and acrylic acid. The results obtained demonstrate the ability to control the physical-chemical properties of the copolymers based on poly(propylene glycol)fumarate and acrylic acid, induced by the polymer composition, which allows the creation of new materials with a predefined program of behavior.

*The work is done within the frameworks of grant financing of scientific researches for 2018–2020 by Ministry of education and science of the Republic of Kazakhstan subject to the project topic*

*No. AP05131541 «Development of theoretical and practical bases of synthesis of new «intellectual» polymers based on polyethylene-(propylene)glycol fumarate».*

## References

1 Wu Y. Acrylated epoxidized soybean oil as a styrene replacement in a dicyclopentadiene-modified unsaturated polyester resin / Y. Wu, K. Li // Journal of Applied Polymer Science. — 2018. — Vol. 135, No. 19. — P. 46212.

2 Strong A.B. Fundamentals of composites manufacturing: materials, methods and applications, 2nd ed. / A.B. Strong. — Society of Manufacturing Engineers: Dearborn, MI, 2008. — 47 p.

3 Бениг Г.В. Ненасыщенные полиэфиры: строение и свойства / Г.В. Бениг. — М.: Химия, 1968. — 253 с.

4 Седов Л.Н. Модифицирование химической структуры полималеинатов и полифумаратов для регулирования свойств сополимеров на их основе / Л.Н. Седов, Г.М. Авдеева, Е.Г. Зильберман, Н.Ф. Пугачевская, О.И. Савичева // Вестн. техн. и эконом. информации. — 1970. — № 2. — С. 16.

5 Анисимов Ю.Н. Привитая сополимеризация винилацетата с ненасыщенной олигоэфирной смолой и характеристики отвержденных композиций / Ю.Н. Анисимов, Н.А. Вонсович, О.Б. Грехова // ЖПХ. — 1996. — Т. 69, № 2. — С. 312–316.

6 Kamel N.A. Biophysical studies on bone cement composites based on polyester fumarate / N.A. Kamel, T.H. Abou-Aiaad, B.A. Iskander, S.K.H. Khalil, S.H. Mansour, S.L. Abd-El Messieh, K.N. Abd-El-Nour // Journal of applied polymer science. — 2010. — Vol. 116, No. 2. — P. 876–885.

7 Hou L.-D. A review on biodegradable materials for cardiovascular stent application / L.-D. Hou, Z. Li, Y. Pan, M. Sabir, Y.-F. Zheng, L. Li // Frontiers of Materials Science. — 2016. — Vol. 10, No. 3. — P. 238–259.

8 Timmer M.D. In vitro degradation of polymeric networks of poly(propylene fumarate) and the crosslinking macromer poly(propylene fumarate)-diacrylate / M.D. Timmer, C.G. Ambrose, A.G. Mikos // Biomaterials. — 2003. — Vol. 24. — P. 571–577.

9 Manavitehrani I. Biomedical Applications of Biodegradable Polyesters / I. Manavitehrani, A. Fathi, H. Badr, S. Daly, Shirazi A. Negahi, F. Dehghani // Polymers. — 2016 — Vol. 8, No. 1. — P. 20.

10 Патент № 31052. Казахстан. Способ получения ненасыщенных полиэфирных смол на основе пропиленгликоля, фталевого ангидрида и фумаровой кислоты / Буркеев М.Ж., Тажбаев Е.М. и др. Опубл. 16.03.2016.

11 Burkeev M.Zh. Nanocatalytic systems based on poly(ethylene glycol maleate)-acrylamide copolymers / M.Zh. Burkeev, E.M. Tazhbaev, A.K. Kovaleva, G.K. Burkeeva et al. // Russ. J. Appl. Chem. — 2015. — Vol. 88, No. 2. — P. 314–319.

12 Burkeev M.Zh. Thermal destruction of copolymers of polypropylene glycol maleate with acrylic acid / M.Zh. Burkeev, A.Zh. Sarsenbekova, E.M. Tazhbaev // Russ. J. Phys. Chem. A. — 2015. — Vol. 89, No. 12. — P. 2183–2189.

13 Burkeev M.Zh. New polyampholyte polymers based on polypropylene glycol fumarate with acrylic acid and dimethylaminoethyl methacrylate / M.Zh. Burkeev, G.K. Kudaibergen, G.K. Burkeeva et al. // Russ. J. Appl. Chem. — 2018. — Vol. 91, No.7. — P. 1145–1152.

14 Гладышев Г.П. Радикальная полимеризация при глубоких степенях превращения / Г.П. Гладышев, В.А. Попов. — М.: Наука, 1974. — 340 с.

15 Kelen T. Analysis of the linear methods for determining copolymerization reactivity ratios. I. A new improved linear graphic method / T. Kelen, F. Tudos // J. Macromol. Sci. Part A-Pure Appl. Chem. — 1975. — Vol. 9, No. 1. — P. 1–27.

16 Finemann M. Linear method for determining monomer reactivity ratios in copolymerization / M. Finemann, S.D. Ross // J. Polym. Sci. — 1950. — Vol. 5. — P. 259–262.

---

М.Ж. Бүркеев, Г.Қ. Құдайберген, Е.М. Тажбаев, Г.К. Бүркеева,
А.Ж. Сарсенбекова, Я. Граничек, Н.А. Есентаева, А.Н. Болатбай, С.Б. Аукадиева

# Полипропиленгликольфумараттың акрил қышқылымен радикалдық сополимерленудің константалары мен параметрлері

Мақалада алғаш рет диоксан ортасында бастапқы мономер қоспасының әртүрлі мольдік қатынасында полипропиленгликольфумараттың акрил қышқылымен бинарлы радикалды сополимерленуі зерттелген. Сополимерлену реакциясының кинетикасы анықталды. Кинетикалық қисықтар ерітіндідегі акрил қышқылының мольдік мөлшерінің көбейген сайын реакция жылдамдығы мен сорбциялық сыйымдылығы артатыны көрсетілді. Хроматография-масс-спектроскопияны қолдану арқылы синтезделген сополимерлердің құрамы анықталды. Радикалды сополимерленудің константалары мен параметрлері Майо-Льюис, Файнман-Росс және Келен-Тюдоштың интегралды әдісімен есептеледі. Сополимерлену тұрақтыларының негізінде *Q-e* параметрлері Алфрей-Прайс теңдеуі бойынша есептелді. Акрил қышқылының полипропиленгликольфумаратпен сополимерлену кезінде соңғысының төмен реактивтілікпен сипатталатыны анықталды. п-ПГФ-АҚ жүйесіндегі $r_1$ салыстырмалы белсенділігі бірден аз. Бұл п-ПГФ басқа мономерлермен сополимерленуге қабілеті, гомополимерленуге қарағанда, жоғары екендігін көрсетеді. Сополимерлердің қанықпағандығы бастапқы мономер қоспасы құрамындағы полиэтиленгликольфумараттың мөлшеріме тура пропорционалды екендігі көрсетілді. Осылайша, зерттеудің нәтижелері п-ПГФ негізіндегі синтезделген полимерлер жақсы қасиеттерге ие және ғылымның әртүрлі салаларында қолданылуы мүмкін.

*Кілт сөздер:* қанықпаған полиэфирлі шайырлар, полипропиленгликольфумарат, акрил қышқылы, сополимерлену константалары, мономерлер белсенділігі, кинетика, сорбция, сополимерлену.

М.Ж. Буркеев, Г.К. Кудайберген, Е.М. Тажбаев, Г.К. Буркеева,
А.Ж. Сарсенбекова, Я. Граничек, Н.А. Есентаева, А.Н. Болатбай, С.Б. Аукадиева

# Константы и параметры радикальной сополимеризации полипропиленгликольфумарата с акриловой кислотой

В статье впервые исследована бинарная радикальная сополимеризация полипропиленгликольфумарата с акриловой кислотой в среде диоксана при различных мольных соотношениях исходной мономерной смеси. Изучена кинетика реакции сополимеризации. Кинетические кривые показывают, что с повышением мольной доли акриловой кислоты в растворе увеличиваются скорость реакции и сорбционная способность сополимеров. С применением хромато-масс-спектроскопии определен состав синтезированных сополимеров. Интегральным методом Майо-Льюиса, Файнмана-Росса и Келена-Тюдоша рассчитаны константы и параметры радикальной сополимеризации. На основании констант сополимеразации по уравнению Алфрея-Прайса рассчитаны параметры *Q-e*. Установлено, что при сополимеризации акриловой кислоты с полипропиленгликольфумаратом последний характеризуется меньшей реакционной способностью. Относительная активность $r_1$ в системе п-ПГФ-АК меньше единицы. Это говорит о том, что способность п-ПГФ к сополимеризации с другими мономерами выше, чем к гомополимеризации. Показано, что степень ненасыщенности сополимеров прямо пропорциональна содержанию полипропиленгликольфумарата в составе исходной мономерной смеси. Таким образом, результаты этого исследования показали, что синтезированные полимеры на основе п-ПГФ имеют хорошие характеристики и могут быть использованы в различных областях науки.

*Ключевые слова:* ненасыщенные полиэфирные смолы, полипропиленгликольфумарат, акриловая кислота, константы сополимеризации, активность мономеров, кинетика, сорбция, сополимеризация.

## References

1 Wu, Y., Li, K. (2018). Acrylated epoxidized soybean oil as a styrene replacement in a dicyclopentadiene-modified unsaturated polyester resin. *Journal of Applied Polymer Science, 135*(19), 46212.

2 Strong, A.B. (2008). *Fundamentals of composites manufacturing: materials, methods and applications, 2nd ed.* Society of Manufacturing Engineers: Dearborn, MI.

3 Benig, G.V. (1968). *Nenasyshchennye poliefiry: stroienie i svoistva [Unsaturated polyesters: structure and properties].* Moscow: Khimiia [in Russian].

4 Sedov, L.N., Avdeyeva, G.M., Zil'berman, Ye.G., Pugachevskaya, N.F., & Savicheva, O.I. (1970). Modifitsirovanie khimicheskoi struktury polimaleinatov i polifumaratov dlia rehulirovaniia svoistv sopolimerov na ikh osnove [Modification of the chemical structure of polymaleinates and polyfumarates to regulate the properties of copolymers based on them]. *Vestnik tekhnicheskoi i ekonomicheskoi informatsii — Technical and Economic Information Bulletin*, *2*, 16 [in Russian].

5 Anisimov, Yu.N., Vonsovich, N.A., & Grekhova, O.B. (1996). Privitaia sopolimerizatsiia vinilatsetata s nenasyshchennoi olihoefirnoi smoloi i kharakteristiki otverzhdennykh kompozitsii [Graft copolymerization of vinyl acetate with an unsaturated polyether resin and characteristics of cured compositions]. *Zhurnal prikladnoi khimii — Journal of Applied Chemistry*, *69*, 2, 312–316 [in Russian].

6 Kamel, N.A., Abou-Aiaad, T.H., Iskander, B.A., Khalil, S.K.H., Mansour, S.H., Abd-El-Messieh, S.L., & Abd-El-Nour, K.N. (2010). Biophysical studies on bone cement composites based on polyester fumarate. *Journal of applied polymer science, 116*(2), 876–885.

7 Hou, L.-D., Li, Z., Pan, Y., Sabir, M., Zheng, Y.-F., & Li, L. (2016). A review on biodegradable materials for cardiovascular stent application. *Frontiers of Materials Science, 10*(3), 238–259.

8 Timmer, M.D., Ambrose, C.G., & Mikos, A.G. (2003). In vitro degradation of polymeric networks of poly(propylene fumarate) and the crosslinking macromer poly(propylene fumarate)-diacrylate. *Biomaterials, 24,* 571–577.

9 Manavitehrani, I., Fathi, A., Badr, H., Daly, S., Negahi Shirazi, A., & Dehghani, F. (2016). Biomedical Applications of Biodegradable Polyesters. *Polymers, 8(1),* 20.

10 Burkeyev, M.Zh., & Tazhbayev, Ye.M. et. al. (2016). Sposob polucheniia nenasyshchennykh poliefirnykh smol na osnove propilenhlikolia, ftalevoho anhidrida i fumarovoi kisloty [Method for the preparation of unsaturated polyester resins based on propylene glycol, phthalic anhydride and fumaric acid]. *Patent No. 31052. Kazakhstan.* Published 16.03.2016 [in Russian].

11 Burkeev, M.Zh., Tazhbaev, E.M., Kovaleva, A.K., & Burkeeva, G.K. et al. (2015). Nanocatalytic systems based on poly(ethylene glycol maleate)-acrylamide copolymers. *Russ. J. Appl. Chem., 88*(2), 314–319.

12 Burkeev, M.Zh., Sarsenbekova, A.Zh., & Tazhbaev, E.M. (2015). Thermal destruction of copolymers of polypropylene glycol maleate with acrylic acid. *Russ. J. Phys. Chem. A., 89*(12), 2183–2189.

13 Burkeev, M.Zh., Kudaibergen, G.K., & Burkeeva, G.K. et al. (2018). New Polyampholyte polymers based on polypropylene glycol fumarate with acrylic acid and dimethylaminoethyl methacrylate. *Russ. J. Appl. Chem., 91*(7), 1145–1152.

14 Gladyshev, G.P., & Popov, V.A. (1974). *Radikalnaia polimerizatsiia pri hlubokikh stepeniakh prevrashcheniia [Radical polymerization with deep degrees of conversion]*. Moscow: Nauka [in Russian].

15 Kelen, T., & Tudos, F. (1975). Analysis of the linear methods for determining copolymerization reactivity ratios. I. A new improved linear graphic method. *J. Macromol. Sci. Part A – Pure Appl. Chem., 9*(1), 1–27.

16 Finemann, M., & Ross, S.D. (1950). Linear method for determining monomer reactivity ratios in copolymerization. *J. Polym. Sci., 5,* 259–262.

DOI: 10.31489/2019Ch1/32-38

UDC 541.64

M.Zh. Burkeev[1], G.K. Kudaibergen[1], Ye.M. Tazhbayev[1],
J. Hranicek[2], G.K. Burkeyeva[1], A.Zh. Sarsenbekova[1]

*[1]Ye.A. Buketov Karaganda State University, Kazakhstan;*
*[2]Charles University, Prague, Czech Republic*
*(E-mail: gulshahar90@mail.ru)*

# Synthesis and investigation of copolymer properties on the basis of poly(ethylene glycol)fumarate and methacrylic acid

In the result of reaction of free radical copolymerization of poly(ethylene glycol)fumarate and methacrylic acid insoluble copolymers of different weight composition were obtained. Influence of ionic strength of the solution, organic solvents on the level of swelling of synthesized copolymers was studied. According to the result of the research, it is possible to make the conclusion that ratio of monomeric units in copolymer, as well as concentration of low-molecular components in the solution significantly influence the perceptivity of polymeric gels to the presence of low-molecular salts (NaCl and $CaCl_2$), organic solvents (DMSO, DMF, and ethanol). When the share of methacrylic acid is decreased in copolymer, the perceptivity of gels to admixtures of low-molecular salts and organic solvents is decreased. This is conditioned both by increase of the content of carboxyl groups in the macrochain, and density decrease of polymer network. Observed influence of ionic strength confirms contribution of both electrostatic and hydrophobic interactions in process of swelling-collapse of samples examined. It is shown that changing the nature of comonomer, we can obtain the hydrogels with the ability to turgesce or collapse at change of ionic strength, thermodynamic quality of the solution, and with variation of ratio of comonomer units it is possible to regulate the intervals of swelling and compression of polymer networks. As well, results of X-ray energy-dispersive microanalysis show that examined polymeric systems based on copolymers p-EGF — MAA might be in demand as sorbent agents in purification and beneficiation technologies.

*Keywords:* poly(ethylene glycol)fumarate, methacrylic acid, copolymer, hydrogel, polycondensation, swelling, collapse, unsaturated polyester, free radical copolymerization.

## *Introduction*

New sphere studying the polymeric materials, whose properties might be changed depending on parameters of environment, appeared and started developing relatively recently. This new generation of materials is called «smart» or «intellectual» polymers. Distinctive features of «intellectual» polymers are in their additional functional abilities, which are out of the properties, defined by the structure of material [1]. Such materials play double or triple role — material itself with necessary characteristics, indicator for external influence, and, in some cases, device, «programmed» for definite behavior. Issue of synthesis, selection of initial reagents at obtaining of such polymer systems and their application, is especially urgent. Perspective reagents for development of intellectual systems are unsaturated polyesters, which are the products of polycondensation of polyatomic alcohols and carboxylic acids. Main feature of unsaturated polyesters is in ability to undergo easily the reaction of copolymerization (solidify) with vinyl monomers at room temperature without application of high pressures, without the release of volatile and other by-products [2–4]. Due to this, it becomes possible to apply the unsaturated polyesters as one of reagents at synthesis of «intellectual» polymers, which are widely applied in medicine, pharmacy, biotechnology, nanotechnology and lots of other branches of human life.

Basing upon the historical data, first time the concept of «copolymerization» of unsaturated polyesters was adopted by German scientist Benig [1]. Thus, multiple scientific works, patents, of both present and past periods, are devoted to the study of copolymerization of unsaturated polyesters with vinyl acetate, styrole and methylmetacrylate, simple and compound allyl ethers [2–4]. Analysis of literary sources showed the absence of information on free radical copolymerization of unsaturated polyesters with unsaturated carboxylic acids.

Earlier we obtained and examined the polymeric hydrogels based on polyglycol maleates with high sorbing properties. Results we obtained demonstrate the perspective of their application as moist sorbent agents in crop production [5] and as effective nanocatalysts [6]. However, with the aim of comprehensive enchanced studying of this unique valuable class, we considered interesting to continue the researches in this direction.

In connection with the abovementioned, this work is devoted to the synthesis and study of physical and chemical properties of new polymeric hydrogels based on unsaturated polyester — poly(ethylene glycol) fumarate (p-EGF) solidified with methacrylic acid (MAA). We carried the analysis of sorbent properties of synthesized samples in water and salt solutions of low-molecular salts (LMS), organic solvents at change of their concentration and basic composition of polymeric network of copolymer.

## *Experimental*

Initial p-EGF was obtained by reaction of polycondensation of fumaric acid and ethylene glycol at the temperature of 403–453 K [7, 8]. Reaction process was controlled by determination of an acid index and by volume of water released. Synthesized polyester is resinous low-melting substance of light-yellow color, soluble in chloroform and dioxane. The resin obtained was separated from the initial monomers by multiple rinsing with acetone.

Molecular mass of p-EGF was established by methods of light-scattering with nephelometer 2100 AN of NACH brand and method of admeasurements of end groups, which amounts 2500 amu [9]. Free radical copolymerization of p-EGF with MAA was carried in the solution of dioxane at different initial mass ratio of comonomers, in the presence of benzoyl peroxide (BP) as initiator, at temperature of 333 K [7, 9]. Synthesized polymers, to separate them from the residuals of unreacted monomers, were multiple rinsed with dioxane and dried with vacuum till the constant mass. Compositions of copolymers obtained were determined with potentiometric titration and according to the residual quantity of monomers by method of chromato-mass spectroscopy with Agilent 7890A mass-selective detector Agilent 5975C [7, 9–11].

Equilibrial level of swelling of hydrogels was determined by gravimetric method. Level of swelling of samples (α) was calculated as the ratio of mass of turgid hydrogel in point of equilibrial swelling to its initial mass in dry condition [1, 5, 6]. IR-spectra of samples were registered in pills with KBr with spectrometer FSM 1201. Electronic microscopic study was held with raster electron microscope (REM) MIRA 3 of TESCAN brand. Studies were carried at accelerating potential 20 kV [11].

## *Results and discussions*

High-turgid polymeric hydrogels are the system that easily react the changes of external environment. Conduct of such hydrogels in solutions of low-molecular salts is studied in details, in particular, the ability of hydrogels to make the redistribution of their concentrations [1, 5, 6, 12]. Researches of copolymers of poly(ethylene glycol) fumarate show that the latter are sensible to the change of environment. This suggests the perceptibility of studied systems to ions of low-molecular salts and organic solvents.

At reaction of p-EGF with MAA in presence of initiator of polymerization reaction, their joint polymerization happens, which leads to the formation of non-fusible polymer of three-dimensionally cross-linked structure [1, 7]. Reaction of free radical copolymerization of p-EGF with MAA proceeds under the following scheme presented in Figure 1.

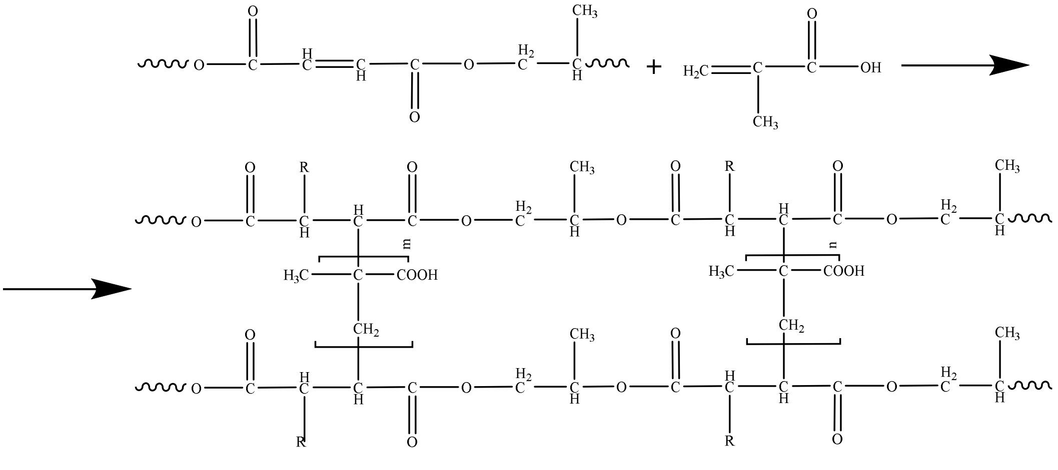

Figure 1. Reaction scheme of free radical copolymerization p-EGF with MAA

Results for copolymerization of p-EGF with MAA are shown in Table. Yield of copolymer amounts 73 to 87 %.

As we see in Table, at any ratio of initial mixture, copolymer is beneficiated with links of MAA, at that yield and level of swelling is decreased progressively as reduction of the latter.

Table

**Dependence of composition of copolymers on composition of initial mixture at free radical copolymerization of p-EGF ($M_1$) with MAA ($M_2$) [BP] = 8 mole/$m^3$, T = 333 K**

| Composition of initial mixture, mass % | | Composition of copolymer, mass % | | Yield, % |
|---|---|---|---|---|
| $M_1$ | $M_2$ | $m_1$ | $m_2$ | |
| 10.03 | 89.97 | 6.65 | 93.35 | 87.30 |
| 15.08 | 84.92 | 10.23 | 89.77 | 80.73 |
| 25.07 | 74.93 | 19.25 | 80.75 | 75.07 |
| 50.05 | 49.95 | 42.09 | 57.91 | 72.52 |

Copolymers were identified according to data of IR-spectra in accordance with the Figure 2. Lines, describing the range 1550 ~ 1620 $cm^{-1}$ are related to the link C = O. At the same time, absorption bands in IR-spectrum copolymers p-EGF-MAA in 1758 ~ 1763 $cm^{-1}$ and 2994 ~ 2997 $cm^{-1}$ characterize the links C=O and $-CH_2$ respectively, and peaks at 1184 ~ 1190 $cm^{-1}$ are peculiar for COC — link. Besides, absorption bands at 1452 ~ 1457 $cm^{-1}$ and 1382 ~ 1389 $cm^{-1}$ conform to link $-CH(CH_2)$.

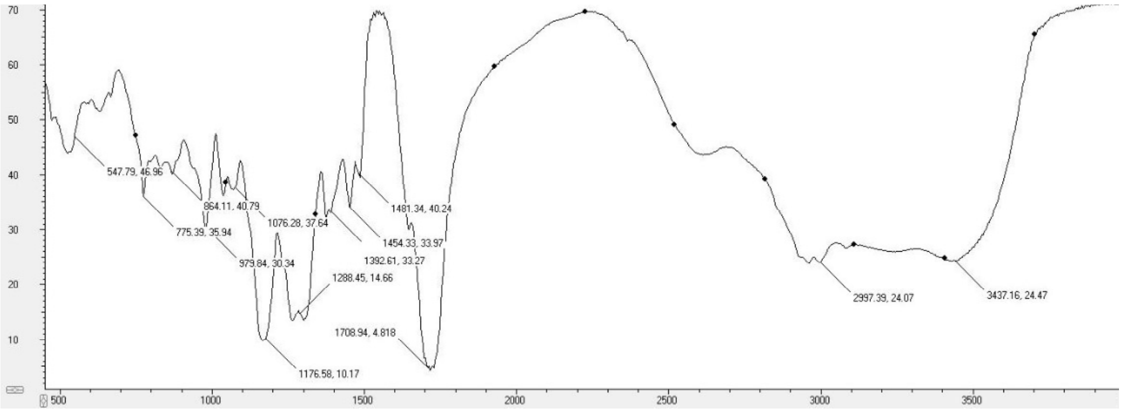

Figure 2. IR-spectrum of p-EGF-MAA

Literature [12] shows that presence of low-molecular component in the solution may cause both swelling, and collapse of polymeric network. According to [12], addition of low-molecular salt influences significantly the polyelectrolytic gels causing the shielding of effects related to the state of charge of the network. Basing upon abovementioned, we can suggest that nature of reaction of linked polymer with ions of mono- and polyvalent salts depends on its chemical composition. Figures 3, 4 show the experimental data of dependence of level of swelling of synthesized samples on concentration of NaCl and $CaCl_2$, respectively.

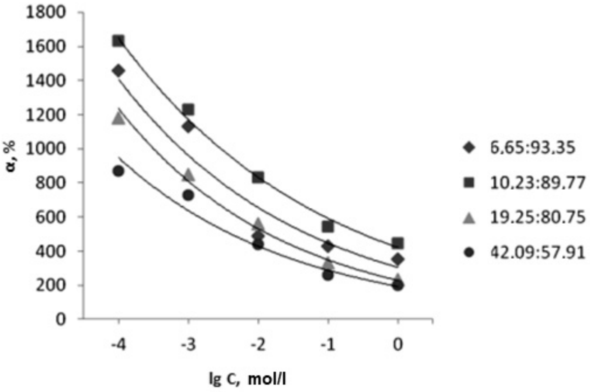

Figure 3. Influence of NaCl salt concentration on level of swelling of copolymers p-EGF-MAA

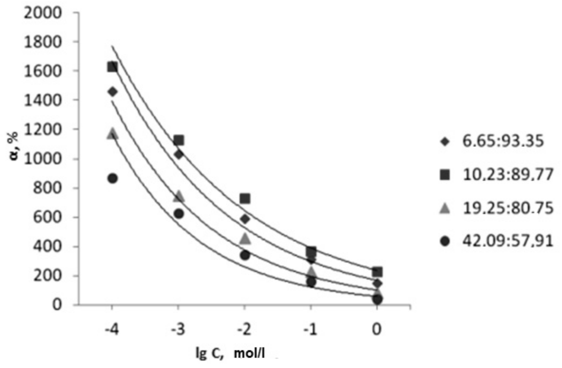

Figure 4. Influence of $CaCl_2$ salt concentration on level of swelling of copolymers p-EGF-MAA

Thus, at adding of low-molecular salt NaCl to the external solution, dimensions of samples of polymeric network are reduced to some minimal value (Fig. 3). According to analysis of hydrogel properties, case of chemical contraction may be implemented at suppression of LMS of electric attraction of like-charged groups. From this viewpoint, such conduct of samples tested in LMS solution is explained by the fact that dependence of level of swelling on salt concentration is subject to polyelectrolytic mode [1, 5, 6, 12].

With concentration increase of low-molecular compositions, we observe the collapse of copolymers tested. It should be emphasized that according to the results obtained, ratio of monomeric units in copolymers to the presence of low-molecular salts influences the conduct of hydrogels. Thus, with increase of share of MAA in copolymers, sensibility of gels to salts admixtures is increased, and transition is observed at higher values of salts.

As continuation of research, we examined the influence of bivalent salt $CaCl_2$ on conduct of hydrogels of p-EGF-MAA. Figure 4 shows the experimental data for swelling in presence of bivalent salt. Comparing these results with the experimental studies of influence of monovalent salt, we can note the fact that curves of dependence of swelling of copolymers tested in the presence of $CaCl_2$ and NaCl are of similar nature. It should be noted that decrease of sorption capacity of hydrogels is observed at lesser concentrations of bivalent salt. This might be related to the number of reasons: first, bivalent ions are stronger attracted by oppositely charged groups of the network, compared to monovalent ones; second, bivalent ions may neutralize the charge of large number of opposed-charged ions inside the network [5, 6]. Experimental data we obtained are coherent with literature data [12].

Considering the abovementioned, basing upon the widely known theoretical principles and processes, peculiar for polyelectrolytic gels, it seemed interesting to study the microstructure of sample of p-EGF-MAA 10.23:89.77 mas.%. With that in mind, electronic and microscopic studies of turgid samples in water and salt solutions of NaCl and $CaCl_2$ were carried out. Results of the research are shown in Figure 5.

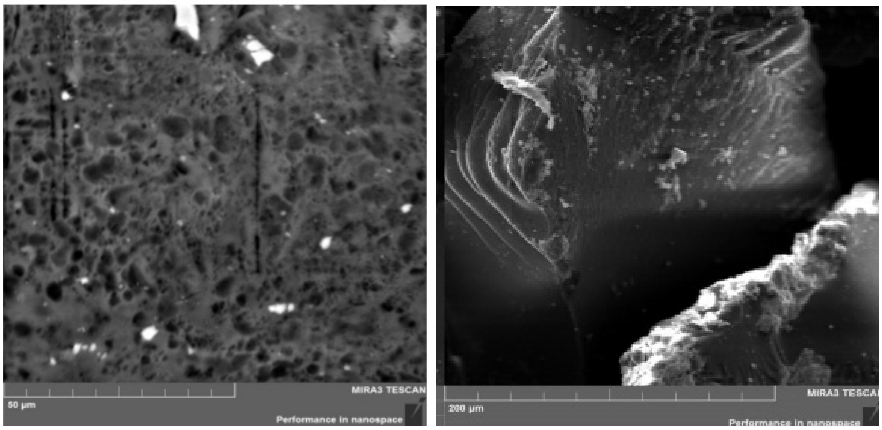

10.23:89.77 mas.% NaCl (at the left) and $CaCl_2$ (at the right)

Figure 5. Electronic and microscopic figures of p-EGF-MAA

To confirm the presence of ions of $Ca^{2+}$ we carried out the X-ray energy-dispersive microanalysis X–Act (Oxford Instruments) of copolymer p-EGF-MAA 10.23:89.77 mas.%. This microanalysis allows detecting locally the elemental composition on the surface of the sample (Fig. 6). Analysis was carried out by the method of mapping of sample surface. At detection, it was considered that the test was carried with carbon adhesive tape, and carbon content was not considered. At imposition of allocation maps of chemical elements, the presence of elements composing this microstructure was obtained.

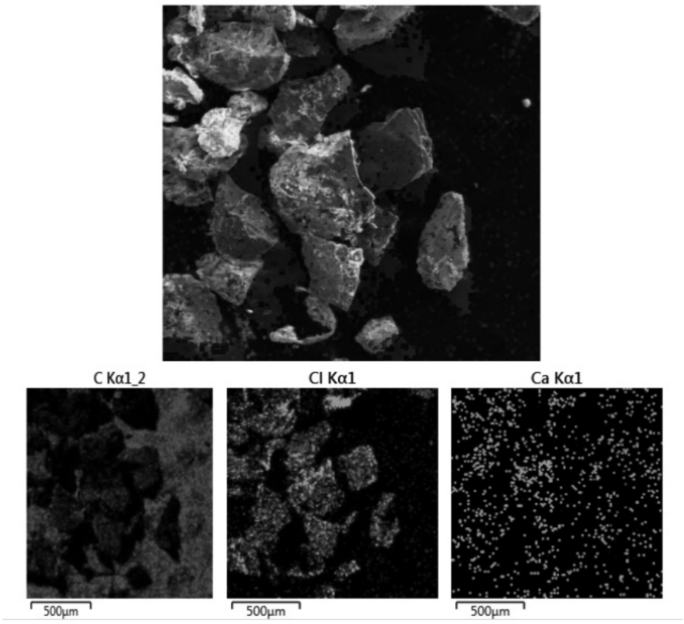

Figure 6. Figure of secondary electrons of copolymer p-EGF-MAA 10.23:89.77 mas.% with ions of $CaCl_2$ salt and mapping in this part

Results of X-ray energy-dispersive microanalysis of the sample fully confirm the composition of the product, and distribution of chemical elements in microstructure confirm the presence of such elements as carbon, chlorine and calcium.

In continuation of researches, to obtain the more aggregate figure of influence of different factors of environment on sorbing ability of samples tested, the influence of organic solvents on level of swelling of p-EGF-MAA with composition of 10.23:89.77 mas.% was studied. As organic component, dimethylformamide (DMF), dimethylsulfoxide (DMSO) and ethanol were selected; their content if the mixture with water varied from 0.1 till 1.0 volume ratios ($n_0$). Selection of these solvents was based upon the difference in their polarity.

At addition to environment, being the polymer turgid in water, among organic solvents gradual reduction of samples dimensions is observed, which is the result of deterioration of thermodynamic quality related to the presence of solvents [1, 5, 12]. It shall be noted that function $\alpha(n_0)$ is not changed in jerks, thus, this process cannot be examined as phase change. As well, it shall be noted that the nature of organic solvents influences the type of influential curves. Thus, hydrogels become most globular in ethanole, compared to the systems DMF–water, DMSO–water. These phenomena might be explained by the volume of polarity and permittivity of examined organic components [12].

## *Conclusions*

Thus, the conclusion might be made that possibilities of control of physical and chemical properties of polymers based on poly(ethyleneglycol) fumarate, demonstrated in the thesis, allow to develop new polymeric materials of polyfunctional destination with preset conduct program. Besides, considering the results of X-ray energy-dispersive microanalysis, we can make a conclusion that tested systems based on copolymer p-EGF might be in demand as sorbents in purification and beneficiation technologies.

*The work is done within the frameworks of grant financing of scientific researches for 2018–2020 by Ministry of education and science of the Republic of Kazakhstan subject to the project topic*

*No. AP05131541 «Development of theoretical and practical bases for the synthesis of new «intelligent» polymers based on polyethylene-(propylene)glycol fumarate».*

## References

1 Burkeev M. Zh. New Polyampholyte polymers based on polypropylene glycol fumarate with acrylic acid and dimethylaminoethyl methacrylate / M.Zh. Burkeev, G.K. Kudaibergen, G.K. Burkeeva et al. // Russ. J. Appl. Chem. — 2018. — Vol. 91, No. 7. — P. 1145–1152.

2 Бениг Г.В. Ненасыщенные полиэфиры: строение и свойства / Г.В. Бениг. — М.: Химия, 1968. — 253 с.

3 Пот У. Полиэфиры и алкидные смолы: монография / У. Пот. — М.: КТС, 2009. — 380 с.

4 Коляго Г.Г. Материалы на основе ненасыщенных полиэфиров / Г.Г. Коляго, В.А. Струк. — Минск: Наука и техника, 1990. — 143 с.

5 Burkeev M.Zh. Effect of external factors on the swelling of hydrogels based on poly(ethylene glycol)maleate with some vinyl monomers / M.Zh. Burkeev, E.M. Tazhbaev, G.K. Burkeeva et al. // Russ. J. Appl. Chem. — 2013. — Vol. 86, No. 1. — P. 63–68.

6 Burkeev M.Zh. Nanocatalytic systems based on poly(ethylene glycol maleate) — acrylamide copolymers / M.Zh. Burkeev, E.M. Tazhbaev, G.K. Burkeeva, A.K. Kovaleva // Russ. J. Appl. Chem. — 2015. — Vol. 88, No. 2. — P. 314–319.

7 Kudaibergen G.K. Constants and parameters of radical copolymerization of poly(ethylene glycol fumarate) with acrylic acid / G.K. Kudaibergen, G.K. Burkeeva et al. // Chemical journal of Kazakhstan. — Vol. 61, No. 1. — 2018. — P. 215–222.

8 Патент № 31052. Казахстан. Способ получения ненасыщенных полиэфирных смол на основе пропиленгликоля, фталевого ангидрида и фумаровой кислоты / Буркеев М.Ж., Тажбаев Е.М. и др. Опубл. 16.03.2016.

9 Burkeev M.Zh. The number average and mass average molecular masses of polyethylene(propylene)glycol fumarates / M.Zh. Burkeev, G. Kudaibergen, G.K. Burkeeva et al. // Bulletin of the Karaganda University. Chemistry series. — 2018. — Vol. 90, No. 2. — P. 17–22.

10 Гольберт К.А. Введение в газовую хроматографию / К.А. Гольберт, М.С. Вигдергауз. — 3-е изд., перераб. и доп. — М.: Химия, 1990. — 352 с.

11 Золотов Ю.А. Физико-химические методы анализа / Ю.А. Золотов, Е.Н. Дорохова, В.И. Фадеева. — М.: Высш. шк., 2000. — 356 с.

12 Филиппова О.Е. «Восприимчивые» полимерные гели / О.Е. Филиппова // Высокомолекулярные соединения. — 2000. — Т. 42, № 12. — С. 2328–2352.

М.Ж. Бүркеев, Г.Қ. Құдайберген, Е.М. Тажбаев,
Я. Граничек, Г.К. Бүркеева, А.Ж. Сарсенбекова

# Полиэтиленгликольфумараттың метакрил қышқылы негізіндегі сополимерлердің синтезі мен зерттелуі

Полиэтиленгликольфумарат пен метакрил қышқылының радикалды сополимерлену реакциясымен әртүрлі массалы қатынастағы ерімейтін сополимерлер алынды. Синтезделген сополимерлердің ісіну дәрежесіне ерітіндінің иондық күші, органикалық еріткіштердің әсері зерттелді. Зерттеу нәтижесі бойынша полимерлі гельдердің сезімталдығына төмен молекулалы тұздардың (NaCl пен $CaCl_2$), органикалық еріткіштер (ДМСО, ДМФА, этанол), сополимердегі буындардың қатынасы, сонымен қатар ерітіндегі төмен компоненттердің концентрациясы айтарлықтай әсер етеді. Сополимердегі метакрил қышқылының мөлшерінің азаюы гельдің төменмолекулалы тұздар мен органикалық еріткіштерге сезімталдығы төмендейді. Бұл макротізбектегі карбоксил топтардың көбеюі мен полимердің тордың тығыздығының азаюымен негізделген. Ионды күшінің бақыланатын әсері зерттеліп жатқан сынамалардың ісінуі-коллапс үрдісі кезінде гидрофобтық және электростатикалық өзара әрекеттесулердің үлесін растайды. Сомономердің табиғатын өзгерте отырып, иондық күш, ерітіндінің термодинамикалық қасиеттерін, ісінуге немесе коллапстауға қабілетті гидрогельдерді алуға болатындығы, сонымен қатар сономердің буындарының қатынасын өзгерте отырып, полимерлі торлардың ісіну мен сығылу интервалдарын реттеуге болатындығы көрсетілді. Ренгтгенді энергодисперсионды микросараптама нәтижелері негізінде п-ЭГФ – МАҚ негізіндегі сополимерлерді полимерлі жүйелер сорбенттер ретінде тазартқыш және байыту технологияларында қолданыла алады.

*Кілт сөздер:* полиэтиленгликольфумарат, метакрил қышқылы, сополимер, гидрогель, поликонденсация, ісіну, коллапс, қанықпаған полиэфирлі шайыр, радикалды сополимерлену.

М.Ж. Буркеев, Г.К. Кудайберген, Е.М. Тажбаев,
Я. Граничек, Г.К. Буркеева, А.Ж. Сарсенбекова

# Синтез и исследование свойств сополимеров на основе полиэтиленгликольфумарата и метакриловой кислоты

Реакцией радикальной сополимеризации полиэтиленгликольфумарата и метакриловой кислоты получены нерастворимые сополимеры различного массового состава. Исследовано влияние ионной силы раствора, органических растворителей на степень набухания синтезированных сополимеров. По результатам исследований можно сделать вывод, что на восприимчивость полимерных гелей к присутствию низкомолекулярных солей (NaCl и $CaCl_2$), органических растворителей (ДМСО, ДМФА, этанол) существенно влияют соотношения мономерных звеньев в сополимере, а также концентрация низкомолекулярных компонентов в растворе. С уменьшением в сополимере доли метакриловой кислоты понижается чувствительность гелей к добавкам низкомолекулярных солей, органических растворителей. Это обусловлено как повышением содержания карбоксильных групп в макроцепи, так и снижением плотности полимерной сетки. Наблюдаемое влияние ионной силы подтверждает вклад как электростатических, так и гидрофобных взаимодействий в процессе набухания-коллапса исследуемых образцов. Показано, что, изменяя природу сомономера, можно получать гидрогели, способные набухать или коллапсировать при изменении ионной силы, термодинамического качества раствора, а варьируя соотношение звеньев сомономеров, можно регулировать интервалы набухания и сжатия полимерных сеток. Также из результатов рентгеновского энергодисперсионного микроанализа следует, что исследуемые полимерные системы на основе сополимеров п-ЭГФ – МАК могут быть востребованы в качестве сорбентов в очистительных и обогатительных технологиях.

*Ключевые слова:* полиэтиленгликольфумарат, метакриловая кислота, сополимер, гидрогель, поликонденсация, набухание, коллапс, ненасыщенная полиэфирная смола, радикальная сополимеризация.

## References

1 Burkeev, M.Zh., Kudaibergen, G.K., & Burkeeva, G.K. et al. (2018). New Polyampholyte polymers based on polypropylene glycol fumarate with acrylic acid and dimethylaminoethyl methacrylate. *Russ. J. Appl. Chem., 91(7),* 1145–1152.

2 Benig, G.V. (1968). *Nenasyshchennye poliefiry: stroienie i svoistva [Unsaturated polyesters: structure and properties].* Moscow: Khimiia [in Russian].

3 Pot, U. (2009). *Poliefiry i alkidnye smoly [Polyesters and alkyd resins].* Moscow: KTC [in Russian].

4 Kolyago, G.G., & Struk, V.A. (1990). *Materialy na osnove nenasyshchennykh poliefirov [Materials based on unsaturated polyesters].* Minsk: Nauka i tekhnika [in Russian].

5 Burkeev, M.Zh., Tazhbaev, E.M., & Burkeeva, G.K. et al. (2013). Effect of external Factors on the swelling of hydrogels based on poly(ethylene glycol)maleate with some vinyl monomers. *Russ. J. Appl. Chem., 86*(1), 63–68.

6 Burkeev, M.Zh., Tazhbaev, E.M., Kovaleva, A.K., & Burkeeva, G.K. et al. (2015). Nanocatalytic systems based on poly(ethylene glycol maleate)acrylamide copolymers. *Russ. J. Appl. Chem., 88*(2), 314–319.

7 Kudaibergen, G.K., & Burkeeva, G.K. et al. (2018). Constants and parameters of radical copolymerization of poly(ethylene glycol fumarate) with acrylic acid. *Chemical journal of Kazakhstan, 61*(1), 215–222.

8 Burkeyev M.Zh., & Tazhbayev Ye.M. et. al. (2016). Sposob polucheniia nenasyshchennykh poliefirnykh smol na osnove propilenhlikolia, ftalevoho anhidrida i fumarovoi kisloty [Method for the preparation of unsaturated polyester resins based on propylene glycol, phthalic anhydride and fumaric acid]. *Patent № 31052. Kazakhstan.* Published 16.03.2016 [in Russian].

9 Burkeev, M.Zh., Kudaibergen, G., & Burkeeva, G.K. et al. (2018). The number average and mass average molecular masses of polyethylene(propylene)glycol fumarates. *Bulletin of the Karaganda University. Chemistry series, 90*(2), 17–22.

10 Golbert, K.A., & Vigdergauz, M.S. (1990). *Vvedenie v hazovuiu khromatohrafiiu [Introduction to Gas Chromatography].* Moscow: Khimiia [in Russian].

11 Zolotov, Yu.A., Dorokhova, E.N., & Fadeeva, V.I. (2000). *Fiziko-khimicheskie metody analiza [Physico-chemical methods of analysis].* Moscow: Vysshaia shkola [in Russian].

12 Filippova, O.E. (2000). «Vospriimchivye» polimernye heli [Susceptible Polymer Gels]. *Vysokomolekulyarnye soedineniia — Polymer Science, 42*(12), 2328–2352 [in Russian].

DOI: 10.31489/2019Ch1/39-47

UDC 547.1

L.K. Salkeyeva[1], P. Vojtíšek[2], Ye.V. Minayeva[1], L.M. Sugralina[1],
A.V. Omasheva[1], A.A. Muratbekova[1], A.K. Salkeyeva[3], K.I. Sadykov[1]

*[1]Ye.A. Buketov Karaganda State University, Kazakhstan;*
*[2]Charles University, Prague, Czech Republic;*
*[3]Karaganda State Technical University, Kazakhstan*
*(E-mail: lsalkeeva@mail.ru)*

# Investigation of interaction between tert.-butyl diamidophosphites and alkyl halides

In this article the interaction of tert.-butyldiamidophosphites with various alkyl halides with a mobile halogen atom, in particular, allyl chloride, benzyl chloride and bromomalonic ester under various conditions was studied. It was established that reactions with benzyl chloride and allyl chloride proceeded according to the classical Arbuzov reaction scheme by quartering the phosphorus atom with the formation of the corresponding benzyl and allyl amidophosphonates as the main reaction products. It was stated that the reaction proceeded ambiguously with the formation of various products mixture. This is due to the structure of the intermediate «quasiphosphonium», which depends on the nature of the solvent: the ionic form predominates in polar solvents, and the pentavalent form predominates in non-polar solvents. In addition it was proved that the direction of the reaction depended on the reaction conditions, namely, the temperature and the solvent nature. It was shown that the reaction with bromomalonic ester proceeded through the initial protonation of the phosphorus atom with the formation of a quasiphosphonium compound, the decomposition of which led to the corresponding tetraethyldiamidophosphorous acid.

*Keywords:* ester amides of P (III) acids, Ester amides of P (III) acids, tert-butyldiamidophosphites, alkyl halides, bromomalonic ester, bromomalonic ester.

Significant advances in the practical use of phosphorus organic derivatives and the important role of phosphorus compounds in vital processes are the basis of a large and undying interest in the chemistry of these compounds. In recent years applied chemistry of organophosphorus compounds was significantly developed, a huge experimental material was accumulated, systematized and summarized in many reviews and monographs [1–4]. At the same time theoretical researches were also developed but a theoretical approach to problems of the reaction mechanism and reactivity of organophosphorus compounds, especially for derivatives of trivalent phosphorus, turned out to be more difficult, and the results were less significant compared with data for objects of classical organic chemistry.

One of the most important and interesting reactions in organophosphorus compounds chemistry was and remains the Arbuzov reaction, or the Arbuzov rearrangement, which had a great influence on the formation and development of the chemistry of organophosphorus compounds.

Ester amides of acids P(III) are of particular interest in a series of compounds of trivalent phosphorus. Due to the presence of the P-N moiety in the molecule composition they possess two nucleophilic centers, namely, a phosphorus atom and a nitrogen atom with respect to electrophilic compounds. The phosphorus atom was believed to be the nucleophilic center in the reactions of ester amides of P(III) acids with alkyl halides occurring with an increase in the valence of the phosphorus atom, and these reactions proceed according to the Arbuzov scheme through formation of the intermediate quasiphosphonium compound. In reactions with H-acids, which occur without changing the valence of the phosphorus atom, according to the scheme of replacing the amide group of the ester amide P(III) with an acid residue, the nitrogen atom of the system plays the role of a nucleophilic center. However a sharp discussion about the mechanism of these reactions is conducted in recent years.

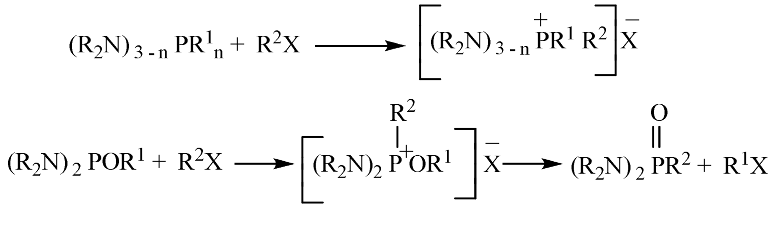

$$(R_2N)_{3-n}PR^1_n + R^2X \longrightarrow \left[(R_2N)_{3-n}\overset{+}{P}R^1R^2\right]\overset{-}{X}$$

$$(R_2N)_2POR^1 + R^2X \longrightarrow \left[(R_2N)_2\overset{R^2}{\overset{|}{\overset{+}{P}}}OR^1\right]\overset{-}{X} \longrightarrow (R_2N)_2\overset{O}{\overset{\|}{P}}R^2 + R^1X$$

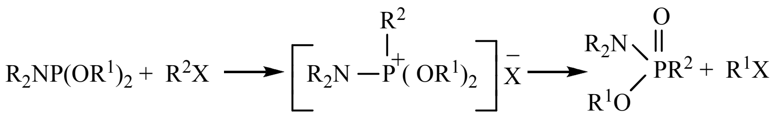

From the standpoint of chemical behavior tert.-butyl esters of amidophosphorous acids have not been practically studied before. Obviously this is due to the fact that according to the literature the tert.-butyl esters of phosphorous acid are thermally unstable compounds which when heated are easily dealkylated with the release of isobutylene. Thus tri-tert.-butylphosphite $(t\text{-}BuO)_3P$ decomposes forming di-tert.-butylphosphite $(t\text{-}BuO)_2PHO$ when heated above 50 °C, diethyl tert.-butylphosphite $(EtO)_2POBu\text{-}t$ decomposes when heated above 70 °C [5]. The cause of the thermal instability of the tert.-butyl esters was not established. It was shown that the second stage of the reaction of $(EtO)_2POBu\text{-}t$ with acrylonitrile and methyl iodide proceeded mainly with the participation of the tert.-butyl radical via the $S_N1$ mechanism (route 1) or E2 (route 2) [6].

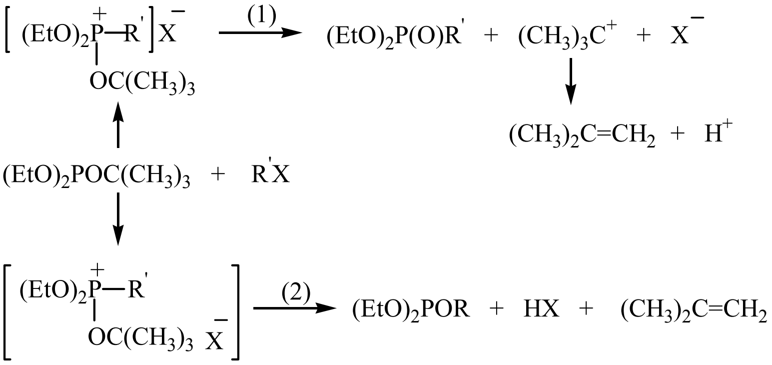

In order to study the issues of thermal stability, reactivity, and also searching for new cost-effective and experimentally convenient methods for synthesizing compounds with a P–C bond we developed effective methods for synthesizing tert.-butyl esters of amidophosphorous acids of cyclic and acyclic structures and studied the regularities of their chemical behavior in reactions with a number of electrophilic compounds. Classical reactions synthesizing ester amides of P (III) acids using a 3–5 % excess of tertiary amine were used to obtain tert.-butyl esters. They are shown on the following schemes:

$$(Et_2N)_2PCl + t\text{-}BuOH + Et_3N \longrightarrow \underset{(1)}{(Et_2N)_2POBu\text{-}t} + Et_3N{\cdot}HCl$$

$$(Me_2N)_2PCl + t\text{-}BuOH + Et_3N \longrightarrow \underset{(2)}{(Me_2N)_2POBu\text{-}t} + Et_3N{\cdot}HCl$$

$$Et_2NPCl_2 + 2\,t\text{-}BuOH + 2\,Et_3N \longrightarrow \underset{(3)}{Et_2NP(OBu\text{-}t)_2} + 2\,Et_3N{\cdot}HCl$$

$$Me_2NPCl_2 + 2\,t\text{-}BuOH + 2\,Et_3N \longrightarrow \underset{(4)}{Me_2NP(OBu\text{-}t)_2} + 2\,Et_3N{\cdot}HCl$$

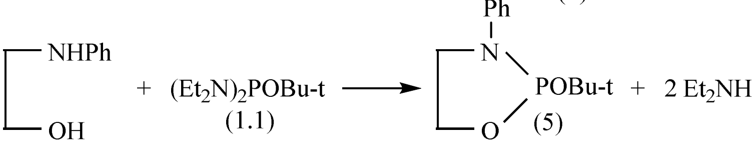

The structure of all phosphorous ester amides obtained was proved by $^{31}P$ NMR and $^{1}H$ NMR spectroscopy. As it was to be expected the signals of the phosphorus atom in the $^{31}P$ NMR spectra are in a weak field in the range from 110 to 130 ppm, which corresponds to the signals of the three-coordinated phosphorus atom.

In the study of tert.-butyl and di-tert.-butyl esters of amidophosphorous acids of cyclic and acyclic structures we showed that they were sufficiently thermally stable compounds. Thus according to the

$^{31}$P NMR spectrum it was found that tert.-butyltetraethyldiamidophosphite (1) retained the configuration of the trivalent phosphorus atom ($\delta_P$124 ppm) when heated above 200 °C.

In accordance with the literature data the studies related to the investigation of the chemical properties of esters with a tert.-butoxyl group are absent, apparently due to the proposed thermal instability of the above-mentioned compounds. However the presence of a tert.-butyl group in many cases can make precise the discussion points mainly related to the ambiguity of many reactions of ambident systems, in particular P(III) ester amides, and also contribute to the uniqueness of the processes, therefore, increase yield of target products.

Thus it is logical to study the Arbuzov reaction involving tert.-butyl esters of amidophosphorous acids, in particular, in reactions with various halide alkyls, both in terms of solving the controversial issues of the reaction mechanism, and in order to find effective ways to create a P–C bond.

We showed that the reaction of phosphite (1) with ethyl bromide proceeded according to the scheme of the classical reaction with the formation of the corresponding tetraethyl diamidoethyl phosphonate (6).

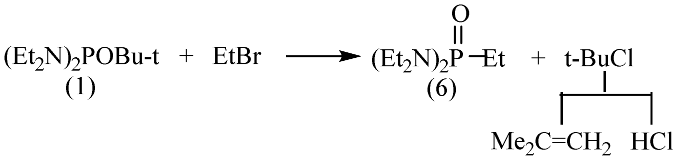

$$\underset{(1)}{(Et_2N)_2POBu\text{-}t} + EtBr \longrightarrow \underset{(6)}{(Et_2N)_2\overset{O}{\overset{\|}{P}}\text{—}Et} + t\text{-}BuCl \rightarrow Me_2C{=}CH_2 + HCl$$

Obviously the reaction mechanism is fully consistent with the classical concepts of the two-stage process. The second stage of the reaction, apparently, proceeds according to the scheme $S_N1$, as a result of which the tert.-butyl cation can be formed, which further regenerates the tert.-butyl bromide or decomposes forming isobutylene, which is fixed quantitatively by water displacement. However during the reaction partial distillation of tert.-butyl bromide was also observed.

If the reaction with ethyl bromide has no deviations from the classical concepts then the study of reactions involving reactive halogen derivatives with a mobile halogen atom encountered some difficulties associated with the ambiguity of the process. So we obtained interesting data when studying the reactions of tert.-butyl esters of amidophosphorous acid with such halide alkyls as benzyl chloride, allyl chloride, which have high mobility of halogen associated with the stability of the allyl and benzyl cation and radical, and also bromomalonic ester [7, 8].

When investigated the reaction of diamidophosphite (1) with benzyl chloride it was shown that the reaction proceeded rather difficult depending on the conditions and a mixture of products was formed.

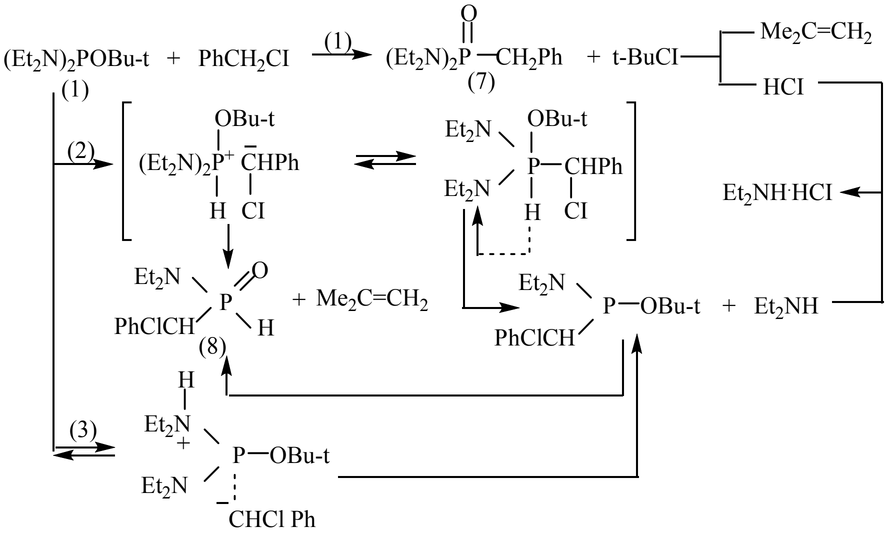

Thus, in particular, when carrying out the reaction without solvent it that the main direction of the reaction was found to be the Arbuzov rearrangement leading to the formation of tetraethyl diamidobenzylphosphonate (7), this is quite consistent with the scheme of the classical Arbuzov reaction. It is known from the literature that diamido esters of benzylphosphonic acid are patented and widely used as herbicides in agriculture and horticulture [9, 10]. Our proposed method of obtaining effective herbicides favorably differs in that the direction of the reaction is well regulated when exposed to external factors (temperature, solvent), does not require the use of catalysts and solvents, sophisticated equipment and has a fairly high yield of the target product. Carrying on the reaction in solvents is significantly different from the usual scheme. It was found that when the reaction proceeded in non-polar aprotic solvents a significant amount of diethylamine hydrochloride (50 %) independent of the nature of the solvent is formed along with the benzylphosphonate. Isobutylene and diethylamido(α-chlorobenzyl)phosphorous acid (8) with δ $^{31}$P 8 ppm, $J_{PH}$ 580 Hz were also recorded as the reaction products; the absorption band characteristic of the P–H bond in the region of 2370 cm$^{-1}$ is in the IR spectrum.

According to our ideas the reaction routes are described in the framework of a scheme involving both isomerization according to the Arbuzov reaction scheme (route 1) and the initial protonation of the phosphorus atom to form a quasiphosphonium compound (route 2), the decomposition of which, apparently, can proceed in several directions.

The structure of the intermediate «quasiphosphonium» depends on the nature of the solvent: the ionic form dominates in polar solvents, and pentacovalent one in non-polar solvents [5, 6]. The formation of acid (8) can be explained within the framework of a scheme taking into account the course of the reaction both through the stage of the phosphorus atom protonation and by the nitrogen atom protonation (route 2) and the decomposition of the resulting intermediate product while maintaining the coordination of the phosphorus atom and further isomerizing the forming phosphite and isobutylene release.

The formation of a significant amount of diethylamine hydrochloride was also explained in the framework of a scheme taking into consideration the initial attack of the acidic proton of benzyl chloride on the phosphorus atom. Moreover, in our opinion, the structure of the intermediate quasiphosphonium compound can be both ionic and pentacovalent one. The decomposition of the pentavalent form of the intermediate product that prevails in the non-polar environment obviously leads to the formation of a compound while maintaining the coordination of the phosphorus atom, which subsequently seems to undergo thermal isomerization leading to an acidic phosphite (8). The ionic form of a quasiphosphonium product can directly lead to phosphite (8).

Thus for the first time in the reaction with alkyl halides containing a mobile hydrogen atom products were obtained, which formation can be explained only from the standpoint of the initial protonation of the phosphorus atom with the formation of an intermediate quasiphosphonium compound.

Carrying out the reaction of phosphite (1) with allyl chloride confirmed the previously obtained results. When carrying out the reaction under the conditions of the Arbuzov reaction, i.e. without a solvent when heated, tetraethyl diamidoallylphosphonate (9) was isolated as a reaction product which according to the literature was patented as an agricultural herbicide [10].

Similarly to the reaction with benzyl chloride the protonation reaction product (10) was isolated, in the IR spectrum of which there is a characteristic absorption band of the P–H bond in the region of 2390 cm$^{-1}$, as well as the absorption band of the C=C bond in the region of 1625 cm$^{-1}$.

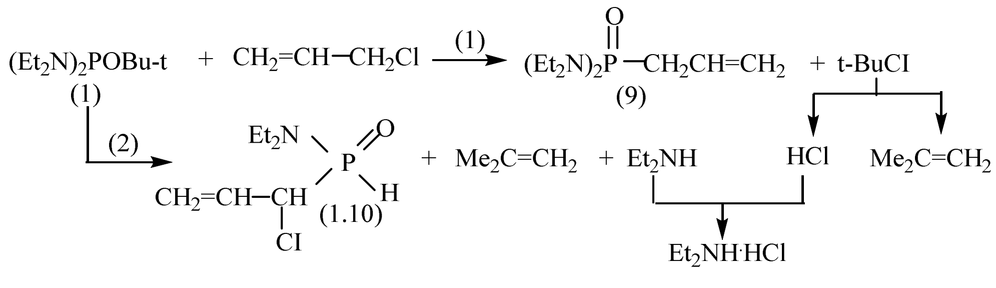

In connection with the research carried out the reaction of tert.-butyltetraethyldiamidophosphite (1) with bromomalonic ester, which also contains both a mobile halogen atom and a mobile hydrogen atom may be of undoubted interest. It was noted that when the reaction was carried out in the absence of a solvent the process proceeded very exothermically with the rapid release of isobutylene and the formation of deliquescent on air oligomer, polyaminophosphine, and ethanetetracarboxylic acid as the reaction products. This route of the reaction is fully consistent with the results of A.E. Arbuzov's work on the interaction of dialkyl esters of phosphorous acid with bromomalonic ester [11], as a result of which polyaminophosphine was also detected.

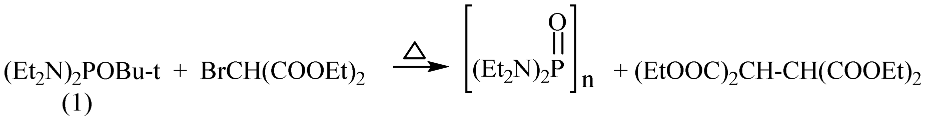

$$\underset{(1)}{(Et_2N)_2POBu\text{-}t} + BrCH(COOEt)_2 \xrightarrow{\Delta} \left[(Et_2N)_2\overset{O}{\overset{\|}{P}}\right]_n + (EtOOC)_2CH\text{-}CH(COOEt)_2$$

When carrying out the reaction in solvents the formation of a significant amount of diethylamine hydrochloride was also detected as the case with benzyl chloride was. In our opinion the explanation for this fact lies in the presence of both a mobile halogen atom and an acid proton which can initially attack the nucleophilic phosphorus atom.

Moreover in the presence of a solvent, the reaction proceeds according to the usual Arbuzov reaction scheme with the formation of tetraethyl diamide phosphon malonic ester (11), and by protonation of the phosphorus atom and further decomposition of the intermediate quasiphosphonium compound in various directions. In contrast to the reaction with benzyl chloride about 25–30 % of the initial bromomalonic ester returns to the reaction mixture, however, the amount of isobutylene released is equimolar, this indicates another possible direction of the reaction, apparently associated with the decomposition of the quasiphosphonium compound with the formation of the corresponding phosphorus ilide, which is unstable and decomposes forming a phosphonate compound.

An interesting fact is the formation, isolation and identification of tetraethyldiamidophosphorous acid (12) as a reaction product, its structure was proved by $^{31}$P NMR and IR spectroscopy. Formation of acidic phosphite (12) with $\delta^{31}$P 19 ppm, $J_{PH}$ 570 Hz is a direct proof of the presence of a competing protonation reaction, with the phosphorus atom being protonated more preferable than the nitrogen atom.

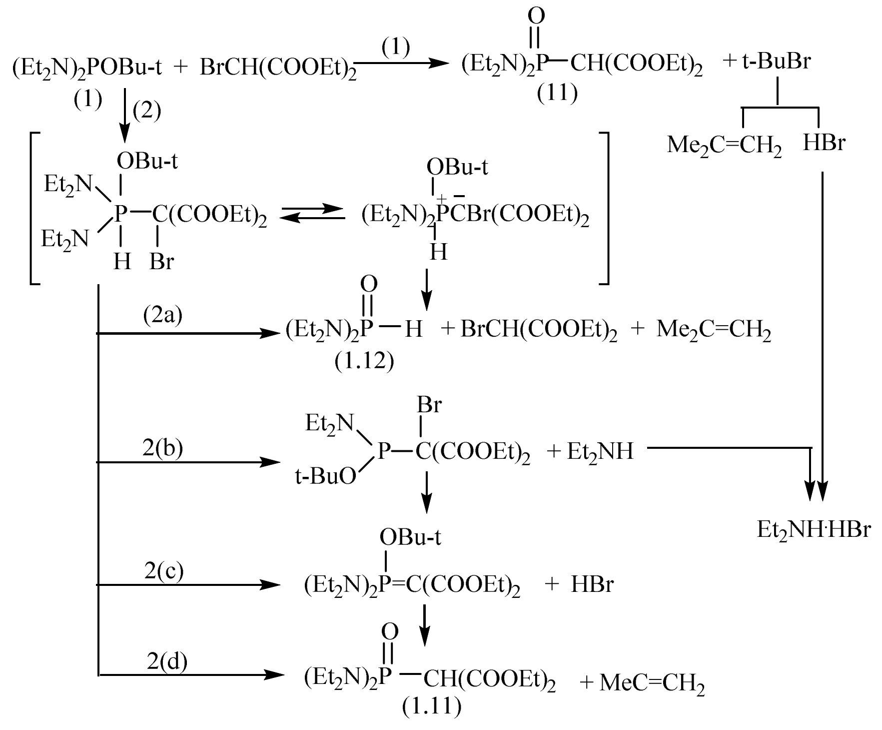

To confirm the proposed scheme we carried out the reaction in the ternary system: tert.-butyltetraethyldiamidophosphite — paraform — malonic ester. Previously the possibility of condensation in the ternary system: malonic ester-aldehyde-trialkylphosphite was shown in the literature [12]. The authors found that the condensation of malonic ester with formaldehyde (paraform) and amidophosphites was complicated by the interaction of malonic ester with amidophosphites and the formation of N,N-diethylaminomalonic acid ethyl ester and the corresponding phosphite.

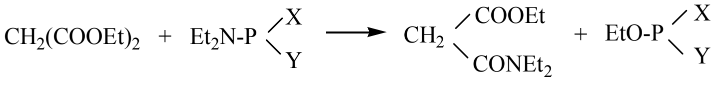

$$CH_2(COOEt)_2 + Et_2N\text{-}P\begin{matrix}\diagup X\\ \diagdown Y\end{matrix} \longrightarrow CH_2\begin{matrix}\diagup COOEt\\ \diagdown CONEt_2\end{matrix} + EtO\text{-}P\begin{matrix}\diagup X\\ \diagdown Y\end{matrix}$$

X=Y=OEt, $NEt_2$

The authors of [12] isolated 2,2-carbethoxyethylphosphonic acid diethyl ester and a small amount of 2-carbethoxy-2-[carbo(N,N-diethylamido)]ethylphosphonic acid diethyl ester during condensation in the ternary system malonic ester–paraform–diethylamidodiethylphosphite. We studied the reaction in the ternary system: tert.-butyltetraethyl diamidophosphite (1) – malonic ester – paraform. It was shown that regardless of the reaction conditions there was observed the initial protonation with the formation of a quasi-phosphonium compound, the decomposition of which led to the corresponding tetraethyldiamidophosphorous acid (12) fixed in the $^{31}$P NMR spectrum with a chemical shift of $\delta^{31}$P 19 ppm, $J_{PH}$ 570 Hz.

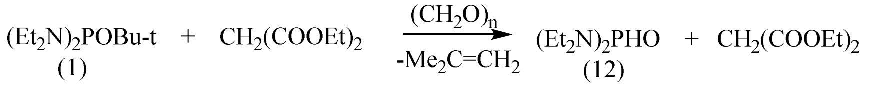

$$\underset{(1)}{(Et_2N)_2POBu\text{-}t} + CH_2(COOEt)_2 \xrightarrow[-Me_2C=CH_2]{(CH_2O)_n} \underset{(12)}{(Et_2N)_2PHO} + CH_2(COOEt)_2$$

Consequently the data obtained confirm our assumptions about the occurrence of competing, and, possibly, ahead of the protonation reaction of ester amide with a sufficiently strong CH-acid, which is a malonic ester. The uniqueness of this process was demonstrated on the reaction of the starting phosphite with malonic ester, as a result of which only diamidophosphorous acid was isolated (12). So the results obtained in aggregate show that tert-butyl esters of amidophosphorous acid are very convenient «tools» in solving a number of issues especially concerning the complex reactions mechanisms, and make it possible to simulate the structure of the intermediate product using the effect of the reaction temperature, solvent, concentration of substances, etc., as well as they are convenient syntons in creating compounds with the P-C bond having wide practical application.

## *Experimental*

*Synthesis of tert.-butyl tetraethyldiamidophosphite (1)*

105.3 g (0.5 mol) of tetraethyldiamidochlorophosphite in 2 liters of benzene was placed in a four-necked flask equipped with a mechanical stirrer, a thermometer, a reflux condenser, and a dropping funnel. At vigorous stirring a mixture of 37.0 g (0.5 mol) of tert.-butyl alcohol and 55.6 g (0.55 mol) of triethylamine in 200 ml of benzene was added at 0–5 ºC. After stirring at room temperature for 2–3 hours the precipitate of triethylamine hydrochloride was filtered, the solvent was removed in a water jet pump vacuum (30–40 mm Hg); 102.9 g (83 %) of phosphite (1) was isolated by distillation of the residue; bp 52–53 ºC (0.07 mmHg), $d_4^{20}$0.8996, $n_D^{20}$ 1.4510. Found, %: C 58.30; H 11.45; N 11.38; P 12.25. $C_{12}H_{29}N_2OP$. Calculated, %: C 58.06; H 11.69; N 11.29; P 12.59. δ $^{31}$P 124 ppm, $\delta^1$H 1.17 ppm ($CH_3$, 12H, t, $^3J_{HH}$ 7 Hz), 1.43 ppm [$(CH_3)_3C$, 9H, s], 3.07 ppm ($CH_2$, 12H, m).

*Interaction of phosphite (1) with benzyl chloride*

*a) without solvent*

12.4 g (0.05 mol) of phosphite (1) and 6.3 g (0.05 mol) of benzyl chloride were mixed in an Arbuzov flask. The reaction mixture was heated on a water bath, partial distillation of t-BuCl was observed; bp 48–50 ºC, $n_D^{20}$ 1.3860 (reference data: bp 51–52 ºC, $n_D^{20}$ 1.3857). Tert.-BuCl mainly decomposes under distillation conditions with the release of isobutylene fixed by the method of water displacement in a gas meter (930 ml, 83 %). The crystallized reaction mass in the flask was treated with water, then the free diethylamine was separated from the aqueous solution of diethylamine hydrochloride by neutralization with alkali, diethylamine has bp 54–55 ºC, $n_D^{20}$ 1.3894 (reference data: bp 55.5 ºC, $n_D^{20}$ 1.3873), yield was 0.4 g (11 %). 4.8 g (34 %) of tetraethyldiamidobenzylphosphonate (7) was isolated by extraction of the aqueous portion with ether, bp 51–52 ºC (reference data [9,10]: bp 51–53 ºC). Found, %: C 63.50; H 10.02; N 9.68; P 10.73. Calculated, %: C 63.83; H 9.57; N 9.93; P 10.98. IR spectrum (ν, cm$^{-1}$): 1220 (P=O), 1400–1600 (Ph).

*b) in a solvent (benzene)*

12.4 g (0.05 mol) of phosphite (1) and 6.3 g (0.05 mol) of benzyl chloride in 50 ml of dry benzene were heated in a flask with reflux condenser. Isobutylene liberation (950 ml, 85 %) was observed. Crystals of diethylamine hydrochloride of mass 2.3 g (yield 42 %) were separated by filtration, bp 220 ºC (reference data: bp 221 ºC). IR spectrum of the reaction mixture (ν, cm$^{-1}$): 1220 (P=O), 2440 (P–H). After distilling off the solvent the precipitated crystals of benzylphosphonate (7) were recrystallized from hexane, bp 51–52 ºC. The residue was distilled in vacuum, yield 2.2 g (18 %) of diethylamido(α-chlorobenzyl)phosphorous acid (8), bp 147–148 ºC (2 mm Hg), $d_4^{20}$ 0.9753, $n_D^{20}$ 1.4740, δ $^{31}$P 8 ppm, $J_{PH}$ 580 Hz.

*The interaction of phosphite (1) with allyl chloride*

*a) without a solvent*

Under reaction conditions with benzyl chloride 12.4 g (0.05 mol) of phosphite (1) and 3.8 g (0.05 mol) of allyl chloride formed 3.7 g (32 %) of tetraethyldiamidoallylphosphonate (9), bp 131–132 ºC (2 mm Hg), $d_4^{20}$ 0.8293, $n_D^{20}$ 1.4485 (reference data [9, 10]: bp 113–114 ºC (0.45 mm Hg).

*b) in a solvent (benzene)*

Under the reaction conditions with benzyl chloride 12.4 g (0.05 mol) of phosphite (1) and 3.8 g (0.05 mol) of allyl chloride formed 2.7 g (28 %) of diethylamido(α-chloroallyl)phosphorous acid (10), bp 115–116 ºC (2 mm Hg), $d_4^{20}$ 0.8623, $n_D^{20}$ 1.4335, δ $^{31}$P 4 ppm, $J_{PH}$ 560 Hz.

*The interaction of phosphite (1) with bromomalonic ester*

*a) without a solvent*

4.8 g (0.02 mol) of bromomalonic ester was added dropwise to 5.0 g (0.02 mol) of phosphite (1). Strong warming up of reaction mixture and rapid release of isobutylene 420 ml (94 %) were observed. The reaction mixture was a yellow crystalline mass, spreading in air, containing polyaminophosphine. White crystals of tetraethanecarboxylic acid ethyl ester mp 73–74 ºC were precipitated during treatment of the reaction mixture with benzene.

*b) in a solvent (benzene)*

12.0 g (0.05 mol) of bromomalonic ester in 100 ml of benzene was added to 12.4 g (0.05 mol) of phosphite (1). Warming up and release of isobutylene of 1040 ml (93 %) were observed. The precipitate $Et_2NH·HBr$ was filtered, mp 210 ºC. According to TLC there were two products in the benzene solution. After the solvent was distilled off by multiple distillation, 1.5 g (16 %) of tetraethyl diamidophosphorous acid (12) were isolated, bp 89–90 ºC (2 mm Hg), $d_4^{20}$ 0.9621, $n_D^{20}$ 1.4540, δ $^{31}$P 19 ppm, $J_{PH}$ 570 Hz, $d_4^{20}$ 0.9600, $n_D^{20}$ 1.4545, δ $^{31}$P 18 ppm, $J_{PH}$ 570 Hz). IR spectrum (ν, cm$^{-1}$): 1255 (P=O), 2370 (P–H). Tetraethyldiamidophosphonomalonic ester (11) is a non-distilling oil, $n_D^{20}$ 1.4358. IR spectrum (ν, cm$^{-1}$): 1215 (P=O), 1700 (C=O). Counter synthesis was carried out as follows. A solution of sodium malonic ester prepared from 4.0 g (0.025 mol) of malonic ester and 0.6 g (0.025 mol) of sodium in benzene was dropped to 5.7 g (0.025 mol) of tetraethyldiamidochlorophosphate in benzene; NaCI was separated by filtration, benzene was distilled off. The residue was oil with $n_D^{20}$ 1.4351.

*c) reaction in the ternary system phosphite: paraform: malonic ester*

A mixture of 5.0 g (0.02 mol) of phosphite (1), 3.2 g (0.02 mol) of malonic ester and 0.6 g (0.02 mol) of paraform was heated in benzene for 1 h before the release of isobutylene in the amount of 370 ml (82 %) was stopped. After distilling off the solvent from the reaction mixture, 0.9 g (28 %) of the malonic ester was isolated, bp 45–46 ºC (2 mm Hg), $n_D^{20}$ 1.4155 (reference data: bp 199ºC, $d_4^{20}$201.4143) and 1.2 g (32 %) of tetraethyl diamidophosphite (12).

*d) reaction of phosphite (1.1) with malonic ester*

A mixture of 5.0 g (0.02 mol) of phosphite (1) and 3.2 g (0.02 mol) of malonic ester was heated in benzene for 1 h before stopping the release of isobutylene in an amount of 400 ml (88 %). After distilling off the solvent 2.6 g (68 %) of tetraethyldiamidophosphite (12) was isolated.

## References

1 Пурдела Д. Химия органических соединений фосфора / Д. Пурдела, Р. Вылчану. — М.: Химия, 1972. — 752 с.

2 Kosolapoff G.M. Organic Phosphorus Compounds: in 7 Vol. — Vol. 1 / G.M. Kosolapoff, L. Maier (eds.). — New York: Wiley Interscience, 1972. — 186 p.

3 Безноско Б.К. Противовоспалительная и анальгетическая активность окисей третичных фосфинов / Б.К. Безноско, В.М. Усанова, Л.В. Журавлева, Н.А. Бондаренко, А.Н. Яркевич, А.Э. Антошин, Е.Н. Цветков // Хим.-фарм. журнал. — 1990. — № 4. — С. 22–24.

4 Тарасова Р.И. Биологически активные производные фосфорилированных карбоновых кислот / Р.И. Тарасова, В.В. Москва // Ж. общей химии. — 1997. — Т. 67, № 9. — С. 1483–1496.

5 Van Wazer M.V. Tert-butylphosphite and some of its reactions / M.V. Van Wazer // J. Org. Chem. — 1964. — Vol. 29, No. 5. — P. 1006–1008.

6 Гусев Ю.К. О реакциях некоторых смешанных эфиров фосфористой кислоты с акрилонитрилом и иодистым метилом / Ю.К. Гусев, В.Н. Чистоклетов, А.А. Петров // Ж. общей химии. — 1977. — Т. 77, № 1. — С. 45–50.

7 Газизов Т.Х. Трет-бутиловые эфиры фосфористой кислоты. Синтез и свойства / Т.Х. Газизов, Ю.В. Чугунов, А.Н. Пудовик // ДАН СССР. — 1987. — Т. 294, № 6. — С. 1382–1386.

8 Салькеева Л.К. Трет-бутиламидофосфиты в реакции Арбузова / Л.К. Салькеева, М.Т. Нурмаганбетова, О.Ш. Курманалиев // Наука и образование — ведущий фактор стратегии Казахстана 2030: тр. Междунар. науч.-практ. конф. — Караганда: КарГТУ, 2001. — С. 334–337.

9 А.С. № 686372. СССР Способ получения тетраэтилдиамидов бензилфосфоновой кислоты / Л.И. Мизрах, Л.Ю. Полонская. Опубл. 05.03.1980.

10 Патент Японии № 48–40740 / Кувахара Масао, Рикукадо Мотоа, Оно Киити, Кавамура Юдзи, Уно Йосинори. Опубл. 03.12.1973.

11 Burgada R. Les Composes Organigues du Phosphore Trivalent. Les du la Liaison Phosphore azote / R. Burgada // Ann. Chim. — 1966. — No. 1. — P. 15–35.

12 Иванов Б.Е. Взаимодействие амидофосфитов с малоновым эфиром и параформом / Б.Е. Иванов, Л.А. Кудрявцева, С.В. Самурина, А.Б. Агеева, Т.И. Карпова // Ж. общей химии. — 1979. — Т. 49, № 8. — С. 1768–1772.

Л.К. Сәлкеева, П. Войтишек, Е.В. Минаева, Л.М. Сугралина,
А.В. Омашева, А.А. Муратбекова, А.К. Сәлкеева, К.И. Садыков

## Үш-бутилдиамидфосфиттердің алкилгалогенидтерімен әрекеттесуін зерттеу

Мақалада үш-бутилдиамидофосфиттер галогеннің жылжымалы атомы бар әртүрлі алкилгалогенидтермен, атап айтқанда, хлорлы аллилмен, хлорлы бензилмен және броммалон эфирімен түрлі жағдайларда әрекеттесуі зерттелген. Хлорлы бензил және хлорлы аллилмен реакциялар негізгі өнімдер ретінде тиісті бензил- және аллиламидофосфонаттардың пайда болуы фосфор атомын кватернизациялау арқылы Арбузов реакциясының классикалық нұсқасына сәйкес өтетіні анықталды. Реакция әртүрлі өнімдердің қоспасын түзе жүретіні белгілі болды. Бұл еріткіш табиғатына тәуелді аралық «квазифосфония» құрылысымен байланысты: иондық пішін полярлы еріткіштерде, пентаковалентті пішін полярлы емес еріткіштерде басым. Сонымен бірге реакцияның бағыты өткізу шарттарына, атап айтқанда, температура мен еріткіштің табиғатына байланысты екендігі дәлелденді. Броммалон эфирімен реакция фосфор атомын бастапқы протондау арқылы квазифосфониялық қосылыстың түзілуімен жүретіні және оның ыдырауы сәйкес тетраэтилдиамидофосфор қышқылына әкелетіні көрсетілді.

*Кілт сөздер*: P(III) қышқылдар эфироамидтері, Арбузов реакциясы, үш-бутил диамидофосфиттер, алкилгалогенидтер, броммалон эфирі, квазифосфониялық қосылыс.

Л.К. Салькеева, П. Войтишек, Е.В. Минаева, Л.М. Сугралина,
А.В. Омашева, А.А. Муратбекова, А.К. Салькеева, К.И. Садыков

## Исследование взаимодействия трет-бутилдиамидофосфитов с алкилгалогенидами

В статье изучено взаимодействие трет-бутилдиамидофосфитов с разнообразными алкилгалогенидами с подвижным атомом галогена, в частности, хлористым аллилом, хлористым бензилом и броммалоновым эфиром в различных условиях. Установлено, что реакции с хлористым бензилом и хлористым аллилом протекают согласно классической схеме реакции Арбузова путем квартенизации атома фосфора с образованием в качестве основных продуктов реакции соответствующих бензил- и аллиламидофосфонатов. Установлено, что реакция протекает неоднозначно с образованием смеси различных продуктов. Это связано со структурой промежуточного «квазифосфония», которая зависит от природы растворителя: ионная форма преобладает в полярных растворителях, пентаковалентная форма — в неполярных растворителях. Кроме того, доказано, что направление реакции зависит от условий проведения, а именно от температуры и природы растворителя. Показано, что реакция с броммалоновым эфиром протекает через первоначальное протонирование атома фосфора с образованием квазифосфониевого соединения, распад которого приводит к соответствующей тетраэтилдиамидофосфористой кислоте.

*Ключевые слова:* эфироамиды кислот P(III), реакция Арбузова, трет-бутилдиамидофосфиты, алкилгалогениды, броммалоновый эфир, квазифосфониевое соединение.

## References

1 Purdela, D., & Vylchanu, R. (1972). *Khimiia orhanicheskikh soedinenii fosfora [Chemistry of Organic Phosphorus Compounds*]. Moscow: Khimiia [in Russian].

2 Kosolapoff, G.M., & Maier, L. (Eds.) (1972). Organic Phosphorus Compounds. New York: Wiley Interscience.

3 Beznosko, B.K., Usanova, V.M., Zhuravleva, L.V., Bondarenko, N.A., Yarkevich, A.N., Antoshin, A.E., & Tsvetkov, E.N. (1990). Protivovospalitelnaia i analheticheskaia aktivnost okisei tretichnykh fosfinov [Anti-inflammatory and analgesic activity of oxides of tertiary phosphines]. *Khimiko-farmatsevticheskii zhurnal — Chemical-pharmaceutical Journal, 4*, 22–24 [in Russian].

4 Tarasova, R.I., & Moskva, V.V. (1997). Biolohicheski aktivnye proizvodnye fosforilirovannykh karbonovykh kislot [Biologically active derivatives of phosphorylated carboxylic acids]. *Zhurnal obshchei khimii — Russian Journal of General Chemistry, 67, 9*, 1483–1496 [in Russian].

5 Van Wazer, M.V. (1964). Tret-butylphosphite and some of its reactions. *J. Org. Chem., 29(5)*, 1006–1008.

6 Gusev, Yu.K., Chistokletov, V.N., & Petrov, A.A. (1977). O reaktsiiakh nekotorykh smeshannykh efirov fosforistoi kisloty s akrilonitrilom i iodistym metilom [On the reactions of some mixed phosphate esters with acrylonitrile and methyl iodide]. *Zhurnal obshchei khimii — Russian Journal of General Chemistry, 77, 1*, 45–50 [in Russsian].

7 Gazizov, T.Kh., Chugunov, Yu.V., & Pudovik, A.N. (1987). Tret-butilovye efiry fosforistoi kisloty. Sintez i svoistva [Phosphorous acid tert.-butyl esters. Synthesis and properties]. *DAN SSSR — Reports of the Academy of Sciences of the USSR, 294, 6*, 1382–1386 [in Russian].

8 Salkeeva, L.K., Nurmaganbetova, M.T., & Kurmanaliev, O.Sh. (2001). Tret.-butilamidofosfity v reaktsii Arbuzova [Tert.-butylamidophosphites in the Arbuzov reaction]. Proceedings from Science and education is a leading factor in the strategy of Kazakhstan 2030: *Mezhdunarodnaia nauchno-prakticheskaia konferentsiia — International scientific and practical conference.* (pp. 334–337). Karaganda: KarGTU [in Russian].

9 Mizrah, L.I., & Polonskaya, L.Yu. (1980). Sposob polucheniia benzilfosfonovoi kisloty [The method of obtaining benzylphosphonic acid tetraethyldiamides]. *Patent No. 686372. USSR.* Publ. 05.03.1980 [in Russian].

10 Kuwahara Masao, Rikukado Motoa, Ono Kiiti, Kawamura Yuji, & Uno Yosinori. (1973). *Japanese Patent No. 48–40740.* Japan Publ. 03.12.1973.

11 Burgada, R. (1966). Les Composes Organigues du Phosphore Trivalent. Les du la liaison phosphore azote. *Ann. Chim., 1*, 15–35.

12 Ivanov, B.E., Kudryavtseva, L.A., Samurina, S.V., Ageeva, A.B., & Karpova, T.I. (1979). Vzaimodeistviie amidofosfitov s malonovym efirom i paraformom [Interaction of amidophosphites with malonic ester and paraform]. *Zhurnal obshchei khimii — Russian Journal of General Chemistry, 49, 8*, 1768–1772 [in Russian].

DOI: 10.31489/2019Ch1/48-53

UDC 541.64

Ye.M. Tazhbayev, M.Zh. Burkeyev, L.Zh. Zhaparova, T.S. Zhumagaliyeva, A.A. Agdarbek

*Ye.A. Buketov Karaganda State University, Kazakhstan*
(*E-mail: lyazzh@mail.ru*)

# Albumin nanoparticles loaded with the antitumor drug «Hydroxycarbamide» by the incorporation method

In this article the possibility of loading the antitumor drug «Hydroxycarbamide» into the polymeric matrix of human serum albumin was studied. Nanoparticles of serum albumin were obtained using desolvation method. Prepared empty human serum albumin nanoparticles have average size of 108.4 nm with narrow particle size distribution, which make them promising in using for the drug delivery purposes. The binding of hydroxycarbamide with the polymer was performed by incorporation of the drug into the medium during the process of crosslinking of albumin macromolecules. Incorporation of the drug into human serum albumin led to the formation of nanoparticles loaded with hydroxycarbamide with satisfactory physico-chemical characteristics (average particle diameters were in the range of 250–350 nm and the value of polydispersity index was 0.2–0.3) with the high value of binding degree (up to 68 %). It was shown that increasing the concentration of the drug in the initial solution led to the increase of binding degree of hydroxycarbamide with human serum albumin nanoparticles. The kinetics of release process of the drug from albumin nanoparticles in the conditions modeling biological medium was studied. As a result of the study of the drug release rate it has been concluded that prolonged release of hydroxycarbamide can be achieved when nanosomal form of the drug is used.

*Keywords:* nanoparticles, human serum albumin, desolvation, antitumor drug, Hydroxycarbamide, incorporation, loading, drug delivery, polymers.

## *Introduction*

Nowadays it is known that the use of prolonged drug dosage forms or «prodrugs» instead of traditional ones have several advantages in comparison with conventional drug delivery systems. First of all it is defined by the increase of therapeutic efficiency of biologically active substance, which takes place due to the localization of needed concentration of drug in the targeted organ or tissue, thus leading to prolongation of the drug effect. Optimization of the effect of drug preparations can be accomplished by «construction» of drug dosage forms on micro- and nano-level on the basis of the polymers, which have wide application in medicine. Among the biocompatible and biodegradable polymers, which can be used as a polymeric basis for developing «prodrugs», a serum albumin is of great interest [1, 2]. For the last decade human serum albumin (HSA) is used as a good transporting agent especially for low molecular compounds including drug preparations. There are known some novel systems in the forms of nanoparticles based on HSA for such drugs of protein origin as «Albuferon» and «Levemir» [2, 3]. Besides, the *in vivo* studies of toxic effects of nanosomal formulations of albumin for the controlled delivery of antitumor drugs have shown the decrease of side effects [2, 3]. «Abraxane» is the example of effective using HSA nanoparticles in tumor chemotherapy [3]. «Abraxane» is the nanoparticulate form of antitumor drug «Paclitaxel» on the basis of albumin and it was approved for the treatment of breast tumor [3]. So HSA nanoparticles allow increasing the solubility of drug preparations, thus improving their uptake by tumor cells.

In this regard, the goal of this work was to study the possibility of binding HSA nanoparticles with antitumor drug preparation «Hydroxycarbamide» with the aim of prolongation of its theraputic efficiency and decreasing undesired toxic effects.

## *Method*

### *Preparation of empty and drug loaded HSA nanoparticles*

Empty HSA nanoparticles were prepared using a desolvation method [4, 5]. Briefly, the pH of HSA solution of albumin (2 %) was adjusted to 8.3 with buffer solution. Then under constant stirring (600 rpm) at room temperature 8 ml of ethanol (96 %) was added to the mixture (1 ml/min) using a tubing pump. After the desolvation process the particles were stabilized by the addition of an aqueous 8 % glutaraldehyde solution (1.175 μl per ml HSA). After that the suspension was stirred for 24 h. The nanoparticles were separated from low molecular components by repeated centrifugation with the Centrifuge MiniSpin Plus 14500 (Eppendorf, Hamburg, Germany) at 14500 rpm and washing them with water.

HSA nanoparticles loaded with the antitumor drug hydroxycarbamide were obtained using the same procedure with the difference that the drug was dissolved in the solution of albumin before carrying out the process of desolvation. The yield of nanoparticles was determined by gravimetric method.

*Measurement of particle size and polydispersity*

The average particle size and polydispersity index (PDI) were measured by photon correlation spectroscopy (PCS) using a Malvern Zetasizer Nano 90S (Malvern Instruments Ltd., Malvern, UK) at a temperature 25 ºC and at a scattering angle 90º.

Pictures of empty HSA nanoparticles and nanoparticles loaded with hydroxycarbamide were made by electron microscopy on MIRA 3 LM TESCAN (Czech Republic).

*Study of binding and drug release of hydroxycarbamide from HSA nanoparticles*

The binding of hydroxycarbamide with nanoparticles was determined from the concentration of drug in the supernatant solution. The analysis of supernatant solution was made on UV-1800 SHIMADZU by UV-spectrophotometry (λ=214 nm). Before measurement the solutions were diluted with water.

The study of *in vitro* drug release was performed in PBS solution (pH 7.4) at 37 ºC within 24 hours. The samples were withdrawn from a beaker and analyzed by UV-spectrophotometry (λ=214 nm).

## *Results and discussion*

Empty HSA nanoparticles have been obtained using desolvation method described above. Physicochemical characteristics (average particle diameter and particle size distribution) are shown in Figure 1. The results of dinamyc light scattering demonstrate that the size of the particles is less than 150 nm and PDI is equal to 0.273. From the given figure it is also clear that there is small amount of big particles of microne size in the system, which were separated from the emulsion by centrifugation at low rate (3000 rpm). Overall obtained HSA nanoparticles have satisfactory parameters, therefore they are applicable as transporting systems for drug preparations.

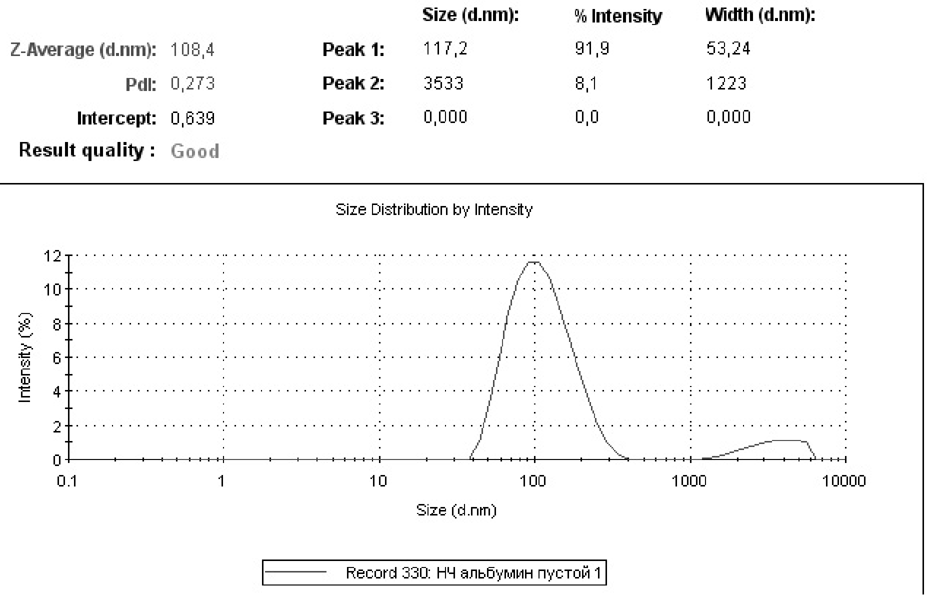

|  |  |  | **Size (d.nm):** | **% Intensity** | **Width (d.nm):** |
|---|---|---|---|---|---|
| **Z-Average (d.nm):** | 108,4 | **Peak 1:** | 117,2 | 91,9 | 53,24 |
| **PdI:** | 0,273 | **Peak 2:** | 3533 | 8,1 | 1223 |
| **Intercept:** | 0,639 | **Peak 3:** | 0,000 | 0,0 | 0,000 |
| **Result quality :** | Good |  |  |  |  |

Figure 1. Particle size distribution of empty HSA nanoparticles

The immobilization of HSA nanoparticles with the drug were performed by incorporation of the drug into the medium during the process of macromolecules crosslinking. An incorporation of the drug into the system when the nanoparticles are formed allow to achieve high loading. The loading of HSA with hydroxycarbamide was performed using three concentrations (0.217 mg/ml, 0.326 mg/ml and 0.484 mg/ml) of the drug. Obtained drug loaded HSA nanoparticles were characterized by photon correlation spectroscopy (PCS), the results are presented in Figure 2 and in Table.

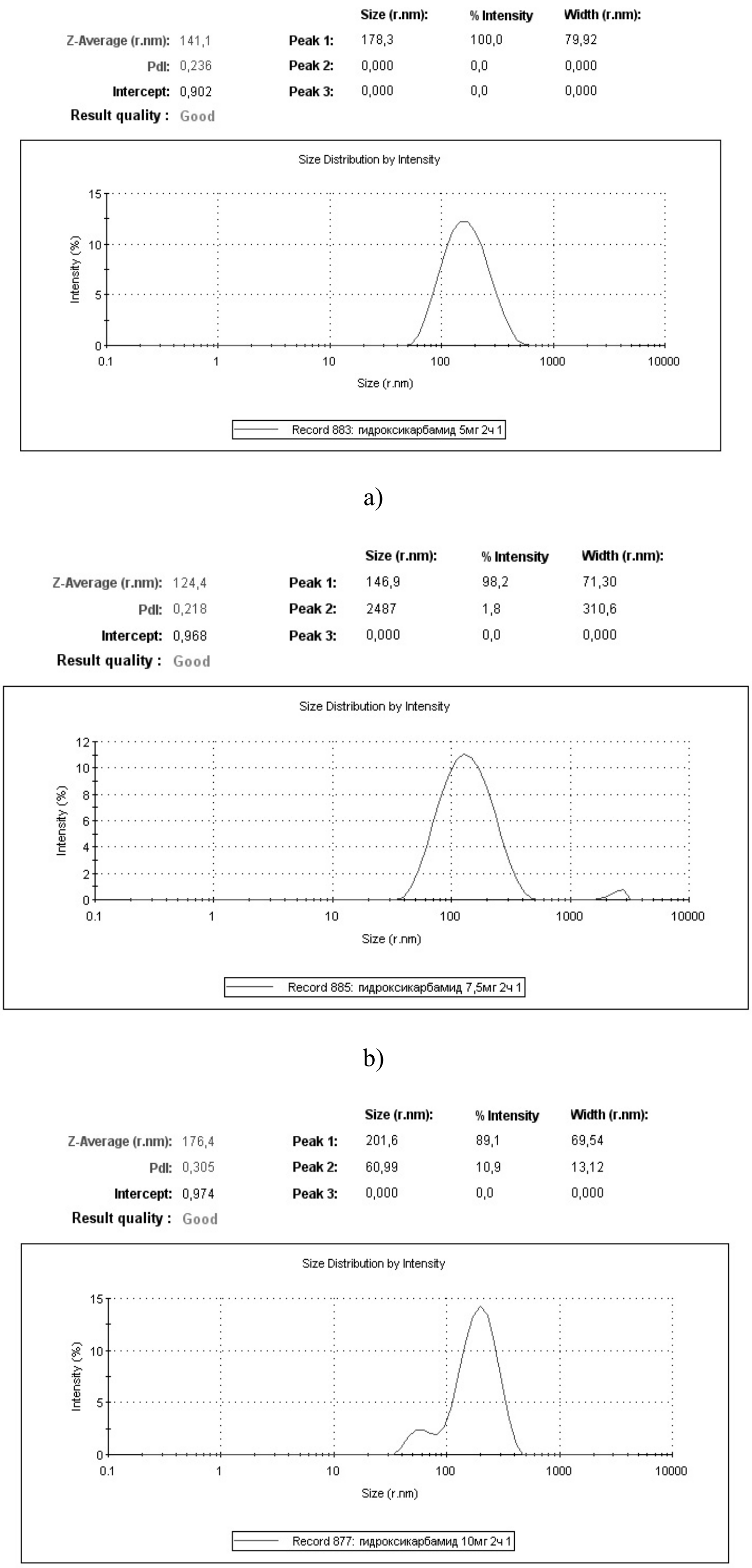

| | | | Size (r.nm): | % Intensity | Width (r.nm): |
|---|---|---|---|---|---|
| Z-Average (r.nm): | 141,1 | Peak 1: | 178,3 | 100,0 | 79,92 |
| PdI: | 0,236 | Peak 2: | 0,000 | 0,0 | 0,000 |
| Intercept: | 0,902 | Peak 3: | 0,000 | 0,0 | 0,000 |
| Result quality : | Good | | | | |

a)

| | | | Size (r.nm): | % Intensity | Width (r.nm): |
|---|---|---|---|---|---|
| Z-Average (r.nm): | 124,4 | Peak 1: | 146,9 | 98,2 | 71,30 |
| PdI: | 0,218 | Peak 2: | 2487 | 1,8 | 310,6 |
| Intercept: | 0,968 | Peak 3: | 0,000 | 0,0 | 0,000 |
| Result quality : | Good | | | | |

b)

| | | | Size (r.nm): | % Intensity | Width (r.nm): |
|---|---|---|---|---|---|
| Z-Average (r.nm): | 176,4 | Peak 1: | 201,6 | 89,1 | 69,54 |
| PdI: | 0,305 | Peak 2: | 60,99 | 10,9 | 13,12 |
| Intercept: | 0,974 | Peak 3: | 0,000 | 0,0 | 0,000 |
| Result quality : | Good | | | | |

c)

*a* — 0.217 mg/ml; *b* — 0.326 mg/ml; *c* — 0.484 mg/ml

Figure 2. Particle size distribution of drug loaded HSA nanoparticles at various concentrations of the drug

Table

**Physico-chemical characteristics of HSA nanoparticles loaded with hydroxycarbamide**

| $C_{\text{Hydrox}}$, mg/ml | Characteristics of nanoparticles | | | Binding degree, % | Yield of nanoparticles, % |
|---|---|---|---|---|---|
| | Average particle diameter, *d*, nm | PDI | Fraction of nanoparticles, % | | |
| 0 | 108.4 | 0.273 | 91.9 | – | 93.3 |
| 0.217 | 282.2 | 0.236 | 100.0 | 13.52 | 84.97 |
| 0.326 | 248.8 | 0.218 | 98.2 | 35.13 | 85.68 |
| 0.484 | 352.8 | 0.305 | 89.1 | 67.56 | 86.75 |

From the graphs it can be seen that the average particle size of nanoparticles ranges between 250–350 nm which is suitable size for the drug delivery systems. The data presented in the table also show that the yields of nanoparticles are also high (84–87 %).

It is important to know the quantity of the drug bond to nanoparticles, which defines the possibility of using particles obtained for the drug delivery purposes. Therefore the binding degree of HSA nanoparticles with hydroxycarbamide was determined using UV-spectroscopy. As it is clear from the table the values of binding degree and the yields of nanoparticles gradually increase with the increasing the concentration of hydroxycarbamide, that means that the amount of the drug can be considerably increased.

The surface and morphology of obtained HSA nanoparticles were observed on MIRA 3 LM TESCAN electron microscope (Czech Republic) (Fig. 3).

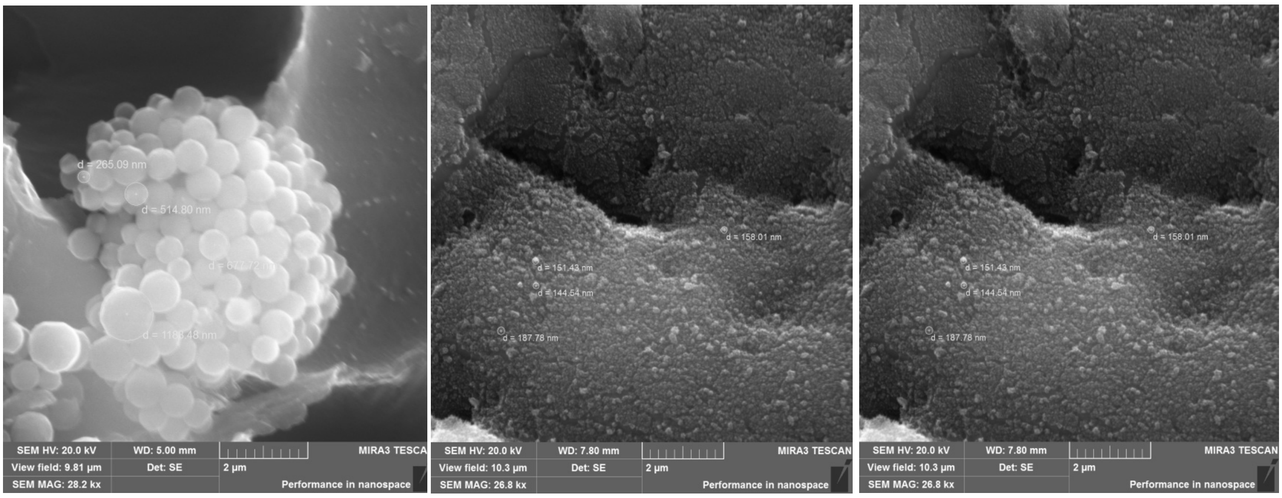

*a* *b* *c*

*a* — 0.217 mg/ml; *b* — 0.326 mg/ml; *c* — 0.484 mg/ml

Figure 3. REM pictures of HSA nanoparticles loaded with hydroxycarbamide at various concentrations

From the given pictures it can be judged that the results of electron microscopy have well correspondence with the results obtained by PCS: HSA nanoparticles loaded with hydroxycarbamide have smooth surface and round shape without any inclusions (Fig. 3). Mainly all three systems consist of the particles of similar size in the interval of 150–300 nm, however bigger particles with the size more than 500 nm also present in the system.

The study of the kinetics of drug release is of great importance as it determines the applicability of prepared HSA nanoparticles loaded with the drug in a treatment of tumor disease. Therefore the release rate of hydroxycarbamide from HSA nanoparticles was observed under *in vitro* conditions (pH 7.4 and T = 37 ºC) within 24 hours. The results of the study are given on the graph below (Fig. 4).

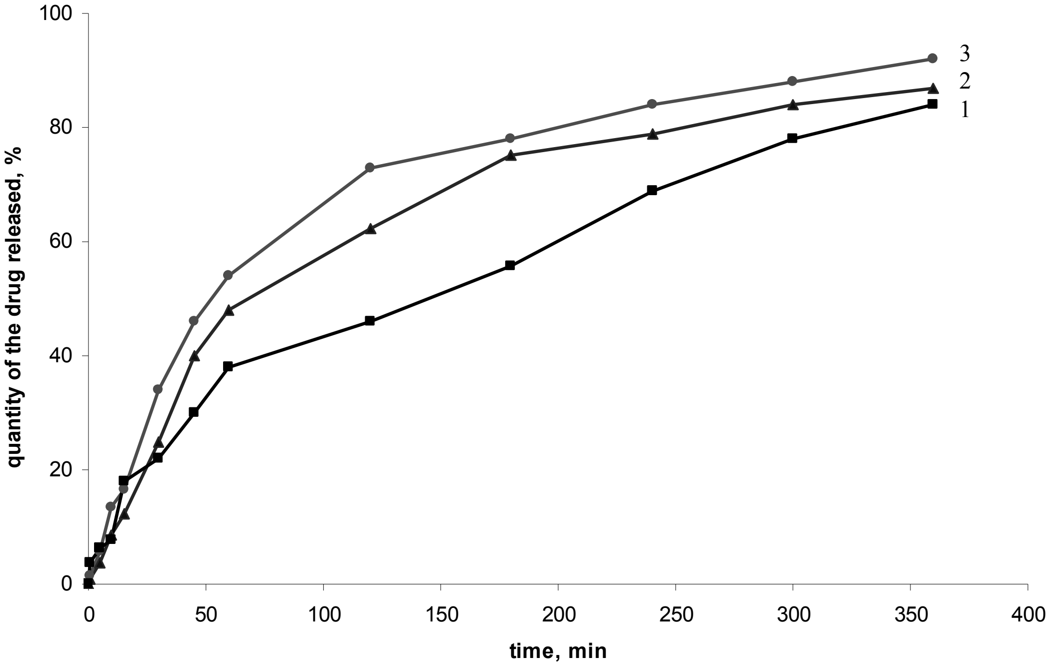

Initial concentrations of the drug are: *1* — 0.217 mg/ml; *2* — 0.326 mg/ml; *3* — 0.484 mg/ml

Figure 4. Release of hydroxycarbamide from HSA nanoparticles

The curves on drug release demonstrate that the higher the amount of hydroxycarbamide bond to nanoparticles the faster the process goes. So at a minimal concentration of the drug (1) the release takes place rather slow whereas when loading HSA nanoparticles with the higher quantity of hydroxycarbamide, it is clearly seen that 50 % of the drug releases to the medium within 60–150 minutes depending on the amount of loaded drug (Fig. 4). However in general it can be concluded that the release rate of hydroxycarbamide from HSA nanoparticles is rather low as in all three cases, i.e. less than 80 % of the loaded drug eliminates to the surrounding medium within 3 hours. It is seen from the graph that after 6 hours approximetaly 80–90 % of the loaded hydroxycarbamide releases from the matrix of nanoparticles. After that time however the release of the rest part of the drug was not observed which is quite regular for this kind of systems and it can be explained by the retardation of elimination caused by crosslinked structure of albumin macromolecules which does not allow to the molecules of the drug to be released outside from the inner part of HSA nanoparticles.

## *Conclusions*

So as a result of the study HSA nanoparticles loaded with antitumor drug «Hydroxycarbamide» by incorporation of the drug during the process of macromolecules crosslinking were obtained. Nanoparticles synthesized have satisfactory characteristics and rather long release rate, which make them promising systems for the drug delivery purposes.

## References

1 Kreuter, J. (1994). *Nanoparticles: Colloidal Drug Delivery Systems.* New-York: Marcel Dekker, USA.

2 Kratz, F. (2008). Albumin as a drug carrier: Design of prodrugs, drug conjugates and nanoparticles. *J. Cont. Rel. 132,* 171–183.

3 Kreuter, J. (2007). Nanoparticles — a historical Perspectives. *Int. J. Pharm., 331,* 1–10.

4 Dreis, S., Rothweiler, F., & Michaelis M., et al. (2007). Preparation, characterization and maintenance of drug efficacy of doxorubicin-loaded human serum albumin nanoparticles. *Int. J. Pharm.*, *341,* 207–214.

5 Langer, K., Balthasar, S., & Vogel, V., et al. (2003). Optimization of the preparation process for human serum albumin nanoparticles. *Int. J. Pharm., 257,* 169–180.

Е.М. Тажбаев, М.Ж. Буркеев, Л.Ж. Жапарова, Т.С. Жұмағалиева, А.А. Ағдарбек

# Қатерлі ісікке қарсы «Гидроксикарбамид» препаратымен енгізу әдісімен иммобилденген альбуминді нанобөлшектер

Мақалада қатерлі ісікке қарсы «Гидроксикарбамид» препаратын адамның сарысулы альбуминінен алынған нанобөлшектерге иммобилдеу мүмкіндігі зерттелді. Адамның сарысулы альбуминді нанобөлшектері десольваттау әдісімен алынды. Синтезделген альбуминді нанобөлшектердің орташа өлшемі 108,4 нм және өлшем бойынша таралуы тар болды. Бұл оларды алдағы уақытта дәрілік заттарды тасымалдауда қолдануға мүмкіндік береді. Дәрілік затты полимермен байланыстыру гидроксикарбамидті ортаға альбуминді нанобөлшектердің түзілуі барысында енгізілуі арқылы жүзеге асырылды. Дәрілік затты альбуминмен енгізу әдісімен байланыстыру қанағаттанарлық сипаттамаларға ие (бөлшектердің орташа өлшемі 250–350 нм, ал полидисперсті мәндері 0,2–0,3) және байланысу дәрежесі жоғары (68 %-ға дейін) гидроксикарбамидпен иммобилденген сарысулы альбуминді нанобөлшектердің түзілуіне әкелді. Бастапқы ерітіндіге енгізілген дәрілік заттың концентрациясын арттыру гидроксикарбамидтің альбуминді нанобөлшектермен байланысу дәрежесінің артуына әкелетіні көрсетілді. Биологиялық шарттарды модельдейтін жағдайда дәрінің альбуминді нанобөлшектерден босап шығу кинетикасы зерттелді. Гидроксикарбамидтің альбуминді нанобөлшектерден босап шығу үрдісін зерттеу нәтижесінде дәрілік препараттың наносомалы үлгісін қолдану арқылы дәрілік заттың ұзағырақ уақыт аралығында босап шығуына қолжеткізуге болатыны туралы қорытынды жасалды.

Кілт сөздер: нанобөлшектер, адамның сарысулы альбумині, десольвация, гидроксикарбамид, енгізу, иммобилдеу, дәрілерді тасымалдау, полимерлер.

Е.М. Тажбаев, М.Ж. Буркеев, Л.Ж. Жапарова, Т.С. Жумагалиева, А.А. Агдарбек

# Наночастицы альбумина, иммобилизованные противоопухолевым препаратом «Гидроксикарбамид» методом включения

В статье изучена возможность иммобилизации противоопухолевого препарата «Гидроксикарбамид» в матрицу наночастиц человеческого сывороточного альбумина. Наночастицы человеческого сывороточного альбумина получали методом десольвации. Полученные наночастицы альбумина имеют средний размер 108,4 нм с узким распределением частиц по размерам, что делает их перспективными при использовании в доставке лекарств. Связывание лекарственного вещества с полимером проведено непосредственным введением гидроксикарбамида в среду в процессе сшивки макромолекул альбумина. Включение лекарственного вещества в наночастицы человеческого сывороточного альбумина привело к образованию наночастиц, иммобилизованных гидроксикарбамидом, с удовлетворительными физико-химическими характеристиками (средний размер частиц составил 250–350 нм, а значения полидисперсности — 0,2–0,3) и высокими значениями степени связывания (до 68 %). Показано, что увеличение концентрации лекарственного вещества, введенного в первоначальный раствор, приводит к увеличению степени связывания гидроксикарбамида с наночастицами сывороточного альбумина. Исследована кинетика процесса высвобождения лекарства из наночастиц альбумина в условиях, моделирующих биологические. По результатам изучения процесса высвобождения гидроксикарбамида из наночастиц альбумина сделан вывод о том, что можно добиться более длительного высвобождения лекарства при использовании наносомальной формы лекарственного препарата.

*Ключевые слова:* наночастицы, сывороточный альбумин человека, десольвация, гидроксикарбамид, включение, иммобилизация, доставка лекарств, полимеры.

# ФИЗИКАЛЫҚ ЖӘНЕ АНАЛИТИКАЛЫҚ ХИМИЯ
# ФИЗИЧЕСКАЯ И АНАЛИТИЧЕСКАЯ ХИМИЯ
# PHYSICAL AND ANALYTICAL CHEMISTRY

DOI: 10.31489/2019Ch1/54-59

UDC 544.08

B.K. Zhanasbayeva, G.K. Bekturganova, V.A. Donbayeva

*Kazakhstan Institute of Metrology, Nur-Sultan, Kazakhstan*
*(E-mail: zhanasbaeva@kazinmetr.kz)*

## Estimation of uncertainty at reference buffer solution certification

The national standard of the pH scale is the primary standard of the Republic of Kazakhstan, which confirmed its equivalence with international comparisons, namely, key comparisons of APMP QM-R19 (2014) and pilot comparisons of COOMET 655/EN/15 (2017). The standard implements the primary method of pH measurements using cells without transfer (Harned cells) with hydrogen and silver chloride electrodes. This cell is characterized by high reproducibility of measurement results. The state reference materials (SRM), which are widely used by laboratories at verification of measuring instruments and internal quality control, are certified with this standard. SRM of pH are the accurate samples of chemicals dissolved in 1 kg of bidistilled deionized water with a specific electrical conductivity of not more than 2·10–4 Cm/m at a temperature of 20 °C. The paper presents an estimation of uncertainty of certified pH values of CRM-standard buffer solutions in the range 9.010–9.280 pH. Determination of the pH of solutions is an indirect type of measurement. The reference pH value is determined from the results of measurements of electromotive force, temperature, pressure and other parameters.

*Keywords:* measurement uncertainty, state standard samples, pH buffer solutions, primary state standard, international comparisons, electromotive force, standard potential.

### *Introduction*

Uncertainty estimation was performed according to [1] using the basic provisions [2]. In general, the combined standard uncertainty of the certified value of pH CRM is evaluated by the equation:

$$u_c^2(A) = u_{char}^2 + u_h^2 + u_{stab}^2, \tag{1}$$

where $u_{char}$ is the uncertainty associated with characterization of certified values; $u_h$ is the standard uncertainty of homogeneity; $u_{stab}$ is the standard uncertainty of long-term instability.

Certified values of the pH CRM as an activity of hydrogen ions expressed in units of pH have been obtained on the state standard of the pH scale. The scientific novelty and purpose of this paper is to assess the measurement capabilities of the State scientific metrological center for further transfer of the pH measurement units and calibration of working standards.

### *Method*

Estimation of solutions pH was carried out as an indirect measurement. The reference value of pH was determined from the results of measurements of the electromotive force (EMF), temperature, pressure and other parameters.

### *Results and discussion*

The entire procedure of determining the pH of reference buffer solutions based on the measurement of the EMF of the cell and has been nominally divided into three stages. The first stage includes the estimation of standard silver chloride electrode potential. Standard silver chloride electrode potential $E^0_{\text{Ag/AgCl}}$ is determined by measuring the EMF of the Harned cells Ag|AgCl|HCl (0.01M)| $H_2$ Pt [3] using the formula:

$$E^0_{\text{Ag/AgCl}} = E + \frac{2RT\ln 10}{F}\left(\lg(m_{\text{HCl}}) + \lg(\gamma_{\pm\text{HCl}}) + 0.25\lg\frac{p^0}{p_{\text{H}_2}}\right., \tag{2}$$

where $E$ is the measured voltage in V; $R$ is the universal gas constant, which is equal to (8.314510 ± ± 0.000070) J×mol$^{-1}$×K$^{-1}$; $T$ is the thermodynamic temperature, K; $F$ is the Faraday constant, which is equal to (9.648530 ± 0.00002)×10$^4$ C×mol$^{-1}$; $m_{\text{HCl}}$ is the HCl molality in the solution; $\gamma_{\pm\text{HCl}}$ is the molality activity coefficient of chloride ions; $P^0$ is the normal atmospheric pressure of 101.325 kPa.

Equation (1) is a measurement model equation in determining of a standard silver chloride electrode $E^0_{\text{Ag/AgCl}}$.

The main components of the uncertainty [4] are as follows:

– the measurement of the EMF of the electrode $E$;
– the measurement of the temperature $T$;
– the molality concentration of the solution of HCl, $m_{\text{HCl}}$;
– the hydrogen partial pressure $P_{\text{H}_2}$;
– the coefficient of ion activity $\text{Cl}^-$ $\gamma_{\pm\text{HCl}}$.

Uncertainties associated with $R$ and $F$ were insignificant and not taken into account during calculating the combined standard uncertainty. Standard silver chloride electrode potential was determined as $E^0_{\text{Ag/AgCl}}$ = = 0.222107 V with a standard uncertainty $u(E^0_{\text{Ag/AgCl}}) = 8.26\cdot10^{-5}$ V.

The second stage includes the determination of the function of acidity $p(\alpha_\text{H}Y_{\text{Cl}})$ and the limit of the function of acidity $p(\alpha_\text{H}Y_{\text{Cl}})^0$. At the second stage EMF, the $E$ of nine Harned cells, has been measured, these cells are filled with the reference buffer solution, whose $pH(X)$ has been determined. These nine cells have been divided into three groups, each containing three cells. The difference between the groups is in the concentration of the alkali metal chloride added to the buffer solution. Usually the following molality of chloride ions is used: $m_{\text{Cl}}$=0.005; 0.010; 0.015 mol/kg.

Values of function of acidity $p(a_\text{H}\gamma_{\text{Cl}})$ in 3 groups of cells have been obtained from the measured EMF and previously determined $E^0_{\text{Ag/AgCl}}$:

$$p(\alpha_\text{H}\gamma_{\text{Cl}}) = \frac{\left(E - E^o_{\text{Ag/AgCl}}\right)F}{RT\ln 10} + \lg m_{\text{Cl}} + 0.5\lg\left(\frac{p^0}{p_{\text{H}_2}}\right). \tag{3}$$

Equation (3) is the measurement model equation for estimate of the function of acidity. The main components of uncertainty in estimation acidity function $p(\alpha_\text{H}\gamma_{\text{Cl}})$ are:

– the estimated value $E^0_{Ag/AgCl}$;
– the determination of the EMF of the electrode $E$;
– the determination of the temperature $T$;
– the molality concentration of the solution of HCl $m_{\text{HCl}}$;
– the hydrogen partial pressure $P_{H_2}$.

Estimates of all the major components have been identified at the first stage and are shown in Tables 1 and 2.

Limit of the function of acidity was specified equal to $p(\alpha_\text{H}Y_{\text{Cl}})^0$= 9.23980 with a standard uncertainty $u(\alpha_\text{H}Y_{\text{Cl}})$ =1.48·10$^{-3}$.

Stage 3 includes calculation of the certified value of the standard sample $pH(X)$

$$pH(X) = p\left(a_\text{H}\gamma_{\text{Cl}}\right)^0 + \lg\gamma^0_{\text{Cl}};$$

$$\lg\gamma^0_{\text{Cl}} = \frac{A\sqrt{I}}{1+1.5\sqrt{I}},$$

where $A$ is the Debye-Hückel constant, $I$ is the ionic strength of the buffer.

Estimates of all the main components identified in the first stage are given in Tables 3 and 4.

Table 1

**Estimation of input values of uncertainty**

| Influencing quantity | Estimated uncertainty |
|---|---|
| Measured value of EMF,<br>$E = 0.463320$ V | $u_B(E) = \frac{\text{error of the multi meter from the certificate}}{\sqrt{3}} = 1.2010^{-5}$ V |
| The temperature of measurement,<br>$T = 298.153$ K | $u(E) = 1.1010^{-2}$ K<br>(specified in the certificate at the thermometer ) |
| Molality of the HCl solution, mol/kg | $u(m_{\text{HCl}}) = 1.2010^{-5}$ mol/kg<br>(specified in the certificate of analysis on a solution*)* |
| The partial pressure of hydrogen, $P_{H2}$ | $u(P_{H_2}) = 5.0$ Pa<br>(determined by the accuracy of measurement of atmospheric pressure) |
| Molality activity coefficient of chloride ions, $\gamma_{\pm HCl}$ | $u(\gamma_{\pm\text{HCl}}) = 9.3\cdot10^{-4}$<br>(from the IUPAC data) |

Table 2

**Uncertainty budget at determination of the capacity of the standard silver chloride electrode $E^0_{\text{Ag/AgCl}}$**

| Quantity $x_i$ | Value $x_i$ | Unit | Standard uncertainty $u(x_i)$ | Sensitivity factor $c_i$ | Unit | Contribution of the uncertainty $c_i \cdot u(x_i)$ | Unit |
|---|---|---|---|---|---|---|---|
| $E$ | 0.463320 | V | $1.20\cdot10^{-5}$ | 1 | – | $1.2\cdot10^{-5}$ | V |
| $T$ | 298.153 | K | $1.10\cdot10^{-2}$ | $\frac{2R\ln10}{F}\begin{pmatrix}\lg(m_{\text{HCl}})+\lg(\gamma_{\pm\text{HCl}})+\\ +0.25\lg\frac{p^0}{p_{\text{H}_2}}\end{pmatrix}= \\ =8.1\cdot10^{-4}$ | V/K | $-8.89\cdot10^{-6}$ | V |
| $m_{\text{HCl}}$ | 0.01 | mol/kg | $1.2\cdot10^{-5}$ | $\frac{2RT}{Fm_{\text{HCl}}}=5.14$ | V·kg/mol | $6.17\cdot10^{-5}$ | V |
| $P_{\text{H}_2}$ | 96686.0 | Pa | 5.0 | $-\frac{2RT}{FP_{\text{H}_2}}=-1.33\cdot10^{-7}$ | V/Pa | $-6.65\cdot10^{-7}$ | V |
| $\gamma_{\pm\text{HCl}}$ | 0.9042 | mol/kg | $9.3\cdot10^{-4}$ | $\frac{2RT}{F\gamma_{\pm\text{HCl}}}=5.68\cdot10^{-2}$ | V·kg/mol | $5.29\cdot10^{-5}$ | V |
| $E^0_{\text{Ag/AgCl}}$ | 0.222107 | V | | | | $8.26\cdot10^{-5}$ | V |

Table 3

**Uncertainty budget for the estimate of function of acidity $p(\alpha_H Y_{Cl})^0$**

| Size $x_i$ | Value $x_i$ | Unit | Standard uncertainty $u(x_i)$ | Sensitivity factor $c_i$ | Unit | Contribution of the uncertainty $c_i \cdot u(x_i)$ | Unit |
|---|---|---|---|---|---|---|---|
| 1 | 2 | 3 | 4 | 5 | 6 | 7 | 8 |
| $E$ | 0.904029 | V | $1.20\cdot10^{-5}$ | $\frac{F}{RT\ln(10)}=16.9$ | 1/V | $2.03\cdot10^{-4}$ | – |
| $E^0_{\text{Ag/AgCl}}$ | 0.222107 | V | $8.26\cdot10^{-5}$ | $-\frac{F}{RT\ln(10)}=-16.9$ | 1/V | $-1.40\cdot10^{-3}$ | – |
| $T$ | 298.152 | K | $1.1\cdot10^{-2}$ | $-\frac{(E-E^0_{\text{Ag/AgCl}})F}{RT^2\ln(10)}=-3.86\cdot10^{-2}$ | 1/K | $-4.25\cdot10^{-4}$ | – |

Continuation of Table 3

| 1 | 2 | 3 | 4 | 5 | 6 | 7 | 8 |
|---|---|---|---|---|---|---|---|
| $m_{\mathrm{HCl}}$ | 0.005 | mol/kg | $2.010^{-6}$ | $\frac{1}{m_{\mathrm{HCl}}\ln(10)} = 86.86$ | kg/mol | $-1.74\cdot10^{-4}$ | – |
| $P_{\mathrm{H_2}}$ | 96457.0 | Pa | 5.0 | $-\frac{0.5}{P_{\mathrm{H_2}}\ln(10)} = -2.25\cdot10^{-6}$ | 1/Pa | $-1.13\cdot10^{-5}$ | – |
| $p\left(a_{\mathrm{H}}\gamma_{\mathrm{Cl}}\right)^0$ | 9.23980 | | | | | $1.48\cdot10^{-3}$ | – |

Table 4

**Uncertainty budget for the determination of acidity function $p(\alpha_{\mathrm{H}}Y_{\mathrm{Cl}})^0$**

| Size $x_i$ | Value $x_i$ | Unit | Standard uncertainty $u(x_i)$ | Sensitivity factor $c_i$ | Contribution of the uncertainty $c_i{\cdot}u(x_i)$ |
|---|---|---|---|---|---|
| $p\left(a_{\mathrm{H}}\gamma_{\mathrm{Cl}}\right)^0$ | 9.23980 | – | $1.48\cdot10^{-3}$ | 1 | $1.48\cdot10^{-3}$ |
| $\lg\gamma^0_{\mathrm{Cl}}$ | –0.05960 | – | $0.58\cdot10^{-5}$ | 1 | $0.58\cdot10^{-5}$ |
| $pH(X)$ | 9.1802 | | | | $1.48\cdot10^{-3}$ |

Thus, the certified value of the standard sample is determined as $pH(X)$ = 9.1802 with the standard uncertainty $u_{char}= 1.48\cdot10^{-3}$.

Stability estimation of CRM is carried out within six months according to the [5].

The obtained data and calculations are shown in Table 5.

Table 5

**The results of stability test of CRM pH = 9.18**

| Time, $n$ | Current value, $Xn$ | Value of difference, $dn$ | $\alpha{\cdot}dn$ | $(1{-}\alpha){\cdot}U$ | $Un$ | Swing, $R$ |
|---|---|---|---|---|---|---|
| 0 | 9.1802 | 0.0000 | 0.0000 | 0 | 0 | |
| 1 | 9.1808 | 0.0006 | 0.0002 | 0 | 0.0002 | 0.0006 |
| 2 | 9.1818 | 0.0016 | 0.0005 | 0.0001 | 0.0006 | 0.0010 |
| 3 | 9.1811 | 0.0009 | 0.0003 | 0.0004 | 0.0007 | –0.0007 |
| 4 | 9.1809 | 0.0007 | 0.0002 | 0.0005 | 0.0007 | –0.0002 |
| 5 | 9.1804 | 0.0002 | 0.0001 | 0.0005 | 0.0005 | 0.0005 |
| 6 | 9.1815 | 0.0013 | 0.0004 | 0.0004 | 0.0008 | –0.0011 |

The standard uncertainty from the instability was calculated according to [1].

Average moving range is as follows:

$$\overline{R} = 0.00022,\ S_D = 0.89\times\overline{R} = 0.89\times0.00022 = 0.000193;$$

$$S_a = \frac{S_D}{\sqrt{\sum_{i=1}^{n} t_i^2}} = \frac{0.000193}{\sqrt{1^2+2^2+3^2+4^2+5^2+6^2}} = 0.0000202\,;$$

$$u_{stab} = 0.0000202\times7 = 0.0001415 = 0.14\cdot10^{-3}.$$

Measurement performed for an estimation of the uncertainty on account of in homogeneity, had pointed, that contribution of $u_h$ was insignificant and it was not taken into account to combined standard uncertainty.

Combined standard uncertainty of certified value of the reference buffer solution of 1th category is estimated using equation (1):

$$u_c\left(A\right) = \sqrt{u_{char}^2 + u_{stab}^2} = \sqrt{\left(1.48\cdot10^{-3}\right)^2 + \left(0.14\cdot10^{-3}\right)^2} = 1.4910^{-3}\,.$$

Extended standard uncertainty is:

$$U(A) = k{\cdot}u_c(A) = 2\cdot1.49\cdot10^{-3} = 2.98\cdot10^{-3} \approx 0.003.$$

Certified value of the pH state certified reference materials, standard buffer solution 1 category, will be equal to (9.1802 ± 0.003) pH at $k = 2$ for 95 % confidence level. Currently work to further improve the state standard is underway [6, 7].

## *Conclusions*

Measurements of pH are influenced by the number of factors. The main contribution to the measurement uncertainty is made by the potential of the chlorine-silver electrode.

## References

1 Государственная система обеспечения единства измерений. Оценивание метрологических характеристик стандартных образцов: РМГ 93–2015. [Введен в действие от 2017–01–01]. — М.: Стандартинформ Российской Федерации, 2016. — 27 с. — (Межгосударственный стандарт).

2 Guide to the expression of uncertainty in measurement. — ISO, Switzerland, 1993. — 120 p.

3 Harned H.S. The Physical Chemistry of Electrolytic Solutions / H.S. Harned, D.D. Owen. — New York: Reinhold, 1958. — 234 p.

4 Measurement of pH. Definition, standards, and procedures. IUPAC Recommendations. 2002.

5 Государственная система обеспечения единства измерений Республики Казахстан. Стандартные образцы состава и свойств веществ и материалов. Методика оценивания характеристики стабильности: СТ РК 2.188–2010. [Введен в действие от 2011–01–07]. — М.: Стандартинформ Российской Федерации, 2010. — 44 с. — (Национальный стандарт Республики Казахстан).

6 APMP.QM-K91 and APMP.QM-P29. APMP comparison on pH measurement of a phthalate buffer. Call and technical protocol. — 2014. — 5 p.

7 Жанасбаева Б.К. Исследования государственного эталона шкалы pH / Б.К. Жанасбаева // Метрология. — 2017. — № 3. — С. 14, 15.

---

Б.К. Жанасбаева, Г.К. Бектұрғанова, В.А. Донбаева

## Эталондық буферлік ерітіндіні аттестаттау кезіндегі белгісіздікті бағалау

pH шкаласының Мемлекеттік эталоны Қазақстан Республикасының бастапқы эталоны болып табылады, ол өзінің халықаралық салыстырмалармен баламалылығын растады: APMP QM-R19 (2014) негізгі салыстырмаларымен және COOMET 655/EN/15 (2017) Пилоттық салыстырмаларымен. Эталон сутекті және хлоркүмісті электродтары бар тасымалсыз (Харнед ұяшықтары) ұяшықтарды қолдана отырып, pH өлшеудің бастапқы әдісін жүзеге асырады. Бұл ұяшық өлшеу нәтижелерінің жоғары жаңғыртылуымен сипатталады. Эталон сондай-ақ өлшеу құралдарын тексеру және сапаны ішкі бақылау кезінде зертханалар кеңінен қолданатын мемлекеттік стандартты үлгілерді (ГСО) әзірлеуге мүмкіндік береді. pH ГСО-20 ºС температурада меншікті электрөткізгіштігі $2\cdot10^{-4}$ См/м аспайтын бидистилденген деионизацияланған судың 1 кг-да ерітілген химиялық заттардың дәл ілімін білдіреді. Жұмыста 9.010–9.280 pH диапазонындағы стандартты буферлік ерітінділердің pH CRM аттестатталған мәндерінің белгісіздігін бағалау ұсынылған. Ерітінділердің pH — анықтау-өлшеудің жанама түрі. pH эталондық мәні электр қозғаушы күштің, температураның, қысымның және басқа да параметрлердің өлшеу нәтижелерінен анықталады. Эталондық электрхимиялық ұяшықтың ЭҚК өлшеулерінің дұрыстығы сутекті және хлоркүмісті электродтардың көрсеткіштеріне тәуелді.

*Кілт сөздер:* өлшеулердің белгісіздігі, мемлекеттік стандартты үлгілер, pH буферлік үйлесімдер, бастапқы мемлекеттік эталон, халықаралық салыстырулар, электрқозғаушы күш, стандартты әлеует.

---

Б.К. Жанасбаева, Г.К. Бектурганова, В.А. Донбаева

## Оценка неопределенности при аттестации эталонного буферного раствора

Государственный эталон шкалы pH является первичным эталоном Республики Казахстан, который подтвердил свою эквивалентность международными сличениями: ключевыми сличениями APMP QM-R19 (2014) и пилотными сличениями COOMET 655/EN/15 (2017). Эталон реализует первичный метод измерений pH с применением ячеек без переноса (ячеек Харнеда) с водородным и хлорсеребряными электродами. Данная ячейка характеризуется высокой воспроизводимостью результатов измерений. На эталоне аттестуются государственные стандартные образцы (ГСО), которые широко используются лабораториями при поверке средств измерений и внутреннем контроле качества. ГСО pH представляют собой точные навески химических веществ, растворенные в 1 кг бидистиллированной деионизированной воды с удельной электрической проводимостью не более $2 \cdot 10^{-4}$ См/м при температуре 20 ºС. В работе представлена оценка неопределенности аттестованных значений pH CRM — стандартных буферных растворов в диапазоне 9,010–9,280 pH. Определение pH растворов — косвенный вид измерений. Эталонное значение pH определяется из результатов измерений электродвижущей силы, температуры, давления и других параметров.

*Ключевые слова:* неопределенность измерений, государственные стандартные образцы, буферные растворы pH, первичный государственный эталон, международные сличения, электродвижущая сила, стандартный потенциал.

## References

1 Hosudarstvennaia sistema obespecheniia edinstva izmerenii. Otsenivanie metrolohicheskikh kharakteristik standartnykh obraztsov [The state system of ensuring the unity of measurements. Evaluation of metrological characteristics of standard samples]. (2017) *RMG 93–2015 from 1th January 2017*. Moscow: Standartinform Rossiskoi Federatsii [in Russian].

2 Guide to the Expression of Uncertainty in Measurement. (1993). ISO, Switzerland.

3 Harned, H.S., & Owen, D.D. (1958). *The Physical Chemistry of Electrolytic Solutions*. New York: Reinhold.

4 Measurement of pH. Definition, standards, and procedures. IUPAC Recommendations (2002).

5 Hosudarstvennaia sistema obespecheniia edinstva izmerenii Respubliki Kazakhstan. Standarnye obraztsy sostava i svoistv veshchestv i materialov. Metodika otsenivaniia kharakteristiki stabilnosti [The state system of ensuring the unity of measurements of the Republic of Kazhakstan. Reference materials of composition and properties of substances and materials. Methods of assessment of stability characteristics] (2010): *ST RK 2.188–2010 from 7th January 2011*. Moscow: Standartinform Rossiskoi Federatsii [in Russian].

6 APMP.QM-K91 and APMP.QM-P29. APMP comparison on pH measurement of a phthalate buffer. Call and technical protocol. (2014).

7 Zhanasbaeva, B.K. (2017). Issledovaniia hosudarstvennoho etalona shkaly pH [Studies of the state standard of the pH scale]. *Metrolohiia — Metrology, 3,* 14–15.

## БЕЙОРГАНИКАЛЫҚ ХИМИЯ
## НЕОРГАНИЧЕСКАЯ ХИМИЯ
## INORGANIC CHEMISTRY

DOI: 10.31489/2019Ch1/60-65

UDC 536.63:546.244:65

K.T. Rustembekov, M.S. Kasymova, D.A. Kaikenov,
V.N. Fomin, S.K. Aldabergenova, A.A. Toybek

*Ye.A. Buketov Karaganda State University, Kazakhstan*
*(E-mail: rustembekov_kt@mail.ru)*

# Calorimetry of new double dysprosium tellurite

New dysprosium-barium double tellurite was synthesized based on ceramic technology. The formation of the equilibrium composition of the compound is controlled by X-ray phase analysis, the results of which revealed that $DyBaTeO_{4.5}$ dysprosium tellurite was synthesized. For the first time, a calorimetric study of the heat capacity of the new double tellurite $DyBaTeO_{4.5}$ was carried out in the temperature range of 298.15–673 K. The calibration of the instrument was carried out on the basis of the determination of the heat meter thermal conductivity. The operation of the calorimeter was checked by measuring the $\alpha$-$Al_2O_3$ heat capacity. The experimental data of the specific and molar heat capacity were processed by the methods of mathematical statistics. The equation for the dependence $C_p^o \sim f(T)$ is derived based on the experimental data. The temperature dependences of the thermodynamic functions $H^o(T)–H^o(298.15)$, $S^o(T)$ and, $F^{xx}(T)$ are determined from $C_p^o \sim f(T)$ and the calculated value of $S^o(298.15)$ of tellurite. Anomalous jumps are observed on the dependence $C_p^o \sim f(T)$, which are probably related to second-order phase transitions. The thermodynamic characteristics of new tellurite can serve as background information for fundamental data banks and reference books, and also used to predict the thermochemical constants of similar compounds.

*Keywords:* dysprosium-barium tellurite, calorimetry, heat capacity, phase transitions, thermodynamic functions.

Modern electronic technology poses the problem of searching for new compounds with valuable electrophysical properties and their in-depth physical and chemical research. Criteria for assessing the prospects of using a particular material put forward the relative cheapness and simplicity of their production, environmental safety as priority requirements, and also one of the decisive factors when choosing a new material is availability of such valuable properties as semiconductor, ferroelectric, piezoelectric and pyroelectric, radioluminescent and superconducting.

Therefore, compounds formed in systems consisting of REE oxides, alkaline earth metals and tellurium are of particular interest for inorganic materials science, since they have promising physical and physicochemical properties [1]. The purpose of this work is a calorimetric study of the heat capacity of new dysprosium double tellurite in the temperature range of 298.15–673 K.

Dysprosium (III), tellurium (IV) and barium carbonate («chemically pure» oxides) were used as starting components for the synthesis in a stoichiometric ratio. Dysprosium-barium tellurite $DyBaTeO_{4.5}$ was synthesized by the method of ceramic technology. The method of synthesis is similar to that given by us earlier in [2]. The formation of the equilibrium composition of the compound was monitored by X-ray phase analysis on a DRON-2.0 diffactometer. X-ray data show that the synthesized compound crystallizes in the structural type of distorted perovskite $P_m3_m$ [3].

The heat capacity of dysprosium-barium double tellurite was studied by dynamic calorimetry on an IT-C-400 serial device in the 298.15–673 K temperature range. The limit of the permissible error of the device is ± 10 % according to passport data [2]. The calibration of the instrument was carried out on the basis of determining the thermal conductivity of the heat meter $K_T$ [4]. For this, several experiments were carried out with a copper sample and an empty ampoule. Thermal conductivity of the heat meter was determined by the formula:

$$K_T = C_{cs} / (\overline{\tau}_{TC} - \overline{\tau}_T^0),$$

where $C_{cs}$ is the total heat capacity of the copper sample, J/(mol×K); $\overline{\tau}_{TC}$ is the average value of the lag time on the heat meter in experiments with a copper sample, s; $\overline{\tau}_T^0$ is the average value of the lag time in experiments with an empty ampoule, s.

The total heat capacity of the copper sample was calculated by the formula:

$$C_{cs} = C_C \times m_s,$$

where $C_C$ is the tabular value of the specific heat capacity of copper, kJ/(kg×K); $m_s$ is the mass of the copper sample, kg.

The value of the specific heat capacity of the analyte was calculated by the formula:

$$C_s = \frac{K_T}{m_0} \times (\tau_T - \tau_T{}^0),$$

where $K_T$ is the heat conductivity of the heat meter; $m_0$ is the mass of the test substance, kg; $\tau_T$ is the lag time of the temperature at the heat meter, s; $\tau_T{}^0$ is the lag time of the temperature on the heat meter in experiments with an empty ampoule, s.

Taking into account the molar mass, the molar heat capacity was calculated using the specific heat capacity by the formula:

$$C_M = C_s \times M,$$

where $C_s$ is the specific heat capacity of substance, J/(g×K); $M$ is the molar mass of the substance, g/mol.

Five parallel experiments were carried out at each fixed temperature, the results of which were averaged and processed by methods of mathematical statistics [5].

At each temperature, the standard deviation $\overline{\delta}$ was estimated for the averaged values of the specific heat capacity using the formula:

$$\overline{\delta} = \sqrt{\sum_{i=1}^{n} \frac{(C_i - \overline{c})^2}{n-1}},$$

where $n$ is the number of experiments; $C_i$ is the measured value of the specific heat capacity; $\overline{c}$ is arithmetic average of the measured values of specific heat capacity.

The random error component was calculated for the average values of the molar heat capacity:

$$\overset{\circ}{\Delta} = \frac{\delta t_p}{\overline{c}} \cdot 100,$$

where $\overset{\circ}{\Delta}$ is the random component of the error in %; $t_p$ is the Student's coefficient (for $n = 5$ $t_p = 2.78$ with $p = 0.95$ confidence interval).

The systematic component of the error was calculated by the formula:

$$\Delta_c = \frac{\overline{C} - C_0}{C_0} \cdot 100,$$

where $\Delta_c$ is the systematic component of the error in %; $C_0$ is the heat capacity value of the model measure taken at the temperature at which the heat capacity was determined.

In our studies, the systematic error and errors in temperature measurements were not included in the calculation, since they were negligible compared to the random component.

The work of the calorimeter was tested by determining the $\alpha$-$Al_2O_3$ heat capacity. The resulting value of $C_p{}^0(298.15)$ for $\alpha$-$Al_2O_3$, which is equal to 76.0 J/(mol×K), is in satisfactory agreement with its recommended value of 79.0 J/(mol×K) [6]. These data show not only the reliability of the results obtained, but also the negligible value of the systematic error, such as the measurement of the temperature error.

The results of calorimetric studies of the heat capacity of tellurite are shown in Table 1.

Table 1

**Experimental values of specific and molar heat capacities $DyBaTeO_{4,5}$**

| $T$, K | $C_p \pm \bar{\delta}$, J/(g×K) | $C_p^0 \pm \overset{0}{\Delta}$, J/mol×K |
|---|---|---|
| 298.15 | 0.5361±0.0312 | 250±15 |
| 323 | 0.5061±0.0811 | 260±24 |
| 348 | 0.5464±0.0643 | 280±26 |
| 373 | 0.6393±0.0521 | 310±27 |
| 398 | 0.7721±0.0251 | 360±1 |
| 423 | 0.9352±0.0651 | 420±29 |
| 448 | 1.1234±0.0721 | 500±34 |
| 473 | 1.3293±0.0452 | 620±2 |
| 498 | 0.8582±0.0187 | 400±4 |
| 523 | 0.6650±0.0335 | 310±16 |
| 548 | 0.6891±0.0295 | 330±12 |
| 573 | 0.7932±0.0445 | 370±19 |
| 598 | 0.9651±0.0362 | 450±16 |
| 623 | 0.8154±0.0257 | 380±10 |
| 648 | 0.7283±0.0452 | 350±21 |
| 673 | 0.6961±0.0329 | 325±2 |

It can be seen from the data presented in Table 1 that the random components of the error of the experimental values of the heat capacities are within the limits of the error of the device over the entire temperature range. The Figure shows the temperature dependence of the heat capacity of the tellurite synthesized.

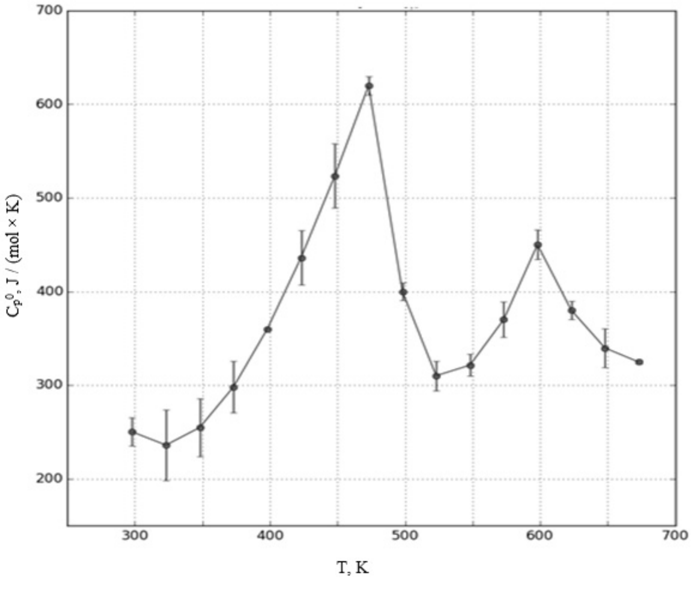

Figure. Temperature dependence of the $DyBaTeO_{4.5}$ heat capacity

Based on the data in Table 1 and the Figure, it was found that the curve of the temperature dependence of the heat capacity of double tellurite $DyBaTeO_{4.5}$ at 473 and 598 K revealed abrupt anomalous λ–shaped jumps, probably due to the second-order phase transitions. These transitions can be associated with cationic redistribution, with changes in the coefficient of thermal expansion, as well as changes in the magnetic moment of the tellurite synthesized or changes in the dielectric constant, electrical resistivity, etc. Due to the presence of the second-order phase transition, the dependence of the compound was described by several equations, the coefficients of which are given in Table 2.

Table 2

**Equations of the temperature dependence of the heat capacity of double tellurite $DyBaTeO_{4.5}$**

| Equation coefficients $C_p^0 = a + bT + cT^{-2}$, J/mol×K | | | $\Delta T$, K |
|---|---|---|---|
| $a$ | $b\cdot10^{-3}$ | $c\cdot10^{5}$ | |
| –(2550.8±76.5) | 5804.6±174.1 | 951.3±28.5 | 298.15–473 |
| –(22283.2±668.5) | 28357.0±850.7 | 21232.6±637.0 | 473–523 |
| –(9319.0±279.6) | 12143.1±364.3 | 8966.9±269.0 | 523–598 |
| –(7443.4±223.3) | 7646.6±229.4 | 11875.2±356.3 | 598–673 |

There were used the values of average random errors for all considered temperature ranges to determine the error coefficients in the equations of dependencies $C_p^0 \sim f(T)$. Due to the fact that the technical characteristics of the device do not allow us to directly calculate the standard entropy $S°(298.15)$ of the test compound from the experimental data on $C_p^0(T)$ it was evaluated using the Kumok ion increment method [7]. Based on the known relations [8, 9] the temperature dependences of the functions were calculated $S°(T)$, $H°(T)–H°(298.15)$ and $F^{xx}(T)$ using experimental data on $C_p^0 \sim f(T)$ and calculated values for $S°(298.15)$. The results are shown in Table 3.

Table 3

**Thermodynamic functions of tellurite $DyBaTeO_{4.5}$ in the temperature range of 298.15–673 K**

| $\Delta T$, K | $C_p^0(T)\pm\overset{\circ}{\Delta}$, J/(mol×K) | $S^0(T)\pm\overset{\circ}{\Delta}$, J/(mol×K) | $H^{\circ}(T)-H^{\circ}(298,15)\pm\overset{\circ}{\Delta}$, J/mol | $F^{xx}(T)\pm\overset{0}{\Delta}$, J/(mol×K) |
|---|---|---|---|---|
| 298,15 | 250±15 | 210±8 | - | 210±6 |
| 323 | 260±24 | 229±7 | 5959±60 | 211±7 |
| 348 | 280±26 | 247±8 | 12033±146 | 213±7 |
| 373 | 310±14 | 266±9 | 18899±187 | 216±8 |
| 398 | 360±7 | 288±11 | 27092±216 | 216±9 |
| 423 | 420±33 | 312±13 | 37018±270 | 226±9 |
| 448 | 500±32 | 339±16 | 48996±357 | 230±10 |
| 473 | 620±15 | 370±19 | 63275±478 | 237±11 |
| 498 | 400±15 | 396±12 | 75726±597 | 244±12 |
| 523 | 310±9 | 413±19 | 84357±788 | 252±12 |
| 548 | 330±17 | 427±10 | 92163±898 | 260±13 |
| 573 | 370±17 | 443±11 | 100733±8 | 267±13 |
| 598 | 450±17 | 460±14 | 110923±998 | 275±14 |
| 623 | 380±18 | 477±11 | 121231±1109 | 282±14 |
| 648 | 350±17 | 491±10 | 130170±1181 | 290±15 |
| 673 | 325±17 | 503±20 | 138424±1219 | 298±15 |

The errors in the temperature dependence of enthalpy were estimated with the average random component of the error in heat capacity, and the errors in temperature dependence $S°(T)$ and $F^{xx}(T)$ were calculated by summing the average error of the experimental determination of heat capacity and the accuracy of the calculation of entropy (±3 %).

Thus, for the first time, the isobaric heat capacity of new double dysprosium tellurite $DyBaTeO_{4.5}$ was investigated by the dynamic calorimetry method in the range of 298.15–673 K.

The standard heat capacity $C_p°(298.15) = 250 \pm 15$ (J/mol×K) was determined for tellurite $DyBaTeO_{4.5}$ experimentally. The equations of temperature dependences of the heat capacity for the compound under study were derived based on the experimental values.

Abrupt anomalous jumps of λ–shaped effects related to the second-order phase transition were detected for the tellurite under study, at 473 and 598 K, on the dependence curve $C_p^{\,0}(T) \sim f(T)$. The standard entropy of the double tellurite under study was calculated by the method of ionic increments. The temperature dependences of the heat capacity were calculated in the range of 298.15–673 K $C_p^0(T)$ and thermodynamic functions such as entropy $S°(T)$, enthalpy $H°(T)–H°(298.15)$ and reduced thermodynamic potential $F^{xx}(T)$ of tellurite $DyBaTeO_{4.5}$.

The presence of the second-order phase transition in the temperature dependence curve of the heat capacity suggests that this compound may have unique electrophysical properties [10]. Thermochemical and thermodynamic characteristics of tellurite can be initial information files of fundamental reference books and data banks and are of interest for chemical informatics, and also have theoretical and practical interest for inorganic materials science in the field of directional synthesis of compounds with polyfunctional properties.

*This work was supported by the Ministry of Education and Science of the Republic of Kazakhstan [grant number AP05132001].*

## References

1 Набока М.Н. Структура и свойства тонких пленок на основе соединений редкоземельных металлов / М.Н. Набока, А.С. Палатник, В.Я. Шевченко // Журн. Всесоюз. хим. общества им. Д.И. Менделеева. — 1981. — Т. 26, № 6. — С. 31.

2 Техническое описание и инструкции по эксплуатации ИТ-С-400. — Актюбинск: Актюбинский завод «Эталон», 1986. — 48 с.

3 Рустембеков К.Т. Диспрозий қос теллуриттерінің синтезі, кристаллохимиясы және құрылысы / К.Т. Рустембеков, А.А. Тойбек, М. Стоев // Вестн. Караганд. ун-та. Сер. Химия. — 2016. — Т. 84, № 4. — С. 49–54.

4 Платунов Е.С. Теплофизические измерения и приборы / Е.С. Платунов, С.Е. Буравой, В.В. Куперин, Г.С. Петров. — Л.: Машиностроение, 1986. — 256 с.

5 Спиридонов В.П. Математическая обработка экспериментальных данных / В.П. Спиридонов, Л.В. Лопаткин. — М.: Изд-во МГУ, 1970. — 221 с.

6 Robie R.A. Thermodynamic Properties of Minerals and Related Substances at 298.15 and ($10^5$ Paskals) Pressure and at Higher Temperatures / R.A. Robie, B.S. Hewingway, I.R. Fisher. — Washington: United States Government Printing Office, 1978. — 456 p.

7 Кумок В.Н. Прямые и обратные задачи химической термодинамики / В.Н. Кумок. — Новосибирск: Наука, 1987. — С. 108.

8 Термодинамические свойства индивидуальных веществ / под ред. В.П. Глушко. — М.: Наука, 1978. — Т. 1. — 496 с.

9 Герасимов Я.И. Химическая термодинамика в цветной металлургии: в 4-х т. / Я.И. Герасимов, А.Н. Крестовников, А.С. Шахов. — М.: Металлургия, 1960. — Т. 1. — 230 с.

10 Rustembekov K.T. X-ray Diffraction and Thermodynamic Characteristics for Tellurite of the Composition $Li_2CeTeO_5$ / K.T. Rustembekov, A.Zh. Bekturganovna // Russian Journal of Physical Chemistry A. — 2017. — Vol. 91, No. 4. — P. 622–626.

К.Т. Рүстембеков, М.С. Қасымова, Д.А. Қайкенов,
В.Н. Фомин, С.К. Алдабергенова, А.А. Тойбек

## Диспрозий жаңа қос теллуритінің калориметриясы

Керамикалық технологиямен жаңа диспрозий-барий қос теллуриті синтезделді. Қосылыстың тепетеңдік құрамының құрылысы рентгенфазалық талдау әдісімен бақыланды. Рентгенфазалық талдау нәтижесі бойынша $DyBaTeO_{4,5}$ қос теллуритінің синтезделгені анықталды. Алғаш рет 298,15–673 К аралығында жаңа $DyBaTeO_{4,5}$ диспрозий қос теллуритінің жылусыйымдылығы калориметрлік әдіспен зерттелді. Құрылғының градуирленуі жылуөлшеуіштің жылуөткізгіштігін анықтау негізінде жүзеге асырылды. Калориметрдің жұмысы α-$Al_2O_3$-тің жылу сыйымдылығын өлшеумен тексерілді. Меншікті және мольдік жылусыйымдылықтарының тәжірибелік мәліметтері математикалық статистика әдістерімен өңделді. Тәжірибелік мәліметтердің негізінде $C_p°{\sim}f(T)$ тәуелділік теңдеуі шығарылды. $C_p°{\sim}f(T)$ және теллуриттің есептелген $S°(298,15)$ мәні бойынша $H°(T)–H°(298,15)$, $S°(T)$ және $Φ^{xx}(T)$ термодинамикалық функцияларының температуралық тәуелділіктері анықталды. $C_p°{\sim}f(T)$ тәуелділігінде, ІІ-текті фазалық ауысумен болуы мүмкін, күрт аномалды секірулер байқалды. Жаңа теллуриттің термодинамикалық сипаттамалары іргелі мәліметтер банкіне және анықтамаларға бастапқы материалдар болуы ықтимал, сол сияқты ұқсас қосылыстардың термохимиялық константаларын болжауда қолданылуы мүмкін.

*Кілт сөздер:* диспрозий-барий теллуриті, калориметрия, жылусыйымдылығы, фазалық түрленулер, термодинамикалық функциялар.

К.Т. Рустембеков, М.С. Касымова, Д.А. Кайкенов,
В.Н. Фомин, С.К. Алдабергенова, А.А. Тойбек

## Калориметрия нового двойного теллурита диспрозия

На основе керамической технологии синтезирован новый двойной теллурит диспрозия-бария. Образование равновесного состава соединения контролировано методом рентгенофазового анализа, по результатам которого было установлено, что синтезирован двойной теллурит диспрозия $DyBaTeO_{4,5}$. Впервые в интервале 298,15–673 К проведено калориметрическое исследование теплоемкости нового двойного теллурита $DyBaTeO_{4,5}$. Градуировку прибора осуществляли на основании определения тепловой проводимости тепломера. Проверку работы калориметра проводили измерением теплоемкости $\alpha$-$Al_2O_3$. Экспериментальные данные удельной и мольной теплоемкости обработаны методами математической статистики. На основе экспериментальных данных выведено уравнение зависимости $C_p^{o}{\sim}f(T)$. По $C_p^{o}{\sim}f(T)$ и вычисленному значению $S^{o}(298,15)$ теллурита определены температурные зависимости термодинамических функций $H^{o}(T){-}H^{o}(298,15)$, $S^{o}(T)$ и $\Phi^{xx}(T)$. На зависимости $C_p^{o}{\sim}f(T)$ наблюдаются аномальные скачки, связанные, вероятно, с фазовыми переходами II рода. Термодинамические характеристики нового теллурита могут служить исходной информацией для включения в фундаментальные банки данных и справочники, а также могут быть использованы для прогнозирования термохимических констант аналогичных соединений.

*Ключевые слова:* теллурит диспрозия-бария, калориметрия, теплоемкость, фазовые переходы, термодинамические функции.

## References

1 Naboka, M.N., Palatnik, L.S., & Shevchenko, V.Ya. (1981). Struktura i svoistva tonkikh plenok na osnove soedinenii redkozemelnykh metallov [Structure and properties of thin films based on rare-earth metal compounds]. *Zhurnal Vsesoiuznoho khimicheskoho obshchestva imeni D.I. Mendeleeva. — The Centenary of the All-Union D.I. Mendeleev Chemical Society*, *26, 6*, 31 [in Russian].

2 *Tekhnicheskoe opisanie i instruktsii po ekspluatatsii IT-S-400 [Technical Description and Operating Instructions for IT-S-400]*. (1986). Aktiubinsk: Aktiubinskii zavod «Etalon» [in Russian].

3 Rustembekov, K.T, Toibek, A.A., & Stoev, M. (2016). Disprozii kos telluritterinin sintezi, kristallokhimiiasy zhane kurylysy [Synthesis, crystal chemistry and structure of the double dysprosium tellurites]. *Vestnik Karahandinskoho universiteta. Seriia Khimiia — Bulletin of the Karaganda University. Chemistry Series, 84, 4,* 49–54 [in Kazakh].

4 Platunov, Ye.S., Buravoi, S.E., Kurepin, V.V., & Petrov, G.S. (1986). *Teplofizicheskie izmereniia i pribory [Thermophysical Measurements and Devices]*. Leningrad: Mashinostroenie [in Russian].

5 Spiridonov, V.P., & Lopatkin, L.V. (1970). *Matematicheskaia obrabotka eksperimentalnykh dannykh [Mathematical Processing of Experimental Data]*. Moscow: MSU Publ. [in Russian].

6 Robie, R.A., Hewingway, B.S., & Fisher, I.R. (1978). *Thermodynamic properties of minerals and related substances at 298.15K and ($10^5$) Paskals pressure and at higher temperatures.* Washington: United States Government Printing Office.

7 Kumok, V.N. (1987). *Priamye i obratnye zadachi khimicheskoi termodinamiki [Direct and inverse problems of chemical thermodynamics]*. Novosibirsk: Nauka [in Russian].

8 Glushko, V.P. (Eds.). (1978). *Termodinamicheskie svoistva individualnykh veshchestv [Thermodynamic properties of individual substances]*. Moscow: Nauka [in Russian].

9 Gerasimov, Ya.I., Krestovnikov, A.N., & Shakhov, A.S. (1960). *Khimicheskaia termodinamika v tsvetnoi metallurhii [Chemical thermodynamics in non-ferrous metallurgy]* (Vols. 1–4; Vol. 1). Moscow: Metallurhiia [in Russian].

10 Rustembekov, K.T., & Bekturganova, A.Zh. (2017). X-ray diffraction and thermodynamic characteristics for tellurite of the composition $Li_2CeTeO_5$. *Russ. J. Phys. Chem. A., 91*(4), 622–626.

DOI: 10.31489/2019Ch1/66-71

UDC 544.38

U. Besterekov[1], S.R. Yermekov[1], I.A. Petropavlovskiy[2]

*[1]M. Auezov South Kazakhstan State University, Shymkent, Kazakhstan;*
*[2]D. Mendeleyev University of Chemical Technology of Russia, Moscow, Russia*
*(E-mail: sajat_78@mail.ru)*

# Values and change laws of atoms and ions radii

In the chemical technology industry many products are produced by aqueous-salt systems. In such systems the charged particles of mineral substances used as raw materials are in the form of ions and play a decisive role in the formation of the target products. Today research results in the theoretical chemistry show that there is no high level scientifically substantiated data on the radii of atoms that are the material basis of such ion particles. The atomic and ion radius values of chemical elements give rise to several values for a single element in known literary data. These data are different from each other. Within the periodic table per each atom and each ion about 30 scaling values are determined by the calculation or physico-chemical methods. According to the results obtained, the values have been found that are close to the known data and preserve their own numerical values within the periodic system. At this point two different equations are used to calculate radii of the atoms and ions of the elements. Version 1 is for elements in the periodic table moving from period to another, while the other is for elements in the 1st and 8th groups in each period of the periodic table. All chemical elements in the periodic table allow calculating the radius values of atoms and ions.

*Keywords:* ion, atom, radius, periodic system, particle, charge, electron, physical and chemical properties.

## *Introduction*

In many areas of chemical technology the processes occurring in aqueous-salt systems are used. In this case the mineral substances used as primary raw materials in the process are the elementary charge particles, ions, and play a decisive role in the formation of target products. Nowadays the research results [1–5] in scientific chemistry have shown that there is no high level scientifically substantiated data on the radii of such ion particles and their material basis. In general within the Periodic Table of Chemical Elements of D. Mendeleyev the data of radii determined by calculation and physico-chemical methods show about 30 scale values for each atom and each ion [6–11]. As examples we can include the research results on the radii of the ionic and atom particles [12] of Melvin-Hughes (MH), Goldschmidt (G), Poling (P), Ingold (In) and Boki (B) that are widely used in educational and scientific practice today (Table 1).

Table 1

**Radii of atoms and ions**

| Elements | Radius of atom, $r_a*10$, nm | | | | Ion charge | Radius of ion, $r_i*10$, nm | | | | |
|---|---|---|---|---|---|---|---|---|---|---|
| | M.H | G | P | B | | M.H | G | P | In | B |
| 1 | 2 | 3 | 4 | 5 | 6 | 7 | 8 | 9 | 10 | 11 |
| Ag | 1.445 | 1.44 | 1.53 | 1.44 | +1 | 1.014 | 1.13 | 1.26 | 1.26 | 1.13 |
| Al | 1.432 | 1.43 | 1.26 | 1.43 | +3 | 0.55 | 0.57 | 0.50 | 0.72 | 0.57 |
| As | 1.248 | 1.22 | 1.18 | 1.48 | +5 | – | 0.46 | – | 0.71 | (0.47) |
| Au | 1.442 | 1.44 | 1.50 | 1.44 | +1 | – | 1.37 | – | 1.37 | (1.37) |
| B | (0.795) | 0.91 | 0.89 | 0.91 | +3 | (0.20) | 0.23 | 0.20 | 0.35 | (0.20) |
| Ba | 2.174 | 2.17 | – | 2.21 | +2 | 1.395 | 1.34 | 1.35 | 1.53 | 1.38 |
| Be | 1.113 | 1.11 | 1.07 | 1.13 | +2 | 0.314 | 0.35 | 0.31 | 0.44 | 0.34 |
| Bi | 1.548 | 1.55 | 1.46 | 1.82 | +5 | – | 0.74 | – | 0.98 | (0.74) |
| Br | 1.1415 | 1.14 | 1.14 | – | +7 | – | – | – | 0.62 | (0.39) |
| C | 0.771 | 0.77 | 0.77 | 0.77 | +4 | 0.195 | 0.16 | 0.15 | 0.29 | 0.2 |
| Ca | 1.974 | 1.37 | – | 1.97 | +2 | 1.051 | 0.99 | 0.99 | 0.99 | 1.04 |
| Cd | 1.490 | 1.48 | 1.48 | 1.56 | +2 | 0.99 | 0.97 | – | 1.14 | 0.99 |
| Cl | 0.994 | 0.99 | 0.99 | – | +7 | – | – | – | 0.49 | (0.26) |
| Co | 1.253 | 1.25 | 1.25 | 1.25 | +3 | 0.65 | 0.63 | – | – | 0.64 |
| Cr | 1.249 | 1.25 | 1.25 | 1.27 | +6 | – | 0.52 | – | 0.81 | 0.35 |
| Cs | 2.655 | 2.62 | – | 2.68 | +1 | 1.678 | 1.67 | 1.69 | 1.69 | 1.65 |

Continuation of Table 1

| 1 | 2 | 3 | 4 | 5 | 6 | 7 | 8 | 9 | 10 | 11 |
|---|---|---|---|---|---|---|---|---|---|---|
| Cu | 1.278 | 1.27 | 1.35 | 1.28 | +2 | 0.47 | 0.72 | – | 0.96 | 0.80 |
| F | 0.709 | 0.64 | 0.64 | – | +7 | – | – | – | 0.10 | – |
| Fe | 1.241 | 1.26 | – | 1.26 | +3 | 0.67 | 0.64 | – | – | 0.07 |
| H | 0.3707 | 0.36 | 0.30 | 0.46 | –1 | – | 1.53 | – | 2.08 | 1.36 |
| Hg | 1.503 | 1.50 | 1.48 | 1.60 | +2 | 0.66 | 1.10 | – | 1.25 | 1.12 |
| I | 1.333 | 2.20 | 1.28 | – | +7 | – | 0.50 | – | 0.77 | (0.50) |
| K | 2.272 | 2.36 | – | 2.36 | +1 | 1.341 | 1.33 | 1.33 | 1.33 | 1.33 |
| La | 1.870 | 1.86 | – | 1.87 | +3 | 1.14 | 1.14 | 1.15 | 1.39 | 1.04 |
| Li | 1.520 | 1.55 | 1.34 | 1.55 | +1 | 0.758 | 0.68 | 0.60 | 0.60 | 0.68 |

## *Results and discussions*

As can be seen form Table 1, there are large quantitative differences that can not be ignored for any element in their atomic and ionic radius values. The research findings show the results of recent research aimed at eliminating such shortcomings. The research has revealed that some of the latest scientific findings about the definite patterns of traction and drainage and the atomic structure, which arise between charged particles, have been used [13–17]. At this point two different equations are used to calculate the atoms and ions of the elements. For elements in version 1 (1–3) elements according to their formula that move from period to period in the periodic table. They are lithium, sodium, potassium, rubidium, cesium, and francium.

$$\frac{Zne^2}{4\pi\varepsilon_0(R_{atom\ of\ previous\ element}+X)^2}=\frac{K\cdot m\cdot v^2}{\left(R_{atom\ of\ previous\ element}+X\right)}. \tag{1}$$

From the 1st formula we find $X$.

$$X=\frac{Zne^2-K4\pi\varepsilon_0 mv^2\cdot R_{atom\ of\ previous\ element}}{K4\pi\varepsilon_0 mv^2}. \tag{2}$$

Next, we find the atomic or ion radius of the element as follows:

$$R_{atom}=R_{atom\ of\ previous\ element}+X. \tag{3}$$

In version 2 (4–6) formulas are for the elements of 1 and 8 groups in each period in the Periodic Table. The laws are known that by an increase in the line number the atoms and ions radius of elements is decreased. Therefore, we deduce $X$ from the radius of the element and ion radius of the element, and we formulate the formula as follows.

$$\frac{Zne^2}{4\pi\varepsilon_0(R_{atom\ of\ previous\ element}-X)^2}=\frac{K\cdot m\cdot v^2}{\left(R_{atom\ of\ previous\ element}-X\right)}. \tag{4}$$

From the 4th formula we find X.

$$X=\frac{K4\pi\varepsilon_0 mv^2 R_{atom\ of\ previous\ element}-Zne^2}{K4\pi\varepsilon_0 mv^2}, \tag{5}$$

here $\varepsilon_0$ — dielectric permeability of vacuum, F/m; $e$ — electron charge, C; $m$ — electron mass, kg; $z$ — number of protons; $R$ — distance between the charged particles, Å; $v$ — velocity of rotating electrons in radius orbitals, m/sec.; $K$ — constant value determining by the arrangement of elements electrons in the cells.

Next, we find the atomic or ion radius of the element as follows:

$$R_{atom}=R_{atom\ of\ previous\ element}-X. \tag{6}$$

The new calculation results obtained for the elements described in Table 1 above are relative to the data given in Table 2, Figure 1.2.

Table 2

**Radii of atoms and ions**

| Elements | Atom radius, $r_a$·10, nm | | | | | | Ion charge | Ion radius $r_i$·10, nm | | | | | | |
|---|---|---|---|---|---|---|---|---|---|---|---|---|---|---|
| | M.H | G | P | B | Average literary | Calculation | | M.H | G | P | In | B | Average literary | Calculation |
| Al | 1.432 | 1.43 | 1.26 | 1.43 | 1.388 | 1.383 | 3 | 0.55 | 0.57 | 0.5 | 0.72 | 0.57 | 0.582 | 0.575 |
| As | 1.248 | 1.22 | 1.18 | 1.48 | 1.282 | 1.256 | 5 | – | 0.46 | – | 0.71 | 0.47 | 0.546 | 0.482 |
| Au | 1.442 | 1.44 | 1.5 | 1.44 | 1.455 | 1.503 | 1 | – | 1.37 | – | 1.37 | 1.37 | 1.37 | 1.377 |
| B | 0.795 | 0.91 | 0.89 | 0.91 | 0.876 | 0.888 | 3 | 0.2 | 0.23 | 0.2 | 0.35 | 0.2 | 0.236 | 0.333 |
| Ba | 2.174 | 2.17 | – | 2.21 | 2.184 | 2.171 | 2 | 1.395 | 1.34 | 1.35 | 1.53 | 1.38 | 1.399 | 1.357 |
| Be | 1.113 | 1.11 | 1.07 | 1.13 | 1.105 | 1.063 | 2 | 0.314 | 0.35 | 0.31 | 0.44 | 0.34 | 0.350 | 0.472 |
| Bi | 1.548 | 1.55 | 1.46 | 1.82 | 1.594 | 1.453 | 5 | – | 0.74 | – | 0.98 | 0.74 | 0.82 | 0.681 |
| Br | 1.141 | 1.14 | 1.14 | – | 1.140 | 1.166 | 7 | – | – | – | 0.62 | 0.39 | 0.505 | 0.383 |
| C | 0.771 | 0.77 | 0.77 | 0.77 | 0.770 | 0.799 | 4 | 0.195 | 0.16 | 0.15 | 0.29 | 0.2 | 0.199 | 0.213 |
| Ca | 1.974 | 1.37 | – | 1.97 | 1.771 | 1.777 | 2 | 1.051 | 0.99 | 0.99 | 0.99 | 1.04 | 1.012 | 1.119 |
| Cd | 1.49 | 1.48 | 1.48 | 1.56 | 1.502 | 1.505 | 2 | 0.99 | 0.97 | – | 1.14 | 0.99 | 1.022 | 1.989 |
| Cl | 0.994 | 0.99 | 0.99 | – | 0.991 | 1.007 | 7 | – | – | – | 0.49 | 0.26 | 0.375 | 0.372 |
| Co | 1.253 | 1.25 | 1.25 | 1.25 | 1.250 | 1.251 | 3 | 0.65 | 0.63 | – | – | 0.64 | 0.64 | 0.333 |
| Cr | 1.249 | 1.25 | 1.25 | 1.27 | 1.254 | 1.278 | 6 | – | 0.52 | – | 0.81 | 0.35 | 0.56 | 0.514 |
| Cs | 2.655 | 2.62 | – | 2.68 | 2.651 | 2.665 | 1 | 1.678 | 1.67 | 1.69 | 1.69 | 1.65 | 1.675 | 1.675 |
| Cu | 1.278 | 1.27 | 1.35 | 1.28 | 1.294 | 1.405 | 2 | 0.47 | 0.72 | – | 0.96 | 0.8 | 0.737 | 0.985 |
| F | 0.709 | 0.64 | 0.64 | – | 0.663 | 0.684 | 7 | – | – | – | 0.1 | – | 0.1 | 0.099 |
| Fe | 1.241 | 1.26 | – | 1.26 | 1.253 | 1.259 | 3 | 0.67 | 0.64 | – | – | 0.07 | 0.439 | 0.404 |
| Hg | 1.503 | 1.5 | 1.48 | 1.6 | 1.520 | 1.488 | 2 | 0.66 | 1.1 | – | 1.25 | 1.12 | 1.032 | 1.097 |
| I | 1.333 | 2.2 | 1.28 | – | 1.203 | 1.283 | 7 | – | 0.5 | – | 0.77 | 0.5 | 0.59 | 0.426 |

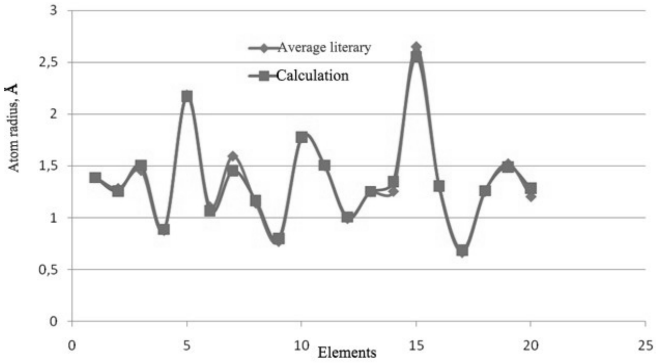

Figure 1. The laws of changes in average literary and calculation values of atomic radii

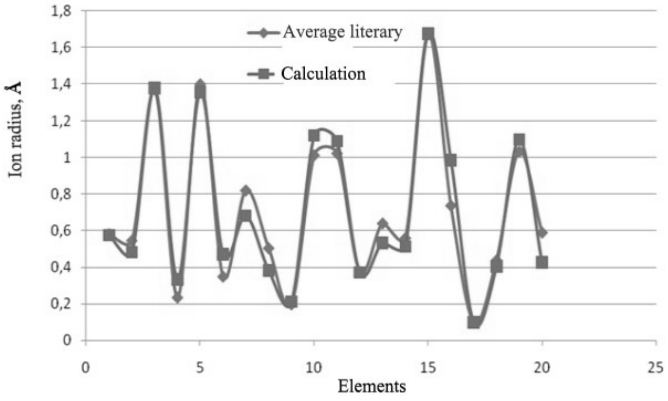

Figure 2. The laws of changes in average literary and calculation values of ion radii

## *Conclusions*

As shown in Table 2 and Figures 1, 2, the results of the study were close to the known data, and the values of the latter were changed within the periodic system, but their numerical values were obtained. In order to verify their superior sequence and authenticity, calculations were made using the atomic and ion radii of any element in the periodic system group before and after of that element, upper and under the certain periods, under certain elements. At the same time, in all four different calculations, the same values of the atom and ion radii of the element under consideration were obtained. This result can be a proof of the novelty of the findings, as well as the high scientific value and significance of it.

Thus, the results of the research can be considered as a new solution for calculating the high values of ion particles and their radicals' radii, which are their material basis in the field of chemistry. The methodology used in the work allow calculation of the radius values of atoms and ions all the chemical elements in the periodic system of D. Mendeleyev.

## References

1 Киселев А.П. Основы общей химии: учебник / А.П. Киселев, А.А. Крашенинников. — СПб.: Балт. гос. техн. ун-т., 2012. — 340 с.

2 Угай Я.А. Общая и неорганическая химия: учебник / Я.А. Угай. — М.: Высш. шк., 2000. — 529 с.

3 Чупахин А.П. Общая химия. Химическая связь и строение вещества: учеб. пособие / А.П. Чупахин. — Новосибирск: Изд-во Новосибир. гос. ун-та, 2003. — 166 с.

4 Тиноко И. Физическая химия. Принципы и применение в биологических науках / И. Тиноко, К. Зауэр, Дж. Вэнг, Дж. Паглиси. — М.: Техносфера, 2005. — 744 с.

5 Сережкин В.Н. Кристаллохимические радиусы и координационные числа атомов / В.Н. Сережкин, Д.В. Пушкин. — Самара: Универс групп, 2005. — 64 с.

6 Потапов А.А. Способ измерения радиуса и энергии связи атомов и ионов / А.А. Потапов. — М.: Ин-т динамики систем и теории управления СО РАН, 2009. — 17 с.

7 Балданова Д.М. Плазменно-гидродинамическая концепция состояния ионов в растворах электролитов в оценке некоторых свойств / Д.М. Балданова, Б.Б. Танганов. — М.: Академия естествознания, 2012. — 99 с.

8 Патент № 2273058. Россия. Способ оценки радиусов атомов химических элементов в различном энергетическом состоянии / Родченко М.Б., Александров Б.Л. — Опубл. 2012.

9 Балданов М.М. Константа экранирования Слейтора-Зинера и радиусы одноатомных ионов / М.М. Балданов, Д.М. Балданова и др. // Известия вузов. Физика. — 2006. — Т. 49, № 3. — С. 59–67.

10 Балданов М.М. К проблеме радиусов гидратированных ионов / М.М. Балданов, Д.М. Балданова и др. // Доклады АН ВШ РФ. — 2006. — № 2(7). — С. 32–38.

11 Балданов М.М. Дисперсионное уравнение Власова и радиусы сольватированных ионов в метаноле / М.М. Балданов, Б.Б. Танганов // Журнал общей химии. — 1994. — Т. 64, № 1. — С. 32–34.

12 Краткий справочник физико-химических величин. — 8-е изд. / под ред. А. Равделя и А.М. Пономаревой. — Л.: Химия, 1983. — 232 с.

13 Сурнин С.П. Структура атома / С.П. Сурнин. — М.: Б.и., 2005. — 88 с.

14 Волков А.И. Строение атомов и периодический закон / А.И. Волков. — М.: Новое знание, 2006. — 196 с.

15 Детлав А.А. Курс физики / А.А. Детлав, Б.М. Яровский. — М.: Академия, 2007. — 720 с.

16 Калашников Н.П. Основы физики: учебник для вузов: в 2-х т. / Н.П. Калашников, М.А. Смондырев. — 3-е изд., стер. — М.: Дрофа, 2007.

17 Карапетьянц М.Х. Общая и неорганическая химия / М.Х. Карапетьянц, С.И. Дракин. — М.: Химия, 2015. — 592 с.

---

У. Бестереков, С.Р. Ермеков, И.А. Петропавловский

# Атомдар мен иондардың радиустары мәндері мен өзгеру заңдылықтары

Химиялық технология салаларында сулы-тұзды жүйелер арқылы көптеген өнімдер өндірілуде. Мұндай жүйелерде шикізаттар ретінде пайдаланылатын минералды заттардың зарядтық бөлшектері иондар түрінде болып, керекті өнімдерді қалыптастыруда шешуші рол атқарады. Ғылыми-ілімдік химия саласында қазіргі кезде қолжеткен нәтижелерді талдау нәтижесі көрсеткендей, осындай иондық бөлшектердің және олардың материалдық негізі болып табылатын атомдардың радиустары туралы шынайылылығы жоғары, толықтама ғылыми дәйектелген мәліметтер жоқ. Химиялық элементтердің атомы мен ионы радиустары мәндері белгілі әдеби мағлұматтарда бір элемент үшін бірнеше мән береді. Олар бір-бірінен өте алшақты мәндер. Химиялық элементтердің периодтық жүйесі кестесі шеңберінде радиустары есептік немесе сан алуан физика-химиялық жолдармен анықталған мәліметтерде әр атом әр ион үшін 30 жуық шкалалық мәндер келтіріледі. Ізденіс нәтижелері бойынша белгілі мәліметтерге жақын және де соңғылардың периодтық жүйе шеңберінде өзгеру заңдылықтарын сақтайтын, бірақ өзіндік сандық нәтижелері бар мәндер алынды. Осы кезде элементтердің атомдары мен иондары радиустарын есептеуде екі түрлі теңдеулер қолданылады. 1-ші нұсқа элементтер периодтық жүйеде периодтан периодқа көшкендегі элементттер үшін, ал екіншісі периодтық жүйедегі әр периодтағы 1-ші және 8-ші топтағы элементттер үшін. Жұмыста қолданылған әдістеме Д. Менделеевтің периодтық жүйесіндегі барлық химиялық элементтердің атомдары және иондары радиустарының мәндерін есептеп анықтауға мүмкіндік береді.

*Кілт сөздер:* ион, атом, радиус, периодтық жүйе, бөлшектер, зарядтар, электрон, физика-химиялық қасиеті.

У. Бестереков, С.Р. Ермеков, И.А. Петропавловский

## Значения и закономерности изменения радиусов атомов и ионов

В отраслях химической промышленности многие продукты производятся с помощью водно-солевых систем. В таких системах заряженные частицы минеральных веществ, используемых в качестве сырья, находятся в форме ионов и играют решающую роль в формировании целевых продуктов. Результаты текущих исследований в области теоретической химии показали, что не существует высокоуровневых научно обоснованных данных о радиусах ионов и атомов. Атомные и ионные радиусы химических элементов имеют несколько значений для одного элемента по некоторым литературным данным. В данных о радиусах химических элементов периодической таблицы, определяемых физико-химическим и расчетным методом, каждый атом и ион имеют около 30 значений. По результатам исследования значения были близки к известным данным. Для вычисления радиусов атомов и ионов элементов используются два разных уравнения. Версия 1 предназначена для элементов в периодической таблице, перемещающихся из периода в период, а другая — для элементов 1-й и 8-й групп в каждом периоде периодической таблицы. Методология, используемая в работе, дает возможность рассчитать атомные и ионные радиусы всех химические элементов в периодической системе Д.И. Менделеева.

*Ключевые слова:* ион, атом, радиус, периодическая система, частицы, заряд, электрон, физико-химические свойства.

## References

1 Kiselev, A.P., & Krasheninnikov, A.A. (2012). *Osnovy obshchei khimii [Basics of general chemistry]*. Saint Petersburg: Baltic STU [in Russian].

2 Ugai, Ya.A. (2000). *Obshchaia i neorhanicheskaia khimiia [General and inorganic chemistry]*. Moscow: Vysshaia shkola [in Russian].

3 Chupakhin, A.P. (2003). *Obshchaia khimiia. Khimicheskaia sviaz i stroenie veshchestva [General chemistry. Chemical bonding and structure of matter]*. Novosibirsk: Novosibirsk SU publ. [in Russian].

4 Tinoko, I., Zauer, K., Veng, J., & Pahlisi, J. (2005). *Fizicheskaia khimiia. Printsipy i primenenie v biolohicheskikh naukakh [Physical chemistry. Principles and applications in biological sciences]*. Moscow: Tekhnosfera [in Russian].

5 Serezhkin, V.N., & Pushkin, D.V. (2005). *Kristallokhimicheskie radiusy i koordinatsionnye chisla atomov [Crystal chemical radii and coordination numbers of atoms]*. Samara: Univers grup [in Russian].

6 Potapov, A.A. (2009). *Sposob izmereniia radiusa i enerhii sviazi atomov i ionov [The method of measuring the radius and binding energy of atoms and ions]*. Moscow: Institute of System Dynamics and Control Theory, Siberian Branch of the Russian Academy of Sciences [in Russian].

7 Baldanova, D.M., & Tanganov, B.B. (2012). *Plazmenno-hidrodinamicheskaia kontseptsiia sostoianiia ionov v rastvorakh elektrolitov v otsenke nekotorykh svoistv [Plasma-hydrodynamic concept of the state of ions in electrolyte solutions in the evaluation of certain properties]*. Moscow: Akademiia estestvoznaniia [in Russian].

8 Rodchenko M.B., Aleksandrov B.L. (2012). Sposob otsenki radiusov atomov khimicheskikh elementov v razlichnom enerheticheskom sostoianii [The method of estimating the radii of atoms of chemical elements in a different energy state]. *Patent No. 2273058 Russia.* [in Russian].

9 Baldanov, M.M., & Baldanova, D.M. et al. (2006). *Konstanta ekranirovaniia Sleitora-Zenera i radiusy odnoatomnykh ionov* [Slater-Zener shielding constant and monatomic ion radii]. *Izvestiia vuzov: Fizika. — Russian Physics Journal, 49, 3,* 59–67 [in Russian].

10 Baldanov, M.M., & Baldanova, D.M. et al. (2006). K probleme radiusov hidratirovannykh ionov [To the problem of hydrated ion radii]. *Doklady Akademii nauk Vysshei shkoly Rossiskoi Federatsii — Reports of Academy of Sciences of Higher School of Russian Federation, 2*, 32–38 [in Russian].

11 Baldanov, M.M., & Tangalov, B.B. (1994). *Dispersionnoe uravnenie Vlasova i radiusy solvatirovannykh ionov v metanole* [Vlasov dispersion equation and the radii of solvated ions in methanol]. *Zhurnal obshchei khimii — Russian Journal of General Chemistry, 64, 1*, 32–34 [in Russian].

12 Ravdel, A., & Ponomareva, A.M. (1983). *Kratkii spravochnik fiziko-khimicheskikh velichin [Quick reference of physico-chemical values]*. (Edition 8). Leningrad: Khimiia [in Russian].

13 Surnin, S.P. (2005). *Struktura atoma [Atom structure]*. Moscow: B.i. [in Russian].

14 Volkov, A.I. (2006). *Stroenie atomov i periodicheskii zakon [Atom structure and periodic law]*. Moscow: Novoe znanie [in Russian].

15 Detlav, A.A., & Yarovskii, B.M. (2007). *Kurs fiziki [Course of Physics]*. Moscow: Akademiia [in Russian].

16 Kalashnikov, N.P., & Smondyrev, M.A. (2007). *Osnovy fiziki [Fundamentals of physics]*. (Vols. 1–2). Moscow: Drofa [in Russian].

17 Karapetyants, M.Kh., & Drakin S.I. (2015). *Obshshaia i neorhanicheskaia khimiia [General and inorganic chemistry]*. Moscow: Khimiia [in Russian].

# ХИМИЯЛЫҚ ТЕХНОЛОГИЯ
# ХИМИЧЕСКАЯ ТЕХНОЛОГИЯ
# CHEMICAL TECHNOLOGY

DOI: 10.31489/2019Ch1/72-77

UDC 666.942:691.542

V.A. Burakhta[1], A.M. Jubanaliyeva[2], S.S. Satayeva[2]

*[1]West Kazakhstan Innovation-Technological University, Uralsk, Kazakhstan;*
*[2]Zhangir khan West Kazakhstan Agrarian-Technical University, Uralsk, Kazakhstan*
*(E-mail: vburakhta@mail.ru)*

## The methods of improving the technology of Portland cement production with the use of Western Kazakhstan local raw materials and industrial wastes

In this paper, one of the most rapidly developing branches in the construction industry in the Republic of Kazakhstan Portland cement production has been examined. In this connection, the main properties of the constituent components for producing Portland cement based on local raw materials in Western Kazakhstan have been studied. The technological burning process of Portland cement clinker has been made and their X-ray phase analysis has been carried out. The cement obtained main characteristics have been determined in order to assess its quality. The technological process of obtaining Portland cement with the use of local raw materials and the addition of pyritic cinders and carbon black has been organized. It has been established that the introduction of technical carbon and pyrite cinders in Portland cement has a positive effect on the rheological properties, as well as on the increase in the strength characteristics of Portland cement. The economic value has been estimated and the profitability of Portland cement production in the West Kazakhstan region has been calculated. An improved technology for the production of Portland cement including the use of local raw materials with the addition of pyritic cinders of more than 2 % and technical carbon in an amount of up to 3 % has been proposed.

*Keywords:* clay, flask, limestone, pyritic cinder, technical carbon, clinker, Portland cement.

One of the key directions of the country's industrial and innovative progress is the development of the chemical industry, which has been repeatedly emphasized by the President of the country N.A. Nazarbayev during the annual Addresses to the people of Kazakhstan [1]. Today, the chemical industry in Kazakhstan is becoming an important issue, which is directly related to the construction industry. Technology of production of building silicate materials is of a significant importance in the modern industry, which is one of the areas that cement industry is involved. Nowadays cement production in Kazakhstan is not sufficiently developed, so our country buys cement mainly from the Russian Federation, which is the main supplier of cement to the Republic of Kazakhstan. In turn, West Kazakhstan remains almost with no supplies of domestic products, so the need for cement in the Western region is almost completely satisfied by import. In this regard, the use of available technologies and the full provision of the region with cement produced by means of local raw materials remains relevant. Currently, Portland cement is widely used among many types of cement. It is a well-known fact that, the main components in the production of Portland cement are carbonate raw materials, aluminosilicate clay rocks, and additives [2].

It was of interest to study the physico-chemical properties of the constituent components to obtain Portland cement based on local raw materials and industrial wastes. Clays of the Pogodaevsk and Taskalinsky deposits, flask of the Taskalinsky deposit and the limestone of the Melovye Gorki deposit (West Kazakhstan region) were taken as raw materials in order to implement experimental studies. Chemical and physico-chemical methods have been used to determine physico-chemical characteristics [3].

After the researches and calculations carried out the technological process of production of Portland cement clinker and Portland cement, including extraction of local raw materials, their crushing, drying, grinding, firing clinker in a rotary furnace, cooling clinker, grinding and obtaining cement was fulfilled. One of the promising methods, namely, X-ray phase analysis has been used to control the quality of the clinker obtained, which allows determining the qualitative and quantitative composition of the clinker with high accuracy. Loss on ignition, fineness of grinding, setting time, insoluble residue content, and strength of Portland cement were determined to assess the quality of the Portland cement obtained.

Earlier, we have studied the chemical composition of raw materials and concluded that the limestone of the deposit of the Melovye Gorki, clay and flask of the Taskalinsky field was expedient for use in Portland cement production. We have set the following mineralogical composition of Portland cement: $C_3S$ — 51 %; $C_2S$ — 29 %; $C_3A$ — 9 % and $C_4AF$ — 11 %. At the same time, we accept that the sum of these basic minerals is 100 %. We give the chemical compositions of the raw material after bringing the sum of oxides $SiO_2+Al_2O_3+Fe_2O_3+CaO$ to 100 % (Table).

Table

**Chemical composition of the raw material after demonstration of the sum of oxides $SiO_2+Al_2O_3+Fe_2O_3+CaO$ to 100 %**

| Materials | $SiO_2$ | $Al_2O_3$ | $Fe_2O_3$ | CaO | Total |
|---|---|---|---|---|---|
| Limestone | 0.3 | 0.7 | 0.2 | 98.8 | 100.0 |
| Taskalinsky clay deposit | 54.7 | 44.4 | 0.4 | 0.5 | 100.0 |
| Pogadaevsk clay deposit | 51.9 | 45.5 | 2.0 | 0.6 | 100.0 |
| Flask | 83.2 | 10.6 | 4.4 | 1.8 | 100.0 |
| Cinder | 15.0 | 6.3 | 77.7 | 1.0 | 100.0 |

Based on the mineralogical composition given, the chemical composition of Portland cement clinker in the main oxides was determined:

$SiO_2 = 0.3\times51+0.3\times29 = 24.0$ %;

$A1_2O_3 = 0.4\times9+0.2\times11 = 5.8$ %;

$Fe_2O_3 = 0.3\times11=3.3$ %;

$CaO = 0.7\times51+0.7\times29+0.6\times9+0.5\times11 = 66.9$ %.

A wide range of different additives is widely used in the technology of Portland cement production. One of these additives is carbon black, which is a waste of chemical industries, unutilized reserves of which cause irreparable harm to the environment [4, 5]. Figure 1 shows the technological process for the production of Portland cement. The technological process of obtaining Portland cement with the use of local raw materials and the addition of pyritic cinders (wastes of sulfuric acid production) and carbon black were carried out. The introduction of pyrite cinder reduced the clinker sintering temperature by 50–100 °C, and the addition of carbon black allowed increasing the activity of Portland cement. Cinder and technical carbon in the amount of 3 %, which allows increasing technological efficiency and environmental safety, were added in order to improve the technology. The X-ray phase analysis was performed on a D2 Phaser Bruker powder diffractometer in order to determine the quality of the Portland cement clinker [6]. The phase composition of the clinker using clay of the Taskalinsky deposit is shown in Figure 2.

The X-ray diffraction pattern obtained as a result of the survey is a broken line with sharp peaks-diffraction reflections. The X-ray diffraction was carried out using the software DIFRAC.EVA (Bruker). From the Figures 2 and 3 it can be seen that minerals such as tricalcium silicate $3CaO\cdot SiO_2$ (alite), dicalcium silicate $2CaO\cdot SiO_2$ (belite), tricalcium aluminate $3CaO\cdot Al_2O_3$, and quartet $4CaO\cdot Al_2O_3\cdot Fe_2O_3$ alumoferrite are present in the clinker composition. The identification of the phase is considered sufficiently reliable, since there are at least three of the most intense diffraction reflections of the phase on the roentgenogram. Thus, the composition of the clinker obtained is consistent with the literature data [7] and corresponds to the composition of Portland cement clinker, which contains four basic minerals.

The main characteristics of Portland cement obtained were determined, namely, loss on ignition, fineness of grinding, setting time, content of insoluble residue and strength of Portland cement. The results of the research showed that the Portland cement parameters determined with the use of the Taskalinsky clay for all characteristics met the requirements of State Standards [8–10] and had improved properties compared to Portland cement with the use of clay of the Pogodaev deposit. In terms of material composition, cements obtained are of the CEM II / A-K Portland cement type with additives up to 20 %. The results of the research have shown that the compressive strength of Portland cement with the use of the clay of the Taskalinsky deposit meets the requirements of State Standard [9], corresponds to the M300 grade and has improved properties compared to Portland cement with the use of clay of the Pogodaev deposit.

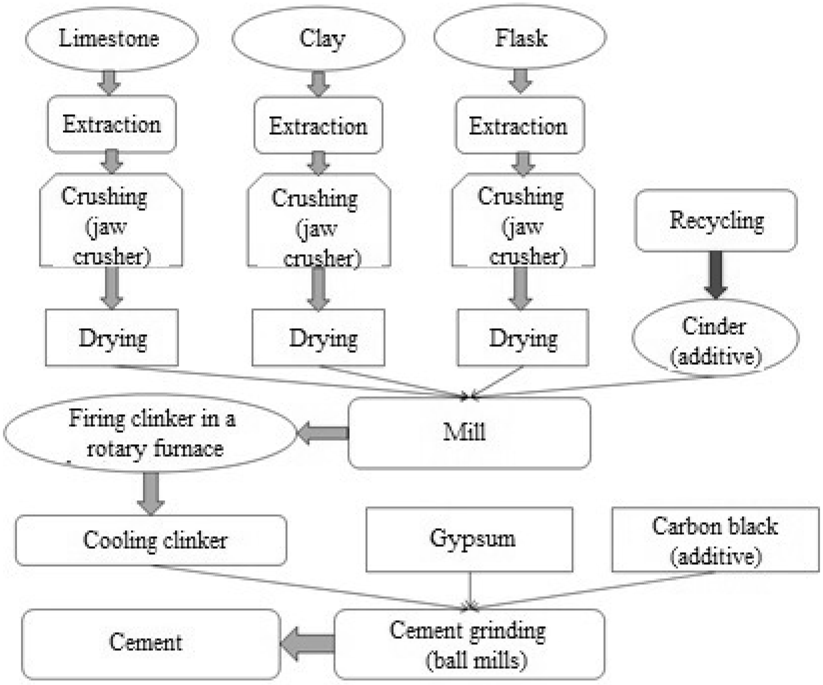

Figure 1. Technological scheme of Portland cement production

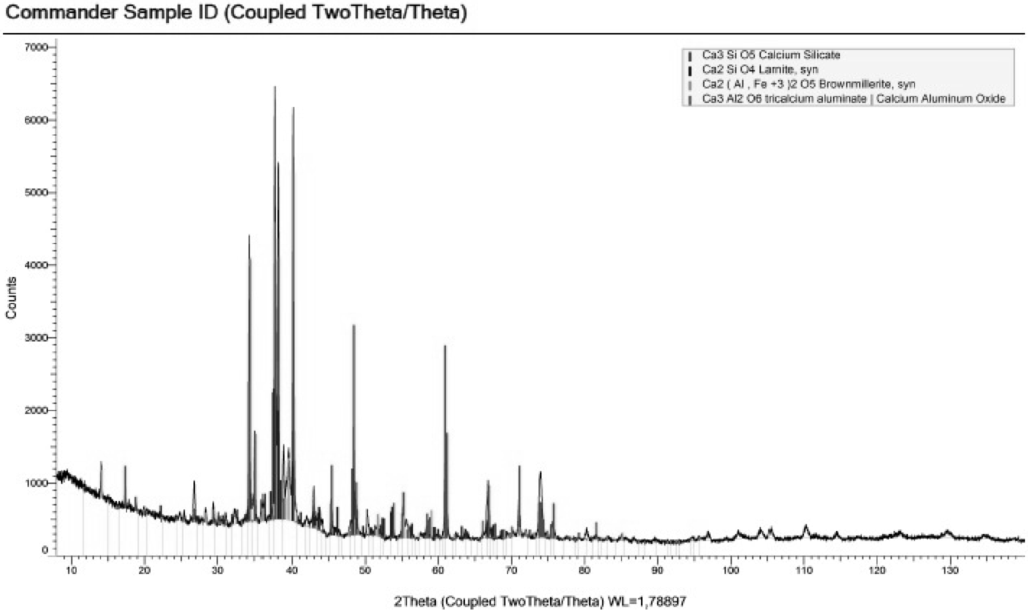

Figure 2. Phase composition of the clinker (using clay of the Taskalinsky deposit)

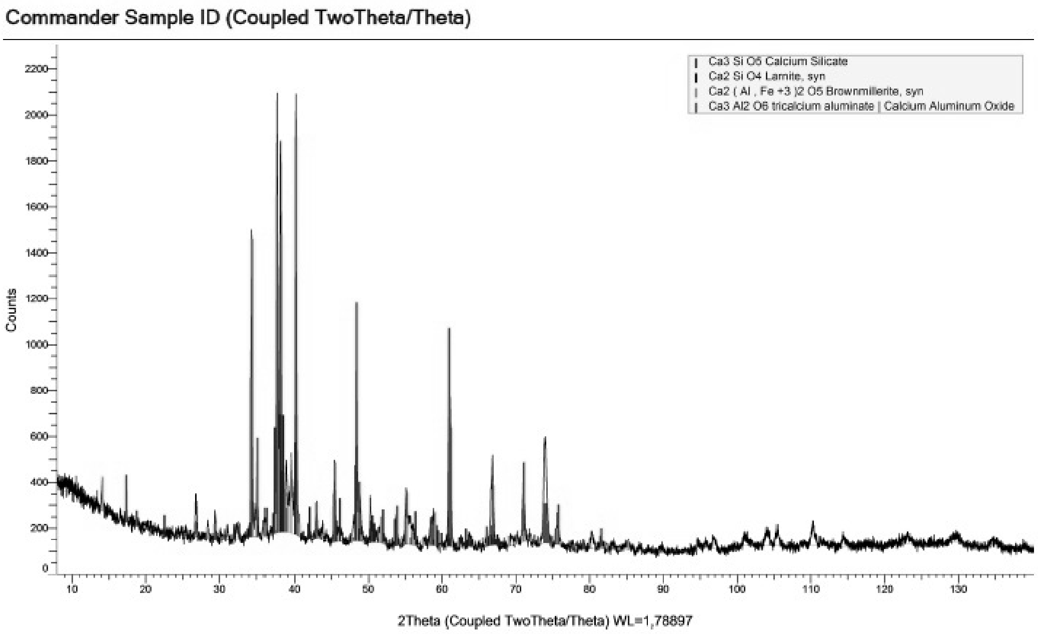

Figure 3. Phase composition of clinker (using clay of the Pogodaev deposit)

Based on the results of the research, we propose an advanced technology for the production of Portland cement, including the use of local raw materials (Limestone of the Melovye Gorki, clay and trough of the Taskalinsky deposit) with the addition of pyritic cinder more than 2 % and carbon black in quantities of up to 3 %. The introduction of pyritic cinders provides reducing the clinker sintering temperature and reducing energy costs. The introduction of carbon black as an additive allowed increasing the activity of cement, as well as to obtain an environmental effect. The economic efficiency of production of Portland cement of local origin in the West Kazakhstan region has been estimated. The profitability of production has been calculated and it has been established that the profit of this technology covers all necessary costs for production and makes up 9891.4 thousand tenge per year. In this way, the expediency of using the clay and the flask of the Taskalinsky deposit, the limestone of the Melovye Gorki deposit as a raw material with the addition of pyrite cinders and carbon black in Portland cement production technology has been established.

## References

1 Послание Президента Республики Казахстан Н. Назарбаева народу Казахстана. Третья модернизация Казахстана: глобальная конкурентоспособность // Казахстанская правда. — № 20 (28399). — 2017. — 31 янв.

2 Колокольников В.С. Производство цемента: учеб. пособие / В.С. Колокольников. — М.: Высш. шк., 1967. — 303 с.

3 Бурахта В.А. Исследование физико-химических свойств глин Западного Казахстана в технологии производства портландцемента / В.А. Бурахта, А.М. Джубаналиева // Казахстанцы — нация единого будущего: материалы Междунар. науч.-практ. конф., посвящ. 25-летию Независимости Республики Казахстан (2016 г.). — Уральск: ЗКИТУ, 2016. — Ч. I. — С. 83–86.

4 Перфилов В.А. Влияние углеродистых добавок на свойства мелкозернистых фибробетонов [Электронный ресурс] / В.А. Перфилов, М.О. Зубова // Интернет-вестн. ВолгГАСУ. Сер. Политематическая. — 2015. — Вып. 1 (37). Ст. 10. — Режим доступа: http://www.vestnik.vgasu.ru/.

5 Перфилов В.А. Применение сажевых отходов (технический углерод) с целью повышения прочностных характеристик тяжелых бетонов / В.А. Перфилов, М.О. Зубова // Качество внутреннего воздуха и окружающей среды: материалы XI Междунар. науч. конф. (23 марта – 5 апреля 2013 г.). — Ханой; Волгоград, 2013. — С. 118–123.

6 Сайт Санкт-Петербургского государственного архитектурно-строительного университета. [Электронный ресурс]. — Режим доступа: http://www.spbgasu.ru/.

7 Бутт Ю.М. Практикум по химической технологии вяжущих материалов: учеб. пособие / Ю.М. Бутт, В.В. Тимашев. — М.: Высш. шк., 1973. — 504 с.

8 Цементы. Методы определения тонкости помола: ГОСТ 310.2–76. [Введен в действие от 01-01-1978]. — М.: ИПК Изд-во стандартов, 2003. — 3 с. — (Межгосударственный стандарт).

9 Цементы. Методы испытаний с использованием полифракционного песка: ГОСТ 30744–2001. — [Введен в действие от 08-20-2001]. — М.: Госстрой России, ГУП ЦПП, 2001. — 19 с. — (Межгосударственный стандарт).

10 Цементы и материалы цементного производства. Методы химического анализа: ГОСТ 5382–91. — [Введен в действие от 07-01-1991]. — М.: ИПК Изд-во стандартов, 2002. — 109 с. — (Межгосударственный стандарт).

В.А. Бурахта, А.М. Джубаналиева, С.С. Сатаева

## Батыс Қазақстанның жергілікті шикізаты мен өндіріс қалдықтарының қолдануымен портландцемент өндірісі технологиясының жетілдіру әдістері

Мақалада Қазақстан Республикасы құрылыс индустриясының қарқынды дамып келе жатқан бағыттарының бірі — портландцемент өндірісі қарастырылған. Осыған байланысты Батыс Қазақстанның жергілікті шикізаты негізінде алынған портландцементтің құрамдас компоненттерінің негізгі қасиеттері зерттелді. Портландцементті клинкердің күйдіру технологиялық процесі жүзеге асырылып, олардың рентгенофазалық талдауы жүргізілді. Алынған портландцементтің сапасын бағалау үшін оның негізгі сипаттамалары анықталды. Жергілікті шикізат пен пирит күлінің қолдануымен портландцемент алу технологиялық процесі іске асырылған. Портландцементке техникалық көміртек және пирит күлін қосу арқылы оның реологиялық қасиеттеріне оң әсер етіп, сондай-ақ портландцементтің беріктік қасиетін арттыратыны анықталды. Батыс Қазақстан облысының жергілікті шыққан портландцемент өндірісінің экономикалық тиімділігі бағаланды және рентабельділігі есептелді. Жергілікті шикізат 2 % астам пирит күлі және 3 % мөлшерінде техникалық көміртекті қосуды қарастыратын портландцемент өндірісінің жетілдірілген технологиясы ұсынылды.

*Кілт сөздер:* саз, опока, әктас, пирит күлі, техникалық көміртек, клинкер, портландцемент.

В.А. Бурахта, А.М. Джубаналиева, С.С. Сатаева

## Методы усовершенствования технологии производства портландцемента с применением местного сырья Западного Казахстана и отходов промышленности

В статье рассмотрена одна из стремительно развивающихся отраслей строительной индустрии в Республике Казахстан — производство портландцемента. В связи с этим исследованы основные свойства составляющих компонентов для получения портландцемента на основе местного сырья Западного Казахстана. Осуществлен технологический процесс обжига портландцементного клинкера и проведен их рентгенофазовый анализ. Для оценки качества полученного портландцемента определены его основные характеристики. Осуществлен технологический процесс получения портландцемента с использованием местного сырья и добавлением пиритных огарков и технического углерода. Установлено, что введение в портландцемент технического углерода и пиритных огарков оказывает положительное влияние на реологические свойства, а также на увеличение прочностных характеристик портландцемента. Оценена экономическая эффективность, и рассчитана рентабельность производства портландцемента местного происхождения Западно-Казахстанской области. Предложена усовершенствованная технология производства портландцемента, включающая использование местного сырья с добавлением пиритных огарков более 2 % и технического углерода в количестве до 3 %.

*Ключевые слова:* глина, опока, известняк, пиритные огарки, технический углерод, клинкер, портландцемент.

## References

1 Poslaniie Prezidenta Respubliki Kazakhstan N. Nazarbaeva narodu Kazakhstana. Tretia modernizatsiia Kazakhstana: hlobalnaia konkurentosposobnost [Message of the President of the Republic of Kazakhstan N. Nazarbayev to the people of Kazakhstan. Third Modernization of Kazakhstan: Global Competitiveness]. (2017, 31 January). *Kazakhstanskaia Pravda — Kazakhstanskaia Pravda, 20 (28399)* [in Russian].

2 Kolokolnikov, V.S. (1967). *Proizvodstvo tsementa [Cement production]*. Moscow: Vysshaia shkola [in Russian].

3 Burakhta, V.A., & Jubanaliyeva, A.M. (2016). Issledovanie fiziko-khimicheskikh svoistv hlin Zapadnoho Kazakhstana v tekhnolohii proizvodstva portlandtsementa [Study of the physical and chemical properties of clays of Western Kazakhstan in the technology of production of Portland cement]. Proceedings from Citizens of Kazakhstan — nation of common future '16: *Mezhdunarodnaia nauchno-prakticheskaia konferentsiia, posviashchennaia 25-letiiu Nezavisimosti Respubliki Kazakhstan — International Scientific and Practical Conference dedicated to the 25th anniversary of Independence of the Republic of Kazakhstan.* (pp. 83–86, part I). Uralsk: ZKITU [in Russian].

4 Perfilov, V.A., & Zubova, M.O. (2015). Vliianiie uhlerodistykh dobavok na svoistva melkozernistykh fibrobetonov [The effect of carbon additives on the properties of fine-grained fiber-reinforced concrete]. *Internet-vestnik VolhHASU. Ser.*

*Politematicheskaia — Internet Bulletin VolgSUACI. Ser. Polythematic,* Issue 1 (37). St. 10. Retrieved from http://www.vestnik.vgasu.ru [in Russian].

5 Perfilov, V.A., & Zubova M.O. (2013). Primenenie sazhevykh otkhodov (tekhnicheskii uhlerod) s povysheniem prochnostnykh kharakteristik tiazhelykh betonov [The use of soot waste (carbon black) in order to increase the strength characteristics of heavy concrete]. Proceedings from Internal air quality and environment'13: *XI Mezhdunarodnaia nauchnaia konferentsiia (23 marta – 5 aprelia 2013 hoda) — XI International Scientific Conference. (pp. 118–123).* Khanoy; Volgograd [in Russian].

6 Sait Sankt-Peterburhskoho hosudarstvennoho arkhitekturno-stroitelnoho universiteta [Site of Saint Petersburg State University of Architecture and Civil Engineering]. *http://www.spbgasu.ru*. Retrieved from http://www.spbgasu.ru [in Russian].

7 Butt, Yu.M., & Timashev, V.V. Praktikum po khimicheskoi tekhnolohii viazhushchikh materialov [Workshop on chemical technology of binders]. Moscow: Vysshaia shkola [in Russian].

8 Cementy. Metody opredeleniia tonkosti pomola [Cements. Methods for determining the fineness of grinding]. (1978). *HOST 310.2–76 from 1st January 1978.* Moscow: IPK Izdatelstvo standartov [in Russian].

9 Cementy. Metody ispytanii s ispolzovaniem polifraktsionnoho peska [Cements. Test methods using polyfraction sand]. (2001). *HOST 30744–2001 from 20th August 2001.* Moscow: Hosstroi Rossii, GUP CPP [in Russian].

10 Cementy i materialy cementnoho proizvodstva. Metody himicheskoho analiza [Cements and materials of cement production. Chemical Analysis Methods]. (1991). *HOST 5382–91 from 1st July 1991.* Moscow: IPK Izdatelstvo standartov [in Russian].

DOI: 10.31489/2019Ch1/78-84

UDC 662. 743

N.I. Kopylov

*Institute of Solid State Chemistry and Mechanochemistry*
*of the Siberian Branch of the Russian Academy of Sciences, Novosibirsk, Russia*
*(E-mail: kolyubov@narod.ru)*

# Phase decomposition of coals of the Tavantolgoyskoye deposit of Mongolia during their roasting

Coals of the Tavantolgoyskoye deposit, by analogy with the coals of other similar deposits, are of interest not only as a fuel and energy resource, but also as raw materials for the metallurgical and chemical industries. In order to prevent contamination of the environment with toxic components when using these coals as fuel for thermal power plant and domestic furnace installations, as well as in industry as a raw material, their special preparation is required. In this regard, investigations were carried out to study the phase decomposition of these coals during their roasting. The results of a comprehensive study of the thermal decomposition of hard coal from this deposit are presented. It is established that this process of phase decomposition is carried out within the temperature range of 300–500 ºC with the release of gas, low-melting and low-boiling phases. At the same time, the mass of the material increases in volume and is sintered with the formation of a solid, porous sinter, the volume of which is 1.5–2 times higher than the volume of the initial sample. It is shown that tavantolgoysky coal can be used to produce fuel briquettes without the addition of a binder.

*Keywords:* coal, phase decomposition, solid residue, resinous fraction, condensate, sublimates, organic fraction.

## *Introduction*

Coals of the Tavantolgoyskoye deposit in Mongolia, by analogy with the coals of other developed deposits, can be valuable raw materials not only for the power industry, but also for the metallurgical and chemical industries [1, 2]. However, the effectiveness of the development of proven reserves is hampered by the high cost of coal mined, and industrial use is hampered by remoteness from industrial centers and the lack of proper transportation routes. Therefore, these coals, as well as products of other fields in Central Asia (for example, Tuva, etc.), are used mainly as fuel for heat and power engineering and private sector units. So, 2.45 million tons were produced for the needs of nearby aimaks and local consumption in the period from 1967 to 2004. In 2006, production amounted to 787.1 thousand tons [3, 4].

The dynamics and nature of thermal decomposition of fossil coal is determined by their composition [1, 2]. Depending on the chemical and phase composition, structure and type of coal, when it is heated, noncondensible gas fractions are removed from the material in a certain sequence, melting and sublimation of condensable products of thermal decomposition takes place. During the coal burning due to incomplete combustion and the formation of sintering with flue gases, the products of this incomplete combustion, in particular, dispersed soot, are emitted into the atmosphere, the particles of toxic decomposition products of coal are sorbed on the surface of the particles. This leads to the release into the environment of environmentally hazardous substances.

The complex geological conditions and extreme continental climate of Central Asia contribute to the formation of stagnant air zones, smog in confined spaces of intermountain valleys. All this leads to the pollution of the atmosphere of rural and urban settlements in these regions by harmful products of flue gases with high concentrations of toxic substances, including carcinogenic polyaromatic hydrocarbons, whose concentrations reach X g/kg [5].

The production and use of environmentally friendly dry coal briquettes will reduce harmful emissions into the atmosphere and reduce the degree of damage to the environment. The resulting thermolysis products can be used to produce mineral oils, motor fuels, and other chemical products. In this regard, in order to obtain baseline data for the technology of producing fuel briquettes for a number of years we have carried out studies on the thermal decomposition of coal from deposits of Tuva and Mongolia [6–8]. This report presents the results of a study of the phase decomposition of hard coal from the Tavantolgoyskoye deposit in Mongolia.

*Experimental*

The object of study was the material of the Tavantolgoyskoye coal deposit (Mongolia) in the form of an average finely ground (~0.02 mm) sample of reservoir VIII, a single lump sample of formation IV and an enlarged average lumpy sample of the field. Technical characteristics and elemental composition of the studied coal samples VIII and IV are presented in Table 1.

Table 1

**Technical characteristics and elemental composition of samples of Tavantolgoysky coal**

| Samples | Technical specifications, % | | | Elemental composition, % | | | $Q^a_s$ kcal/kg |
|---|---|---|---|---|---|---|---|
| | $W^a$ | $A^a$ | $V^{daf}$ | $C^{daf}$ | $H^{daf}$ | $S^d_{gen}$ | |
| Seam IV | 0.9 | 10.6 | 30.1 | 84.0 | 5.4 | 0.67 | 6828.3 |
| Seam VIII | 0.9 | 14.7 | 35.8 | 76.0 | 4.4 | 0.69 | 6763.5 |

Thermal analysis was performed using a derivator of the model «Paulik, Paulik-Erdey», type IOM-1000 (Hungary). The maximum heating temperature was limited to 650–700 ºC. The heating rate was maintained at 10 ºC/min. The magnitude of the sample was 1.0 ± 0.2 g. Experiments were carried out under conditions that ensure free diffusion of the gas components and prevent contact of the material with the air medium.

Determination of quantitative and aggregate changes in the heating process with capturing sublimates of coal fractions was carried out in a laboratory setup that includes a furnace with a reactor in which a crucible with a weight of 50–100 g was placed and collector of condensed sublimates connected to it with the help of a branch pipe.

*DTGA samples of coal seam VIII.*

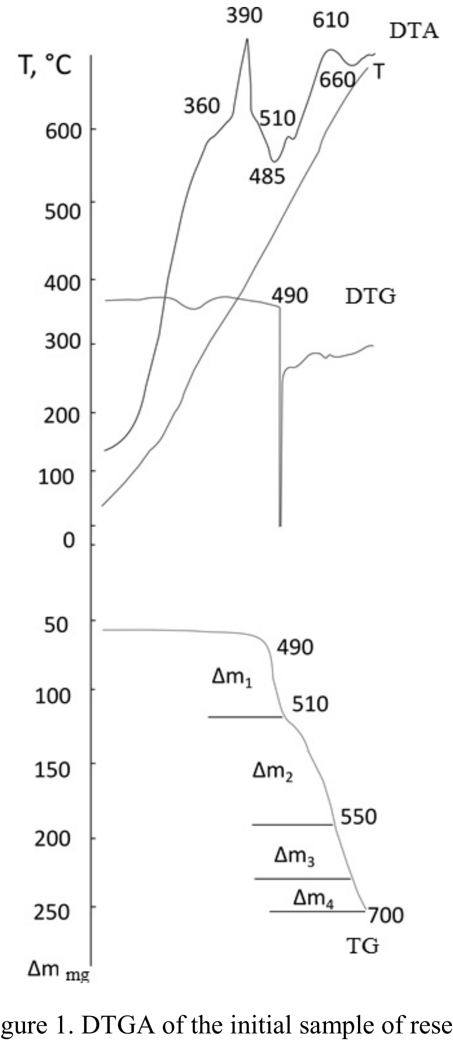

Figure 1. DTGA of the initial sample of reservoir VIII

The beginning of thermal decomposition (Fig. 1) is marked a sharp explosive endoeffect (at 420–490 ºC) associated with the evolution of gaseous components (with a weight loss of 5–7 %) and at the same time the appearance of a low-melting fraction. The subsequent stages of thermolysis possess monotonous step character. The total weight loss is 14–15 %. A characteristic feature of the thermolysis of this sample is the appearance of an acute exo peak on the DTA curve at 360–410 ºC, the nature of which was not entirely clear from the start. This effect does not appear on the TG and DTG curves. Therefore, one would assume that there is a phase or structural transformation with the release of heat. However, more likely, the appearance of this exoeffect is due to heating due to the oxidation reaction of the sample material by sorbed oxygen contained in the starting material with a high degree of dispersion. The process can occur without the formation of gaseous products. In the case of the formation of gaseous products, their removal may be slowed down due to sorption or delayed diffusion.

In all experiments carried out on the whole volume, the material is sintered and compacted.

*DTGA samples of coal seam IV.* Pre-lumpy material was crushed (to a particle size of ≤ 0.5 mm). When the sample is heated, exoeffects at 380, 500 and 520 ºC and endoeffects at 420, 590 and 640 ºC are detected on the DTA curve (Fig. 2).

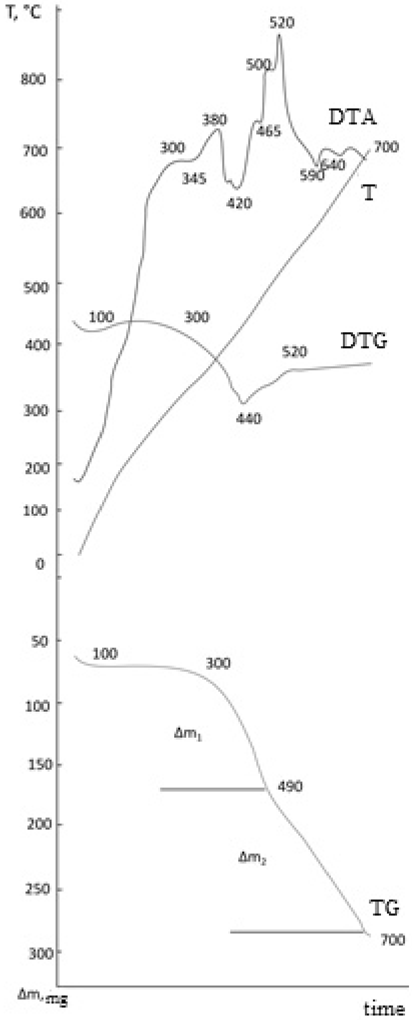

Figure 2. DTGA of the initial sample of reservoir IV

Such dynamics of decomposition is due to the fact that several processes are simultaneously or sequentially realized during heating: an exothermic structural transition, melting, boiling and sublimation of hydrocarbon components, distillation of the gas fraction and its ignition at the crucible exit (exoeffect at 500–520 ºC). When this occurs, the sample mass decreases (TG and DTG curves) at 90–100 ºC by ~0.8 %, possibly due to the loss of sorbed moisture, and further from 300 ºC with an increase in intensity to 440–480 ºC and uniform up to 700 ºC. In this case, the total mass loss is equal to 25.8 %, which exceeds the mass loss of a sample of coal from reservoir VIII, for the reason that sample IV is prepared from lump monolith, and sample VIII is from the initial dispersed, finely ground material from which, due to a large contact surfaces with the external environment; during storage a significant part of the gas component evaporates. At 450–480 ºC, a swelling and increase in the volume of the material occurs with the formation of a viscous mass. When cooled, a sufficiently solid porous column is formed.

DTGA samples of the enlarged batch (mass ~ 3 kg), which consisted of a mixture of fines and a lump material of various sizes, gave the following results.

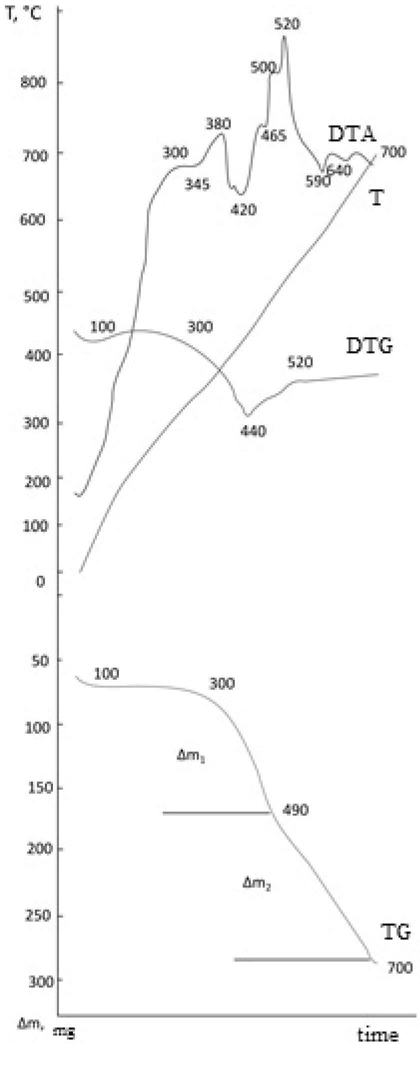

Figure 3. DTGA enlarged batch of coal Tavantolgoyskoye field

When heated, the phase and chemical changes in the material have a complex dynamics (see Fig. 3). Already in the areas of DTA, DTG and TG curves, corresponding to a temperature of 100–140 °C, a small effect is noted, accompanied by a small weight loss. At ~300 ºC, the effect appears with a slight increase (0.5 %) and a subsequent decrease in mass (~1.8 %). In this temperature range, the total mass loss of the sample was 2.4 %.

The subsequent explosive effect at 405–440 ºC is observed on the DTG and DTA curves with a sharp weight loss ($\Delta m^2$ ~8.2 %). Phase transformations (DTA: 480, 540, 590 and 610 ºC) are accompanied by a consistent decrease in mass, a total of 11.0 %, and further in the range of 610–680 ºC — 3.5 %. The total cumulative mass loss is ~25 %. At the same time, intensive swelling of the material, the formation of porous sinter in the upper part of the sample and dense sintering in its bottom part are noted.

*Enlarged experiments of thermal decomposition of coal.* According to the data of experiments, the mass loss of the sample when heated to 600 ºC and exposure at this temperature is in the range of 29.35–25.45 %

(average — 22.78 %), except for the decrease in the mass of the sample prepared from small rashes, equal to 10.45 %, which does not fit in with the results of other experiments. This is probably due to the aggregate composition of the source material and the initial low content of the gas component in the composition of the coal. Prolonged contact with the air environment of coal in the form of a small rash contributes to the intensive diffusion of the gas component from coal, as well as chemical and physical weathering of the easily oxidizable and removed to the environment components of this type of coal.

The amount of condensate produced by sublimates of low-boiling fractions on average reaches ~ 9 % of the initial sample mass. The maximum value (10.09 %) was obtained in the experiment, where the initial sample was prepared from lump material. At the same time, data on the mass of condensate (8.9 %) for the experiment, where the source material was trifle from the package of the enlarged batch, agrees well with the data of other experiments.

The results of experiments with heating samples up to 600 ºC with holding for 2 hours every 100 ºC showed that the process of thermal decomposition for averaged samples prepared with the grinding of bulk material of different sizes, and for the sample obtained by grinding a part of the whole monolith, implemented by a single mechanism.

Intensive thermolysis occurs in the temperature range of 400–500 ºC with maximum sublimation of gaseous and easily volatile components of coal within up to 15 % of the initial mass of the sample, from which 10–12 % is due to removal of the gas component, i.e. 70–80 % of the total mass loss of the original sample.

The mass loss of the material when heated to 300 ºC reaches almost 3 % for medium samples and 4 % for lumpy samples. Condensate is released evenly in all temperature stages: starting with low concentrations (0.5 %) at ≤ 200 °C and 1.5–3.0 % at each subsequent temperature stage. The total weight loss in all experiments is comparable and amounts to 21.74–23.32 % of the initial mass of the sample. This value is composed of the mass of sublimate condensate (within 7.12–9.04 %) and the gas component (within 13.85–14.62 %). This series of experiments is characterized by the absence of swelling and an increase in the volume of the material. After each stage, starting from 300 ºC, sintering of the material in the bottom part of the crucible was observed with preservation of the upper free-flowing layer.

Table 2

**The results of experiments with heating and exposure (1 hour) at 600 ºC samples of Tavantolgoysky coal**

| Ex. No. | Material | $t$, ºC | $\sum\Delta m$, % | Condensate, % | Gas. fraction, % | Note |
|---|---|---|---|---|---|---|
| 1 | Average sample | 600 | 24.6 | 7.9 | 16.7 | Swelling, sintering |
| 2 | Average sample | 600 | 25.45 | 9.3 | 16.15 | Swelling, sintering |
| 3 | Average sample | 600 | 20.7 | 8.73 | 12 | Swelling, sintering |
| 4 | Trifle from the package | 600 | 10.45 | 8.9 | 1.6 | No swelling, sintering |
| 5 | Monolith sample | 600 | 20.35 | 10.09 | 10.26 | Porous sinter |
| 6 | Average $\sum$ exp. 1–3;5 | 600 | 22.78 | 9 | 13.78 | Swelling, sintering |

The results of experiments on thermal decomposition of the coal batch under study are summarized in Table 2. As follows from the data presented, the results of all experiments (with and without stage aging) correlate well with each other, with the exception of experience data with breakdown of the bulk material (experiment 5), where the amount of condensate is comparable to average values (8.9 %), and the amount of gas fraction is an order of magnitude less (1.6 %). As a result, the total mass loss for this sample during thermal decomposition is 10.45 %. This is less than half the weight loss of the averaged samples and the monolith sample.

It should be noted that the characteristic feature of the behavior of this type of coal during its thermal decomposition is that the volume of the material increases 1.5–2.0 times when heated in continuous mode to ≥ 600 ºC and at the same time with step-by-step temperature exposures this phenomenon is not observed, but the sintering of the material in the bottom part is preserved. Apparently, this is due to the drainage of the liquid fractions during their formation and subsequent heating.

## *Conclusions*

A preliminary thermal analysis of samples of coal VIII and IV of the layers showed that when they are heated, the gaseous components of the coal are distilled, and the solid hydrocarbons are sequentially melted and sublimated. The depth and quantitative characteristics of thermolysis are largely determined by the initial state of aggregation (size of material, preparation conditions, heating mode and the final temperature of the experiment). So, a fine sample of reservoir VIII with DTGA up to 660–700 ºC has a relatively low mass loss (13–15 %). A sample of the original lump monolith of coal seam IV has a slightly different pattern of thermal decomposition. The DTA curve shows more prominently the effects of gas component sublimation, melting, sublimation, and burning at the crucible outlet of the hydrocarbon solid phases. In this case, the mass loss reaches 26 %.

Comparison of DTGA data from initial samples of a finely dispersed formation VIII and a large-size formation IV indicates a sharp difference in the content of the gas component in them (~2 times). This is probably due to more affordable storage conditions for diffusion from the material of the gas component of the dispersed coal product of the sample from reservoir VIII, rather than lump material from the sample from formation IV.

The studies carried out of the enlarged batch showed that the thermal decomposition of hard coal from the Tavantolgoyskoye deposit was determined by the initial aggregate state of the samples, i.e. the size of the material, as well as the final temperature of thermolysis.

The total weight loss during thermal decomposition of the averaged samples of the starting material with continuous heating to 600 °C and exposure for 2 hours at this temperature is in the range of 20.35–25.45 %. It consists of the mass of the condensate formed sublimates (7.90–10.09 %) and the magnitude of the gas component (10.26–16.70 %).

The data on thermal decomposition of a sample prepared from a fine, loose part of batch material differs sharply from those for averaged samples at close concentrations of sublimates concentrates (8.9 %) and almost an order of magnitude (1.6 %) less than the gas component. This is consistent with the data obtained during thermolysis of a single dispersed sample of reservoir VIII.

The total decrease in the mass of the samples in experiments with a stepwise temperature exposure (21.74–23.32 %) is comparable with the data obtained with continuous heating. This value is composed of the mass of sublimate condensate (7.12–9.04 %) and the gas component (13.85–14.62 %). The process of thermolysis begins already at ≤ 250 ºC and intensively develops at 400–500 ºC. With continuous heating, sintering and intensive swelling of the material occurs, its volume increases by ~1.5–2.0 times. The material is a porous, dry product with a denser bottom part. With stage-by-stage aging, starting at 300 ºC and at all subsequent stages, the material is sintered in the bottom part, and in the upper part the bulk structure is preserved at the initial sample volume. From the results of the research it follows that the coals of the Tavantolgoyskoye deposit can be used for briquetting (without any addition of binders) and obtaining valuable coal-chemical products.

## References

1 Горная энциклопедия: в 5 т. — Т. 5. / под ред. Е.А. Козловского. — М.: Сов. энцикл., 1991. — С. 227.

2 Краткая химическая энциклопедия: в 5 т. — Т. 2, 5. / под ред. И.Л. Кнунянца. — М.: Сов. энцикл., 1963–1967. — С. 330, 326.

3 Геология Монгольской Народной Республики / под ред. Н.А. Миронова, Р.А. Хасина, Ч. Хурц. — М.: Недра, 1977.

4 Erdenetsogt, Bat-Orshikh Mongolian coal-bearing basins: Geological settings, coal characteristics, distribution, and resources / Bat-Orshikh Erdenetsogt, Insung Lee, Delegiin Bat-Erdene, Luvsanchultem Jargal // Int. Coal geol. — 2009. — Vol. 80, Iss. 2. — P. 87.

5 Шибанов В.И. Обобщение результатов геологоразведочных работ по Улуг-Хемскому угольному бассейну по состоянию на 01.01.1993. — Кызыл: ТТФГИ, 1994. — 33 с.

6 Копылов Н.И. Термическое разложение углей Тувинского месторождения / Н.И. Копылов // Химия в интересах устойчивого развития. — 2013. — Т. 21, № 1. — С. 1–6.

7 Kopylov N.I. Thermolysis of brown coal from the Baganursky deposit (Mongolia) / N.I. Kopylov // Bulletin of the Karaganda University. Chemistry series. — 2017. — No. 4(88). — P. 80–87.

8 Kopylov N.I. Thermolysis of coal from the deposits of Tuva and Mongoliya // Theoretical and experimental chemistry: Proceedings of the VI$^{th}$ International scientific conference, dedicated to EXPO-2017 (15–17 June 2017). — Karaganda: KSU Publ., 2017. — P. 120.

Н.И. Копылов

## Моңғолияның Тавантолгой кен орны тас көмірлерінің күйдіру кезіндегі фазалық ыдырауы

Тавантолгой кен орнының тас көмірлері, басқа кен орындары көмірлері сияқты, отын-энергетикалық ресурс тұрғысынан, сонымен қатар металлургия және химия өнеркәсібінде шикізат ретінде үлкен қызығушылық туғызады. Қоршаған ортаның улы заттармен ластануын алдын алу мақсатында бұл көмірді ЖЭС және тұрмыстық пеш қондырғылары үшін отын ретінде және өнеркәсіпте бастапқы шикізат ретінде пайдалану кезінде арнайы дайындықтан өткізуді қажет етеді. Сондықтан көмірдің күйдіру кезіндегі фазалық ыдырауы зерттелді. Тавантолгой кен орнындағы тас көмірдің термиялық ыдырау зерттеулерінің нәтижелері көрсетілген. Зерттеудің нәтижесінде фазалық ыдырау процесі 300–500°С температурасы аралығында газ, тез балқитын және жылдам қайнайтын фазалардың бөлінуімен жүретіні анықталды. Бұл кезде материал массасының көлемі бойынша артатындығы және қатты, кеуекті өнім түзіп бірігетіні байқалды, оның көлемі бастапқы сынамадан 1,5–2 есе артатыны анықталды. Тавантолгой көмірлерін байланыстырғыш заттарды қоспай отындық брикеттерді алуда қолдануға болатындығы көрсетілді.

*Кілт сөздер:* тас көмір, фазалық ыдырау, қатты қалдық, шайырлы фракция, конденсат, возгондар, органикалық фракция.

Н.И. Копылов

## Фазовое разложение каменных углей Тавантолгойского месторождения Монголии при их обжиге

Каменные угли Тавантолгойского месторождения по аналогии с углями других подобных месторождений представляют интерес не только как топливно-энергетический ресурс, но и как сырьё для металлургической и химической отраслей промышленности. В целях предотвращения заражения окружающей среды токсичными компонентами при использовании этих углей в качестве топлива для ТЭЦ и бытовых печных установок, а также в промышленности в качестве исходного сырья, требуется их специальная подготовка. В связи с этим были проведены исследования по изучению фазового разложения этих углей при их обжиге. Представлены результаты комплексного исследования термического разложения каменных углей данного месторождения. Установлено, что этот процесс фазового разложения осуществляется в пределах температур 300–500 ºС с выделением газовой, легкоплавкой и легкокипящей фаз. При этом масса материала увеличивается в объёме и спекается с образованием твёрдого, пористого спёка, объём которого в 1,5–2 раза превышает объём исходной пробы. Показано, что тавантолгойские угли можно использовать для получения топливных брикетов без добавок связующего.

*Ключевые слова:* каменный уголь, фазовое разложение, твёрдый остаток, смолистая фракция, конденсат, возгоны, органическая фракция.

## References

1 Kozlovsky, E.A. (Eds.). (1991). *Hornaia entsiklopediia [Mountain Encyclopedia]* (Vols. 1–5: Vol. 5). Moscow: Sovetskaia entsiklopediia [in Russian].

2 Knunyats, I.L. (Eds.). (1963–1967). *Kratkaia khimicheskaia entsiklopediia [Brief chemical encyclopedia].* (Vols. 1–5: Vol. 2, 5). Moscow: Sovetskaia entsiklopediia [in Russian].

3 Mironova, O.N., Hasina, R.A., & Hurz, C. (1977). *Heolohiia Monholskoi Narodnoi Respubliki [Geology of the Mongolian People's Republic]*. Moscow: Nedra [in Russian].

4 Erdenetsogt, B.-O., Lee, I., Delegiin, B.-E., & Jargal, L. (2009). Mongolian coal-bearing basins: Geological settings, coal characteristics, distribution, and resources, *Int. Coal geol.*, *80*(2), 87.

5 Shibanov, V.I. (1994). *Obobshchenie resultatov heolohorazvedochnykh rabot po Ulug-Khemskomu uholnomu basseinu po sostoianiiu na 01.01.1993 [Generalization of the results of geological exploration of the Ulug-Khemky coal basin as of 01/01/1993].* Kyzyl: TTFGI [in Russian].

6 Kopylov, N.I. (2013). Termicheskoe razlozhenie uhlei Tuvinskoho mestorozhdeniia [Thermal decomposition of coal from the Tuva deposit]. *Khimiia v interesakh ustoichivoho razvitiia — Chemistry for Sustainable Development*, *21, 1,* 1–6 [in Russian].

7 Kopylov, N.I. (2017). Thermolysis of brown coal from the Baganursky deposit (Mongolia). *Bulletin of the Karaganda University. Chemistry series*, *(4)88,* 80–87.

8 Kopylov, N.I. Thermolysis of coal from the deposits of Tuva and Mongoliya. Proceedings from Theoretical and experimental chemistry: the VI$^{th}$ International scientific conference, dedicated to EXPO-2017, 15–17 June 2017 (p. 120). Karaganda: KSU Publ.

DOI: 10.31489/2019Ch1/85-90

UDC 544.653.1

Sh.T. Koshkarbaeva, M.S. Sataev, P.A. Abdurazova, K.B. Amanbaeva, Ye.B. Raiymbekov

*M. Auezov South Kazakhstan State University, Shymkent, Kazakhstan*
*(E-mail: eplusr@bk.ru)*

# Investigation of chemical nickel plating of powdered carborundum

The technology of application of metal coatings on the surface of powder carborundum was developed. At the same time, the process of chemical nickel plating was used for this purpose. It was found that carborundum, although not included in the number of catalysts of this process, could contribute to the reduction of nickel ions. It was assumed that in the high-temperature decomposition of the hyposphyte ion, hydrogen evolution took place at the carborundum surface with a slowed-down stage by recombining hydrogen atoms into the molecule. The high reactivity of hydrogen atoms leads to the reduction of nickel ions. This makes it possible to activate the surface of carborundum and to further build up the metal under conditions typical for chemical nickel plating. Experiments in which the surface of the powder was investigated by means of a scanning electron microscope showed that such a mechanism for activating the powder surface was valid. Testing of this technology under laboratory conditions allowed obtaining a coating having the necessary adhesion to carborundum particles and containing 95 % of chemical nickel.

*Keywords*: carborundum, silicon carbide, chemical nickel plating, composite material, hydrogen atoms, activation, nickel-phosphorous coating.

## *Introduction*

Carborundum (silicon carbide) is a refractory (melting point 2830 ºC), chemically permanent, second in hardness to diamond and boron nitride. Silicon carbide has high thermal, chemically and radiation permanent, stands out for its oxidation resistance among many metal-resistant alloys and chemical compounds. These properties contributed to its widespread use as a material of ceramic composite materials and coatings [1–4].

But at the same time, in order to ensure adhesion between the individual components, it becomes necessary to clad the surface of powdered carborundum with various metals. The coated particles of carborundum can be used for the manufacture of abrasive tools and composite materials such as metal-ceramics. Such materials are used for the manufacture of corrosion and erosion-resistant nozzle inserts; for the manufacture of parts of heat exchange equipment and parts of pumps for pumping acidic solutions and other corrosive liquids [1–4].

Known methods of applying metal coatings on dielectric powders can be divided into physical and chemical methods [5–7]. Physical methods, when the metal is first converted into vapor or liquid applying to the surface to be coated, where they again turn into a compact solid metal, forming a coating [8–10]. Chemical methods, when a metal is formed during a chemical reaction and, settling on the surface to be coated, create metallic coatings [6, 7]. Chemical methods are more convenient for the metallization of powders since in this case, it is easier to obtain coatings from particles uniformly distributed over the entire surface.

So for the metallization in the gas phase, the reaction of thermal decomposition of metal carbonyls can be used [11]. During the course of the reaction, they decompose, leaving the metal on the surface to be coated and release carbon monoxide, which can again be used to produce metal carbonyl. Currently, using carbonyl technology, it is possible to apply dielectric powders of iron, nickel, cobalt, tungsten, and chromium coatings. The disadvantage of this method is the use of high temperatures necessary for the decomposition of carbonyl compounds, and the high cost of carbonyls.

Plasma-chemical method [9] allows obtaining a metal coating on the surface of the powder material located in the pseudo-boiling layer. The disadvantage of this method is the need to obtain high temperatures, the complex design of the reactor, the use of the working gas, additionally purified from oxygen, the fragility of the electrodes.

The electrochemical method [12] requires preliminary deposition of a metallic sublayer on dielectric materials using other methods. The method does not have the disadvantages of the above analogues, allows obtaining higher performance, however, in the case of obtaining powders with a metal content of up to 50 %, the quality of the coating deteriorates significantly.

The chemical method of precipitation from solution involves the pretreatment of the starting powder in solutions of the palladium and tin salts in order to obtain active catalytic sites [6, 13]. Then, in solutions containing a compound of the corresponding metal, the reducing agent and the complexing agent are chemically coated with copper or Nickel coating. The disadvantages of this method are the high cost of palladium salts used to activate the surface of the powder particles and the possibility of desorption of palladium from the surface of the particles, leading to the formation of a coating metal in a solution outside the surface of the powder particles.

Palladium-free methods for powder metallization are proposed. So in [14, 15], pretreatment is carried out by creating on the surface of powdered particles a layer of copper sulphate, which is then transferred with the help of a phosphine gas to a metal-like layer of copper phosphide. This film allows to further obtaining a metallic coating by chemical or electroplating. But the use of phosphine requires a process in sealed conditions, which creates additional difficulties.

The analysis shows the relevance of the metallization of the carborundum surface and the need to develop new alternative methods for this purpose.

## *Experimental*

In this work, it was proposed to use a process of chemical nickel plating for the application of a metallic coating. Chemical nickel plating was carried out in electrolytes containing a nickel salt, a reducing agent: sodium hypophosphite, as well as buffering additives (salts of organic acids). The process flows at a high temperature on the surface of metals that are catalysts for the decomposition of hypophosphite. Thus, the process begins spontaneously on metals such as nickel, iron, aluminum, and palladium at temperatures above 50–70 °C. The process of chemical nickel plating was accompanied by the release of hydrogen. Moreover, there is often a relationship between the amount of the deposited nickel-phosphorus coating and the volume of hydrogen released [6].

$$NaH_2PO_2 + H_2O \rightarrow NaH_2PO_3 + 2H^+ + 2e^- \qquad (1)$$

$$NaH_2PO_2 + 2H_2O \rightarrow NaH_2PO_4 + H_2 + 2H^+ + 4e^- \qquad (2)$$

$$3NaH_2PO_2 - 2e^- \rightarrow Na_3PO_3 + 2P + 3H_2O \qquad (3)$$

$$5NaH_2PO_2 - 4e^- \rightarrow Na_3PO_4 + 4P + 2NaOH + 4H_2O \qquad (4)$$

The electrons formed by reactions (1, 2) reduce the $Ni^{2+}$ and $H^+$ ions in the electrolyte solution.

$$Ni^{2+} + 2e^- \rightarrow Ni \qquad (5)$$

There are other hypotheses explaining the mechanism of chemical nickel plating. So the process of deposition of coatings can be linked by the reactivity of hydrogen atoms.

$$2H + Ni^{2+} \rightarrow Ni + 2H^+ \qquad (6)$$

In this case, part of the hydrogen released, always accompanying the process of chemical Nickel plating, is the result of a side reaction.

The study of the mechanism of chemical nickel plating by measuring the stationary potential of some metals in solutions containing 10 and 50 g/L of sodium hypophosphite in the temperature range of 20–100 °C showed that the stationary potential of the nickel electrode sharply shifts to the negative nickel at temperatures above 70 °C [16]. In addition, spontaneous chemical nickel plating on copper phosphides deposited on dielectric materials is noted, although in this case this potential is not reached. Moreover, even after the deposition of a layer of chemical nickel, the stationary potential was in a more positive area than the reduction potential of nickel ions. Therefore, the reduction of nickel ions can occur only at the expense of atomic hydrogen.

The study of chemical nickel plating was carried out on carborundum powder 93CF40. Samples of powders at various stages of the process were studied using an ISM-6490-LV scanning electron microscope (JEOL, Japan), which allowed obtaining electronic images (photographs) of individual sections (spectra) of the surface at given magnifications. The microscope made it possible at the same time to obtain elemental compositions of the spectra in the form of a table.

The initial powders were decreased in a 20 % solution of sodium carbonate at a temperature of 40–500 °C until the surface of the particles was completely wetted and washed in hot running water. The powder prepared in this way was placed in a Petri dish and dried at 50 °C to constant wt. Then 10 g of the powder was placed in a heat-resistant beaker, poured 100 ml of $NiSO_4 \cdot 7H_2O$ solution — 30 g/L. $NaH_2PO_2$ — 10 g/L, $CH_3COONa$ — 10 g/L and subjected to activation. For this, the solution was heated to boiling. The heating process was carried out on a hotplate and usually took about 10 minutes. After boiling the solution, heating was stopped and the solution was allowed to cool to 70 °C. At the same time, visual observations show that when the temperature rises, hydrogen evolution is practically absent. But after boiling it is already visually possible to observe the release of gaseous hydrogen. Consequently, silicon carbide, which has semiconducting properties, can be a catalyst for the decomposition of hypophosphite ions after such activation, and there is slow recombination of adsorbed hydrogen atoms. The temporary existence of hydrogen atoms and can lead to the process of chemical nickel plating.

## *Results and discussion*

Figure 1 shows the electron image of the carborundum powder after such an activation cycle. This figure, it is possible to distinguish light areas characteristic of the metal phase and dark areas of carborundum. The spectral analysis presented in the table shows that the content of carborundum (Si + C) is over 94 % in dark areas, and the content of nickel phosphorus coating (Ni + P) is over 90 % in light areas.

At the same time, even in the dark area, nickel is released (3.28 %), which indicates the initial stage of activation of these areas. It also draws attention to the fact that when nickel is released, no phosphorus is released. Perhaps this is due to the fact that when activated, reaction (6) is predominant. In general, after activation, the nickel extraction process takes up about 36 % of the total carborundum.

Experiments have shown that after carrying out the activation process three times, a nickel layer is formed that is sufficient for carrying out the process at usual temperatures (80–95 ºC). This technique should be considered more preferable than prolonged boiling in the electrolyte of chemical nickel plating, in which undesirable decomposition of hypophosphite and nickel release outside the surface of carborundum is possible.

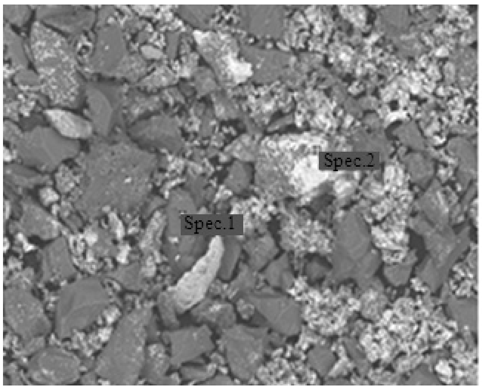

| Element | Weight, % | | |
|---|---|---|---|
| | Total | Spec-1 | Spec-2 |
| C | 20.01 | 31.58 | 4.97 |
| O | 6.45 | 5.33 | - |
| Al | 0.42 | - | - |
| Si | 36.78 | 61.84 | 2.84 |
| P | 2.09 | - | 9.73 |
| Fe | 0.24 | - | - |
| Ni | 34.02 | 1.26 | 82.46 |

Figure 1. Electronic image after one activation cycle
(the Table shows the elemental composition common to the whole powder and for individual spectra)

Further growth of the metal film was carried out by chemical nickel plating in the usual solution of the following composition: $NiSO_4 \cdot 7H_2O$ — 30 g/L, $NaH_2PO_2$ — 10 g/L, $CH_3COONa$ — 10 g/L, at an electrolyte temperature of 90 ºC for 30 minutes.

The data of the spectral analysis of the powder (Fig. 2) show that the carborundum particles are 95 % coated with a nickel-phosphorus coating.

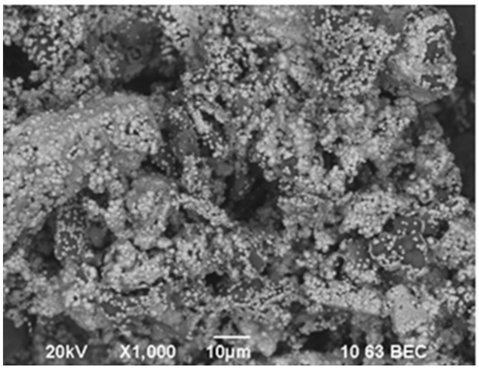

| Element | Weight, % |
|---|---|
| C | 1.54 |
| Si | 3.15 |
| P | 8.75 |
| Ni | 86.46 |

Figure 2. Electronic image of carborundum powder after three cycles of activation
and chemical nickel plating at 90 ºC in ordinary acid electrolyte

A photograph of the powder, taken at a magnification of 8,000 times (Fig. 3), shows that the coating is formed in the form of spherical particles, the average diameter of which ranges from 300 to 750 nanometers. It is also seen from this figure that the individual spherical particles are collected in large agglomerates having a dense packing.

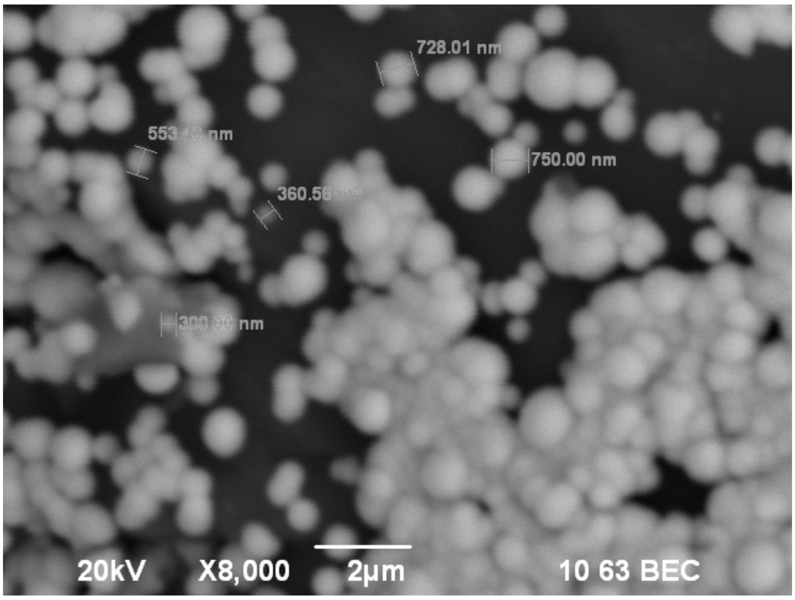

Figure 3. The structure of metallic nickel particles deposited on particles of carborundum powder after one cycle of activation in a solution of chemical nickel plating

It can also be seen from the above figures that the formation of a coating occurs only on the surface of the carborundum particles. Consequently, such a coating will provide the necessary adhesion between the particles of carborundum and the matrix in obtaining composite products or coatings.

### *Conclusions*

Silicon carbide can be a catalyst for chemical nickel plating. However, this catalytic activity is manifested at high temperatures, which are achieved by boiling the electrolyte of chemical nickel plating. Such activation is explained by the decomposition of hypophosphite ions, leading to the release of hydrogen. The intermediate stage of the process is the formation of atomic hydrogen adsorbed on the surface of silicon carbide. As a result, the interaction of nickel ions with hydrogen atoms on the surface of carbide particles forms a metallic nickel film, which makes it possible to carry out the process at lower temperatures. In addition, for solutions for chemical nickel plating, electrolyte regeneration methods have been developed that make this process cheaper and more technologically advanced.

## References

1 Ахметов Н.С. Общая и неорганическая химия / Н.С. Ахметов. — СПб.: Лань, 2014. — 495 с.

2 Патент Российской Федерации МПК C23F1/14 — № 2544319. Способ химического никелирования и раствор для его осуществления / Каблов Е.Н., Щетанов Б.В., Ефимочкин И.Ю., Севостьянов Н.В., Мурашева В.В., Вдовин С.М., Нищев К.Н. Заяв. 17.12.2013, Опубл. 20.03.2015.

3 Патент Российской Федерации МПК C23C4/12 — № 2542199. Способ получения композиционных покрытий из порошковых материалов / Григорьев С.Н., Тарасова Т.В., Попова Е.В., Смуров И.Ю. Заяв. 16.07.2013, Опубл. 20.02.2015.

4 Ferrante M. Metallization of silicon carbide with chromium powder / M. Ferrante, E. Pigoretti // Journal of Materials Science Letters. — 1992. — Vol. 11, No. 24. — P. 1687–1688.

5 Гамбург Ю.Д. Гальванические покрытия: справочник по применению / Ю.Д. Гамбург. — М.: Техносфера, 2006. — 215 с.

6 Вишенков С.А. Химические и электрохимические способы осаждения металлопокрытий / С.А. Вишенков — М.: Машиностроение, 1975. — 312 с.

7 Хокинг М. Металлические и керамические покрытия: подготовка, свойства, применение / М. Хокинг, В. Васатасри, П. Сидки. — М.: Мир, 2000. — 516 с.

8 Besov A.V. A method of manufacturing powder materials for plasma spraying retention coatings / A.V. Besov // Inventions in mechanical engineering. — 2001. — No. 2. — P. 14, 15.

9 Patent of the United States of America MPK C23C16/4417 — No. 5489449. Coated particles of inorganic or metallic materials and processes of producing the same / Kaoru U., Yukiyoshi Y., Tadashi F., Eisuke K., Satoshi A. Decl. 18.07.1994, Publ. 06.02.1996.

10 Patent of the United States of America MPK C09K3/1445 — No. 5250086. Multi-layer metal coated diamond abrasives for sintered metal bonded tools / Roger M., Edward J.C., David E.S. Decl. 25.03.1992, Publ. 05.10.1993.

11 Патент Российской Федерации МПК C23C24/04 — № 2257423. Портативное устройство для газодинамического напыления покрытий / Каширин А.И., Клюев О.Ф., Буздыгар Т.В., Шкодкин А.В. Заяв. 21.08.2003, Опубл. 10.03.2005.

12 Патент Российской Федерации МПК C23C24/04 — № 2247174. Устройство газодинамического напыления порошковых материалов / Косарев В.Ф., Лаврушин В.В., Спесивцев В.П., Сюн Т., Цзе У., Цзинь Х. Заяв. 30.04.2003, Опубл. 27.02.2005.

13 Хоперия Т.Н. Химическое никелирование неметаллических материалов / Т.Н. Хоперия. — М.: Металлургия, 1982. — 144 с.

14 Sataev M.S. A galvanic-chemical method for preparing diamond containing coatings / M.S. Sataev, S.T. Koshkarbaeva, S. Perni, S.Z. Nauryzova, P. Prokopovich // Colloids and Surfaces A: Physicochemical and Engineering Aspects. — 2015. — Vol. 480. — P. 384–389.

15 Sataev M.S. A low-temperature gold coating of the dielectric surfaces employing phosphine gas as a reducing agent / M.S. Sataev, P.A. Abdurasova, Sh.T. Koshkarbaeva, A.A. Bolisbek, N.K. Saripbekova, G.A. Kambarova, O.N. Koblanova, S. Perni, P. Prokopovich // Colloids and Surfaces A: Physicochemical and Engineering Aspects. — 2017. — Vol. 521. — P. 86–91.

16 Kozhakulov N.K. Stationary potential of metals and alloys in the process of chemical nickel plating / N.K. Kozhakulov, Sh.T. Koshkarbaeva, M.S. Sataev // Kazakhstan industry. — 2009. — Vol. 6, No. 57. — P. 56, 57.

---

Ш.Т. Қошқарбаева, М.С. Сатаев, П.А. Абдуразова, К.Б. Аманбаева, Е.Б. Райымбеков

## Ұнтақ тәрізді карборундты химиялық никельдендіруді зерттеу

Ұнтақ тәрізді карборундтың бетіне металл жабындысын қолдану үшін технология әзірленді. Бұл мақсатта химиялық никель қаптамасы қолданылды. Бұл үрдістің катализаторлар қатарына кіре алмаса да, карборунд никель иондарының азаюына ықпал ететіндігі анықталды. Гипосфит ионының жоғары температурадағы ыдырау кезінде карборундтың бетінде молекулаға сутегі атомдарын рекомбинациялау арқылы баяулау сатысында жүреді деп болжануда. Сутегі атомдарының жоғары реактивтік қабілеттілігі никель иондарының азаюына әкеледі. Бұл карборундтың бетін белсендіруге және химиялық никель қаптамасына тән жағдайда металды одан әрі үдетуге мүмкіндік береді. Растрлы электронды микроскоп арқылы ұнтақ беті зерттелген тәжірибелерде ұнтақ бетін белсендірудің осындай механизмі жарамды екенін көрсетті. Осы технологияны зертханалық жағдайларда сынау карборундты бөлшектерге қажетті адгезиясы бар және құрамында 95 % химиялық никель бар жабынды алуға мүмкіндік берді.

*Кілт сөздер*: карборунд, кремний карбиді, химиялық никельдендіру, композициялық материал, сутегі атомдары, белсендіру, никель-фосфорлы қаптама.

---

Ш.Т. Кошкарбаева, М.С. Сатаев, П.А. Абдуразова, К.Б. Аманбаева, Е.Б. Райымбеков

## Исследование химического никелирования порошкообразного карборунда

Разработана технология нанесения металлического покрытия на поверхность порошкообразного карборунда. При этом для этой цели использован процесс химического никелирования. Найдено, что карборунд, хотя и не входит в число катализаторов этого процесса, может способствовать восстановлению ионов никеля. Предполагается, что при высокотемпературном разложении гипосфит-иона выделение водорода происходит на поверхности карборунда с замедленной стадией рекомбинации атомов водорода в молекулу. Высокая реакционная способность атомов водорода приводит к восстановлению ионов никеля. Это позволяет активировать поверхность карборунда и проводить дальнейшее наращивание металла в условиях, обычных для химического никелирования. Эксперименты, в которых поверхность порошка исследовалась при помощи растрового электронного микроскопа, показали справедливость такого механизма активирования поверхности порошка. Проверка данной технологии в лабораторных условиях позволила получить покрытие, имеющее необходимое сцепление с частицами карборунда и содержащее 95 % химического никеля.

*Ключевые слова*: карборунд, карбид кремния, химическое никелирование, композиционный материал, атомы водорода, активация, никель-фосфорное покрытие.

## References

1 Akhmetov, N.S. (2014). *Obshchaia i neorhanicheskaia khimiia [General and Inorganic chemistry]*. Saint-Petersburg: Lan [in Russian].

2 Kablov, E.N., Shchetanov, B.V., Ephimochkin, I.Y., Sevostiyanov, N.V., Murasheva, V.V., Vdovin, S.M., & Nishev, K.N. (2015). Sposob khimicheskoho nikelirovaniia i rastvor dlia eho osushchestvleniia [Method of chemical nickel-plating and solution for its realization]. *Patent of the Russian Federation MPK C23F1/14 — No. 2544319.* Decl. 17.12.2013, Publ. 20.03.2015 [in Russian].

3 Grigorev, S.N., Tarasova, T.V., Popova, E.V., & Smurov, I.Y. (2015). Sposob polucheniia kompozitsionnykh pokrytii iz poroshkovykh materialov [Method for preparing composite coatings of powder materials]. *Patent of the Russian Federation MPK C23C4/12 — No. 2542199*. Decl. 16.07.2013, Publ. 20.02.2015 [in Russian].

4 Ferrante, M., & Pigoretti, E. (1992). Metallization of silicon carbide with chromium powder. *Journal of Materials Science Letters, 11(24)*, 1687–1688.

5 Hamburg, U.D. (2006). *Halvanicheskie pokrytiia. Spravochnik po primeneniiu [Electroplated coatings. Application Guide]*. Moscow: Tekhnosfera [in Russian].

6 Vishenkov, S.A. (1975). *Khimicheskie i elektrokhimicheskie sposoby osazhdeniia metallopokrytii [Chemical and electrochemical methods of metal plating]*. Moscow: Mashinostroienie [in Russian].

7 Hawking, M., Vasatasri, V., & Sidky, P. (2000). *Metallicheskie i keramicheskie pokrytiia: podhotovka, svoistva, primenenie [Metallic and ceramic coatings: preparation, properties, application]*. Mosow: Mir [in Russian].

8 Besov, A.V. (2001). A method of manufacturing powder materials for plasma spraying retention coatings. *Inventions in mechanical engineering, 2*, 14–15.

9 Kaoru, U., Yukiyoshi, Y., Tadashi, F., Eisuke, K., & Satoshi, A. (1996). A. Coated particles of inorganic or metallic materials and processes of producing the same. *Patent of the United States of America MPK C23C16/4417 — No. 5489449*. Decl. 18.07.1994, Publ. 06.02.1996.

10 Roger, M., Edward, J.C., & David, E.S. (1993). Multi-layer metal coated diamond abrasives for sintered metal bonded tools. *Patent of the United States of America MPK C09K3/1445 — No. 5250086.* Decl. 25.03.1992, Publ. 05.10.1993.

11 Kashirin, A.I., Kliuev, O.F., Buzdygar, T.V., & Shkodkin A.V. (2005). Portativnoie ustroistvo dlia hazodinamicheskoho napyleniia pokrytii [Portable apparatus for gasodynamic deposition of coatings]. *Patent of the Russian Federation MPK C23C24/04 — No. 2257423.* Decl. 21.08.2003, Publ. 10.03.2005 [in Russian].

12 Kosarev, V.F, Lavrushin, V.V., Spesivtsev, V.P., Sjun, T., Tsze, U., Tszin, K. (2005). Ustroistvo hazodinamicheskoho napyleniia poroshkovykh materialov [Apparatus for gasodynamic deposition of powder materials]. *Patent of the Russian Federation MPK C23C24/04 — No. 2247174.* Decl. 30.04.2003, Publ. 27.02.2005 [in Russian].

13 Hoperia, T.N. (1982). *Khimicheskoe nikelirovanie nemetallicheskikh materialov [Chemical nickel plating of non-metallic materials]*. Moscow: Metallurhiia [in Russian].

14 Sataev, M.S., Koshkarbaeva, S.T., Perni, S., Nauryzova, S.Z., & Prokopovich, P. (2015). A galvanic-chemical method for preparing diamond containing coatings. *Colloids and Surfaces A: Physicochemical and Engineering Aspects, 480*, 384–389.

15 Sataev, M.S., Abdurasova, P.A., Koshkarbaeva, Sh.T., Bolisbek, A.A., Saripbekova, N.K., & Kambarova, G.A., et al. (2017). A low-temperature gold coating of the dielectric surfaces employing phosphine gas as a reducing agent. *Colloids and Surfaces A: Physicochemical and Engineering Aspects, 521*, 86–91.

16 Kozhakulov, N.K., Koshkarbaeva, Sh.T., & Sataev, M.S. (2009). Stationary potential of metals and alloys in the process of chemical nickel plating. *Kazakhstan industry, 6(57),* 56–57.

DOI: 10.31489/2019Ch1/91-95

UDC 665.5

Fengyun Ma[1], Xintai Su[1], M.I. Baikenov[2], A.B. Tateyeva[2],
G.G. Baikenova[3], S.K. Mukhametzhanova[2], D.Ye. Aitbekova[2]

*[1]Xinjiang University, Urumqi, China;*
*[2]Ye.A. Buketov Karaganda State University, Kazakhstan;*
*[3]Karaganda Economic University of Kazpotrebsoyuz, Kazakhstan*
*(E-mail: murzabek_b@mail.ru)*

# Modeling of catalytic-cavitation processing of middle oil fraction (200–300 ºC)

Experiment planning is the optimal control of an experiment in the context of incomplete information about the process mechanism. Interest in the science of experiment is associated with a wide range of experimental studies and a significant economic effect from the optimal organization of the experiment. An optimal experiment is a way to save time and cash, increase reliability of results. Middle fraction of Kumkol oil (200–300 ºC) was used to study the cavitation effect on fuel oil. The following catalytic systems were used, namely, modified $FeS_2$, nanocatalysts ε-$Fe_2O_3/SiO_2$, α-$Fe_2O_3/SiO_2$ spherical catalyst, β-FeOOH, and $Fe(OA)_3$. By quantifying the individual composition of the middle fraction (200–300 ºC) of Kumkol oil, a general pattern of the effect of catalytic-cavitation processing on the hydrocarbon composition of the middle fraction (200–300 ºC) of Kumkol oil was established. The optimal conditions and a number of factors affecting the cavitation processing of the middle oil fraction (200–300 ºC) in the presence of a $FeS_2$ catalyst were determined. In accordance with the regression equation obtained, the optimal conditions for cavitation processing are the following: $\tau$ = 90–120 s, the amount of added catalyst is 0.7–1 g and the amount of added water is 1.5–2 ml.

*Keywords:* nanocatalytic systems, cavitation processing, Kumkol oil, experiment planning, middle fraction, iron (III) oxides, polymorphic modifications, hydrocarbon composition.

## *Introduction*

A large number of experimental problems in chemistry and chemical technology are formulated as extremal problems: determining the optimal process conditions, the optimal composition and etc. Due to the optimal location of points in the factor space and the linear transformation of coordinates, it is possible to overcome the drawbacks of classical regression analysis, in particular the correlation between the coefficients of the regression equation. The choice of the experiment plan is determined by the formulation of the research problem and the features of the object. The research process is usually divided into separate stages. The information obtained after each stage determines the further strategy of the experiment. Thus, the possibility of optimal control of the experiment arises. Planning an experiment allows all the factors to be varied simultaneously and to obtain quantitative estimates of the main effects and interaction effects. The effects of interest to the researcher are determined with a smaller error than with traditional research methods. Ultimately, the use of planning methods significantly increases the efficiency of the experiment [1].

Middle fraction of Kumkol oil (200–300 ºC) was used to study the cavitation effect on fuel oil. The individual chemical composition of the middle fraction of Kumkol oil (200–300 ºC) is presented in Table 1.

Table 1

**Individual chemical composition of the middle fraction (200–300ºC) of Kumkol oil**

| Exit time, min | Chemical composition | Content, % |
|---|---|---|
| 1 | 2 | 3 |
| 2.477 | Methylcyclodecane | 0.46 |
| 3.589 | 2-Methyldodecanol | 3.92 |
| 3.755 | 1,2,4-Trimethylbenzene | 4.15 |
| 4.629 | 2-Hexyloctanol | 10.87 |
| 4.758 | 2-Hexyldecanol | 10.05 |
| 5.963 | Cyclodecane | 2.4 |
| 6.049 | 2-Ethyl-1,4-dimethylbenzene | 2.56 |
| 7.912 | Decane | 5.87 |
| 9.129 | Undecane | 3.63 |

Continuation of Table 1

| 1 | 2 | 3 |
|---|---|---|
| 9.664 | 2,6,11-Trimethyldodecane | 6.35 |
| 10.138 | 2,7-Dimethylnaphthalene | 3.68 |
| 10.986 | 1-Hexadecene | 3.4 |
| 11.620 | 2,3,6-Trimethylnaphthalene | 4.3 |
| 12.357 | 2-Dodecyloxyethanol | 2.34 |
| 12.517 | Dodecane | 2.82 |
| 13.304 | Tridecan | 10.62 |
| 13.390 | 2,6,10-Trimethyltetradecane | 0.62 |
| 14.534 | 2-Methylheptadecane | 1 |
| 14.768 | 1,1-Hydroxybishexadecane | 13.05 |
| 15.635 | 2-Methylhexadecane | 0.79 |
| 15.819 | Tetradecane | 2.33 |
| 16.194 | 8-Methylpentadecane | 1.59 |
| 20.197 | Pentadecane | 3.1 |

The following catalytic systems were used, namely, modified $FeS_2$, nanocatalysts $\varepsilon$-$Fe_2O_3/SiO_2$, $\alpha$-$Fe_2O_3/SiO_2$ spherical catalyst, $\beta$-FeOOH, and $Fe(OA)_3$.

## *Experimental*

Experiments on the cavitation processing of the middle fraction of oil (200–300 ºC) were performed in a ultrasonic disperser MEF-92, which allows high-intensity processing of small volumes of liquids under laboratory conditions.

A sample of the treated liquid with a volume of 0.05 ml was subjected to a cavitation effect for 7–10 minutes. The amount of the introduced catalytic additive was 1 % of the volume of the treated substance. The parameters of the ultrasonic cavitator MEF-92 are as follows: the oscillation frequency is 22 kHz, the intensity of the ultrasonic effect is up to 250 W/cm$^2$, the power is 600 W.

The study of products of the middle fraction of oil (200–300 ºC) before and after cavitation processing was determined by gas chromatography-mass spectrometry using an HP 5890/5972 MSD instrument from Agilent (USA). Chromatography conditions are DB-XLB-5 column, 30 mm × 0.5 μm; gas — helium, 0.8 ml/min; in the temperature range of 50 ºC — 4 min, 50–150 ºC — 10 ºC/min, 150–300 ºC — 20 ºC/min, 300 ºC — 4 min; evaporator: 200–300 ºC. Identification of substances was carried out according to the NIST 98 mass spectral database.

## *Results and discussion*

One of the ways to successfully solve the technological problem of cavitation processing of oil fuels is to determine the optimal process conditions, namely, the duration of the cavitation processing, the amount of catalyst added and water. As optimization parameters ($y$), the dynamic viscosity of the average fraction of oil was considered, since viscosity is the main physico-chemical parameter of the properties of oil fuels. The following factors have been chosen as independent factors, namely, $z_1$ is duration of cavitation treatment (s); $z_2$ is the amount of catalyst (g); $z_3$ is the amount of water added (ml).

The influence of various factors on the reduction of viscosity during cavitation processing of the middle fraction of oil (200–300 ºC) was determined by the method of full factorial experiment design [1]. To derive a linear regression equation, an extended planning matrix of the full factorial experiment of type 23 was used (the number of levels was 2, the number of factors was 3), where all possible combinations of factors were implemented at the levels chosen for the study [2]. The coordinates of the center of the plan, the intervals of variation and the levels of research are shown in Table 2.

Table 2

**Experimental Conditions**

| | $z_1$ | $z_2$ | $z_3$ |
|---|---|---|---|
| Main level, $z^o_j$ | 90 | 0.75 | 1.5 |
| Variation interval, $\Delta z_j$ | 30 | 0.25 | 0.5 |
| +1 | 60 | 1 | 2 |
| –1 | 120 | 0.5 | 1 |

Table 3 presents the plan of the extended planning matrix of the full factorial experiment $2^3$ on a dimensionless scale.

Table 3

**Expanded matrix of planning full factor experiment $2^3$**

| Experience number | $x_0$ | $x_1$ | $x_2$ | $x_3$ | $x_1x_2$ | $x_1x_3$ | $x_2x_3$ | $x_1x_2x_3$ | $Y_{exp}$, $Pa{\cdot}s$ |
|---|---|---|---|---|---|---|---|---|---|
| 1 | +1 | –1 | –1 | –1 | +1 | +1 | +1 | –1 | 2.52 |
| 2 | +1 | +1 | –1 | –1 | –1 | –1 | +1 | +1 | 2.34 |
| 3 | +1 | –1 | +1 | –1 | –1 | +1 | –1 | +1 | 2.4 |
| 4 | +1 | +1 | +1 | –1 | +1 | –1 | –1 | –1 | 2.28 |
| 5 | +1 | –1 | –1 | +1 | +1 | –1 | –1 | +1 | 2.37 |
| 6 | +1 | +1 | –1 | +1 | –1 | –1 | –1 | –1 | 2.4 |
| 7 | +1 | –1 | +1 | +1 | –1 | –1 | +1 | –1 | 2.26 |
| 8 | +1 | +1 | +1 | +1 | +1 | +1 | +1 | +1 | 2.16 |

Using the plan presented in Table 3, the coefficients of the full linear regression equation were calculated:

$$\hat{y} = b_0 + b_1x_1 + b_2x_2 + b_3x_3 + b_{12}x_1x_2 + b_{13}x_1x_3 + b_{23}x_2x_3 + b_{123}x_1x_2x_3 . \tag{1}$$

Any coefficient of the regression equation $b_j$ is determined by the scalar product of the column $y$ on the corresponding column $x_j$ divided by the number of experiments in the planning matrix $N$:

$$b_j = \frac{1}{N}\sum_{i=1}^{N} x_{ji}y_i . \tag{2}$$

In accordance with equation (2), the following coefficients of the regression equation were obtained: $b_0 = 18.9$; $b_1 = –0.44$; $b_2 = –0.34$; $b_3 = –0.36$; $b_{12} = –0.89$; $b_{13} = –4.6$; $b_{23} = –0.16$; $b_{123} = 0.04$.

To determine the dispersion of reproducibility ($s^2_{\text{reprod.}}$) and check the significance of the regression coefficients and the adequacy of the equation, three additional experiments were put in the center of the plan and the following values of $y$ were obtained:

$$y_1^0 = 2.42;\ \ y_2^0 = 2.3;\ \ y_3^0 = 2.37;$$

$$\bar{y}^0 = \frac{\sum_{u=1}^{3} y_u^0}{3} = 2.36;$$

$$s^2_{\text{reprod.}} = \frac{\sum_{u=1}^{3}(y_u^0 - \bar{y}^0)^2}{2} = 0.0016;\ \ s_{\text{reprod.}} = 0.04 .$$

The diagonal elements of the covariance matrix are equal to each other; therefore all the coefficients of equation (1) are determined with the same accuracy:

$$s_{b_j} = \frac{s_{\text{reprod.}}}{\sqrt{\text{N}}} . \tag{3}$$

According to the formula (3):

$$s_{b_j} = 0.04/\sqrt{8} = 0.014 .$$

The significance of the coefficients of the regression equations was estimated by the Student's criterion using the formula:

$$t_j = \frac{|b_j|}{s_{b_j}} \tag{4}$$

According to the formula (4) $t_0 = 1334.1$; $t_1 = 31.05$; $t_2 = 24$; $t_3 = 25.4$; $t_{12} = 62.8$; $t_{13} = 324.7$; $t_{23} = 11.3$; $t_{123} = 2.82$. The tabular value of the student's criterion for the significance level $p = 0.05$ and the number of degrees of freedom $f = 2$ $t_p(f) = 4.30$. Consequently, the coefficient $b_{123}$ is insignificant and should be excluded from the regression equation (1), and the equation takes the form:

$$\hat{y} = 18.9 - 0.44x_1 - 0.34x_2 - 0.36x_3 - 0.89x_1x_2 - 4.6x_1x_3 - 0.16x_2x_3 \,. \qquad (5)$$

The adequacy of the obtained regression equation (5) experiment was tested by the Fisher criterion:

$$F = s^2_{\text{residual}} / s^2_{\text{reprod.}} \,;$$

$$s^2_{\text{residual}} = \frac{\sum_{i=1}^{8} (y_i - \hat{y}_i)^2}{N - l} = 0.0225 \,,$$

where $l$ is the number of significant coefficients in the regression equation, equal to 4. Then $F = 0.0225 / / 0.0016 = 14.06$. The tabular value of the Fisher criterion for $p = 0.05$, $f_1 = 1$, $f_2 = 2$, $F_{1-p}(f_1, f_2) = 18.5$, i.e. $F < \underline{F}_{1-p}(f_1, f_2)$.

Consequently, the resulting regression equation (5) adequately describes the experiment.

In accordance with Figure, we find that according to the obtained mathematical calculations, the optimal conditions for cavitation processing are the following: τ = 90–120 s, the amount of added catalyst is 0.7–1 g and the amount of added water is 1.5–2 ml.

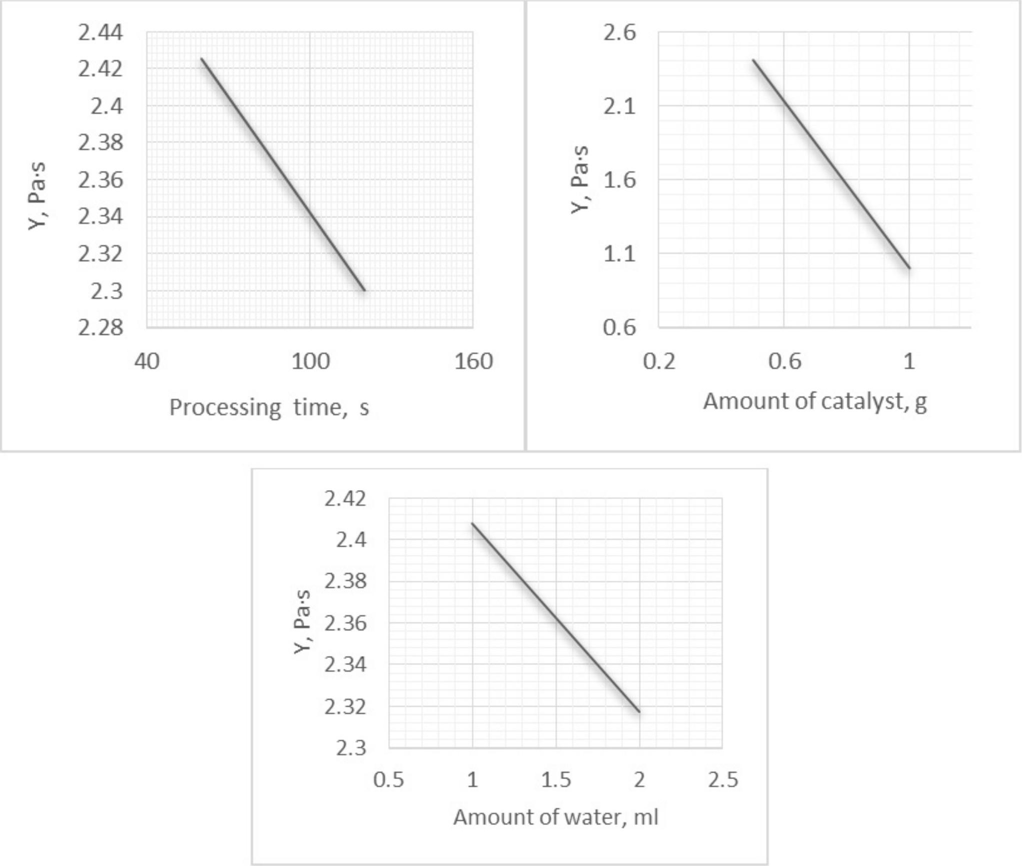

Figure. The influence of factors $z_1$, $z_2$, $z_3$ on the reduction of viscosity during cavitation processing of the middle fraction of oil (200–300 ºC)

## *Conclusions*

Thus, optimal conditions and a number of factors affecting the cavitation treatment of the middle oil fraction (200–300 ºC) in the presence of a $FeS_2$ catalyst are determined. In accordance with the obtained regression equation, the optimal conditions for cavitation processing are the following: τ = 90–120 s, the amount of added catalyst is 0.7–1 g and the amount of water added is 1.5–2 ml.

## References

1 Ахназарова С.Л. Методы оптимизации эксперимента в химической технологии / С.Л. Ахназарова, В.В. Кафаров. — М.: Высш. шк., 1985. — 327 с.

2 Experiment Design and Data Processing. — Shanghai: Mathematical Institute of the Academy of Sciences of PRC, 2006.

---

Фэнъюнь Ма, Синтай Су, М.И. Байкенов, А.Б. Татеева,
Г.Г. Байкенова, С.К. Мухаметжанова, Д.Е. Айтбекова

# Мұнайдың орта фракциясын (200–300 ºС) каталитикалық-кавитациялық өңдеу процесін модельдеу

Экспериментті жоспарлау — бұл үрдіс механизмі туралы толық емес ақпарат арқылы эксперименттi оңтайлы бақылау. Эксперименттік ғылымға деген қызығушылық экспериментaлды зерттеулердің кең ауқымымен және тәжірибенің оңтайлы ұйымдастырылуынан айтарлықтай экономикалық әсерге байланысты. Оңтайлы эксперимент деп уақыт пен қаржыны үнемдеуді, нәтижелердің сенімділігін арттыруды айтады. Мұнай отындарына кавитациялық әсерді зерттеу үшін құмкөл мұнайының (200–300 ºС) орташа үлесі пайдаланылды. Келесі каталитикалық жүйелер қолданылды: модификацияланған $FeS_2$; ε-$Fe_2O_3/SiO_2$ нанокатализаторы; α-$Fe_2O_3/SiO_2$ сфералық катализаторы; β-FeOOH және $Fe(OA)_3$. Құмкөл мұнайының орта фракциясының (200–300ºС) жеке құрамын анықтау арқылы каталитикалық-кавитациялық өңдеудің көмірсутегі құрамына әсері анықталды. $FeS_2$ катализаторының қатысуымен мұнайдың орта фракциясын (200–300 ºС) кавитациялық өңдеуге әсер ететін оңтайлы жағдайлар мен бірқатар факторлар анықталды. Алынған регрессиялық теңдеуге сәйкес, кавитациялық өңдеудің оңтайлы шарттары мынадай: τ = 90–120 с, катализатордың мөлшері 0,7–1 г, ал қосылған судың мөлшері 1,5–2 мл.

*Кілт сөздер:* нанокаталитикалық жүйелер, кавитация үрдісі, құмкөл мұнайы, эксперименттік жоспарлау, орта фракция, темір (III) оксидтері, полиморфты модификациялар, көмірсутектік құрам.

---

Фэнъюнь Ма, Синтай Су, М.И. Байкенов, А.Б. Татеева,
Г.Г. Байкенова, С.К. Мухаметжанова, Д.Е. Айтбекова

# Моделирование процесса каталитическо-кавитационной обработки средней фракции нефти (200–300 ºС)

Планирование эксперимента — это оптимальное управление экспериментом в условиях неполной информации о механизме процесса. Интерес к науке об эксперименте связан с широкими масштабами экспериментальных исследований и значительным экономическим эффектом от оптимальной организации. Оптимальный эксперимент — это путь к экономии времени и средств, увеличению надежности и достоверности результатов. Для исследования кавитационного воздействия на нефтяные топлива была использована средняя фракция кумкольской нефти (200–300 ºС). В качестве каталитических систем были использованы: модифицированный $FeS_2$; нанокатализаторы ε-$Fe_2O_3/SiO_2$; α-$Fe_2O_3/SiO_2$ сферический катализатор; β-FeOOH и $Fe(OA)_3$. Путем количественного определения индивидуального состава средней фракции (200–300 ºС) кумкольской нефти была установлена общая закономерность влияния каталитическо-кавитационной обработки на углеводородный состав средней фракции (200–300 ºС) кумкольской нефти. Определены оптимальные условия и ряд факторов, влияющих на проведение кавитационной обработки средней фракции нефти (200–300 ºС) в присутствии катализатора $FeS_2$. В соответствии с полученным регресионным уравнением оптимальные условия для кавитационной обработки следующие: τ = 90–120 с, количество добавляемого катализатора 0,7–1 г и количество добавляемой воды 1,5–2 мл.

*Ключевые слова:* нанокаталитическая система, процесс кавитации, кумкольская нефть, экспериментальное планирование, средняя фракция, оксиды железа (III), полиморфные модификации, углеводородный состав.

## References

1 Akhnazarova, S.L., Kafarov, V. V. (1985). *Metody optimizatsii eksperimenta v khimicheskoi tekhnolohii [Methods of experiment optimization in chemical technology]*. Moscow: Vysshaia shkola [in Russian].

2 *Experiment Design and Data Processing*. (2006). Shanghai: Mathematical Institute of the Academy of Sciences of PRC.

DOI: 10.31489/2019Ch1/96-99

UDC 537.527+66.021.1

A.M. Pudov[1], E.S. Mustafin[1], D. Havlicek[2],
Kh.B. Omarov[1], A.S. Borsynbayev[1], D.A. Kaikenov[1]

*[1]Ye.A. Buketov Karaganda State University, Kazakhstan;*
*[2]Charles University, Prague, Czech Republic*
*(E-mail: pudovam@list.ru)*

# Extraction of copper from the waste of the Karagayly concentrator under the action of an electric hydro-pulse discharge depending on the pH of the medium in the cell

In the work, the waste of the Karagayly concentrator was processed at the experimental hydro pulse discharge (HPD) laboratory set-up in order to transfer the copper contained in them (0.11–0.14 %) into the solution and then partially precipitate it in the process of pulsed electrolysis. Pulp from waste (waste + water 1:1) was poured into the cell, then an acidic medium was adjusted to the value pH = 1.0–3.0 using a mixture of reagents. Under the action of electro-hydro pulse the process of pulsed electrolysis occurs simultaneously. Then the lid was tightly closed and a hydro-pulse discharge (HPD) was performed for 5–20 minutes. Under the action of the discharge, all the metals contained in the pulp went into solution and simultaneously precipitated, except for copper ions, which remained in the solution and partially deposited on the cathode. As a result, after processing the pulp with HPD, 20 solutions with a precipitate were obtained. All solutions and precipitates were studied on a copper content by an atomic absorption spectrometer. The optimal conditions for the extraction of copper into solution, namely, the duration of discharge HPD for 20 minutes at pH = 1 and presence of silicate and phosphate ions, were established. All interfering ions of other metals remain in the sediment, since copper is to the right of other metals in the galvanic series.

*Keywords:* waste, copper, hydro-pulse discharge, pH medium, cell, pulp, sediment, solution.

Integrated use of mineral resources and the development of technologies for their complete processing, providing access to high quality products, taking into account the demand of external and internal markets is one of the most important areas of the mining and metallurgical complex of Kazakhstan [1]. To date, the state of the mining industry in Kazakhstan is characterized by the lack of significant capital investments in the industry, the lag in the development of the mineral resource base, the deterioration of geological and mining conditions for the development of deposits. The increase in production and processing volumes will be possible only through the development of new fields and the involvement of imbalance ores, dumps and waste after enrichment in the complex processing.

Worldwide, the process of mining and processing of metal ores is associated with the formation of a large amount of waste of various aggregative states. Currently, they contain billions of tons of ore processed. Further accumulation of waste from the mining complex is fraught with serious environmental degradation in the Republic of Kazakhstan. In this regard, the question of creating new environmentally friendly technologies for mining focused on their maximum usage [2].

The main advantage of non-ferrous metallurgy of Kazakhstan is the presence of its own mineral resource base. Kazakhstani ores containing non-ferrous metals are complex and have a complex structural and mineralogical composition. They include a wide range of rare and trace elements. At the same time, the structure, physical, chemical and other characteristics of Kazakhstani ores during mining, enrichment and metallurgical processing require an individual technology for each field. Existing technologies in Kazakhstan in the production of non-ferrous and rare metals do not fully meet the modern requirements of ecology, economics and integrated using of mineral raw materials. At present, the possibility of recycling the valuable components of metallurgical wastes is negligible, and the extraction of these components into such wastes is incomplete [3].

In Kazakhstan, the State Program of Industrial and Innovative Development of the Republic of Kazakhstan for 2015 — 2019 has been implementing, in order to ensure the sustainable development of the country. The program highlights the main problems of the metallurgical industry, namely:

– depletion of the resource base;

– low complexity of the raw materials used;

– a high degree of depreciation of fixed production assets;

- high degree of environmental pollution;
- technological lag;
- lack of integrated complexes with a full production cycle from mining to production with a high degree of product readiness;
- low capacity and distribution of the internal market;
- high energy, labor and material consumption of products.

In order to solve these problems, the state policy in the development of the mining and metallurgical complex of the country provides for:

- the organization of production of final products of high processing on the basis of base metals by small and medium-sized enterprises;
- stimulation of reducing the share of exports of ores and concentrates to ensure the integrated processing of mineral raw materials.

The promising areas of technological development of non-ferrous metallurgy are the production of pure metals (aluminum, copper, gold, and titanium) and products from them (wire rod, wire, rolled products, profiles and alloys, as well as jewelry) [4].

One of these technologies is the use of electro-hydraulic effect (EHE) to extract non-ferrous metals from mining waste, by passing energy-consuming enrichment technologies. In the series of electro-physical technologies, including laser, ultrasonic, plasma, electronic, electroerosion, electro-hydraulic technologies occupy a separate niche. Electrohydraulic (EH) technologies are based on the use of EH-effect (effect of Yutkin) [5].

EH-effect is a set of phenomena observed in a high-voltage pulsed discharge in a liquid (usually in water). There are only a few studies of electrolyte solutions [6].

High-voltage pulsed discharge in a liquid is accompanied by light and electromagnetic radiation, the formation of shock, ultrasonic and sound waves of a wide frequency range, pulse pressure (with an amplitude reaching tens of thousands of atmospheres under certain conditions), powerful hydrostream with cavitations [7, 8].

In our work, the waste of the Karagayly concentrator was processed at an experimental hydro pulse discharge (HPD) laboratory set-up in order to transfer the copper contained in them (0.11–0.144 %) into the solution and then was partially precipitated in the process of pulsed electrolysis. The presence of other metals in the waste is as follows: Zn — 0.12 %, Ni — 0.08 %, Fe — 0.04 %, the rest is less than 0.01 %. Metals standing to the left in the galvanic series are stronger reducing agents than metals to the right. They displace the latter from solutions of salts. For example, the interaction of $Zn + Cu^{2+} \rightarrow Zn^{2+} + Cu$ is possible only in the forward direction. Zinc displaces copper from an aqueous solution of its salt. At the same time, if a compound with which zinc forms an insoluble precipitate is present in the solution, for example $OH^-$, $CO_3^{2-}$, $SiO_3^{2-}$, $PO_4^{3-}$ ions, then zinc ions precipitate, and copper ions or metallic copper remain in solution. These processes and the effects of HPD allow copper ions to be transferred into solution and partially precipitate pure copper on the cathode.

## *Experimental*

Test Specifications:

- capacitance of the storage capacitor C = 0.4 μF;
- switch operating voltage ~30 kV;
- energy storage of about 200 J;
- geometry of the anode of conical shape to the top of the cone covered with an insulator with a base diameter of 10 mm;
- the cathode was a cylindrical cell with a diameter of 120 mm and a height of 100 mm with a tip in the center of the bottom with a base diameter of 10 mm and a height of 12 mm;
- pH 1.0–3.0.

Pulp from waste (waste + water 1:1) was poured into the cell, then an acidic medium pH = 1.0–3.0 was adjusted using a mixture of reagents (reagents are selected for each type individually); in this case, under the action of an electro-hydro pulse, at the same time there is a process of pulsed electrolysis. Then the lid was tightly closed and a hydro-pulse discharge (HPD) was performed for 5–20 minutes. Under the action of the discharge, all the metals contained in the pulp went into solution and were simultaneously precipitated, except copper ions, which remained in solution and partially deposited on the cathode. As a result, after processing the pulp with HPD, 20 solutions with a precipitate were obtained, which were filtered through a paper filter (red ribbon).

All solutions and precipitates were studied on a copper content by an atomic absorption spectrometer. The data are given in the Table.

Table

**The output of copper from the pulp into the solution, depending on the pH of the medium and the duration of discharge HPD, % (P = 0.95)**

| No. | pH | Time, minutes | | | | | | | |
|---|---|---|---|---|---|---|---|---|---|
| | | 5 | | 10 | | 15 | | 20 | |
| | | Sediment | Solution | Sediment | Solution | Sediment | Solution | Sediment | Solution |
| 1 | 3.0 | 80.1±3.8 | 18±1.3 | 78.9±3.5 | 21±2.3 | 71.3±5.3 | 22±1.4 | 72.2±2.7 | 26±2.3 |
| 2 | 2.0 | 75.4±4.1 | 23±1.5 | 70.1±2.9 | 28±1.9 | 68.7±4.2 | 31±1.6 | 69.0±4.3 | 32±3.3 |
| 3 | 1.0 | 62.2±2.2 | 37±2.4 | 49.6±3.6 | 49±2.6 | 48.4±2.6 | 53±2.9 | 42.3±2.6 | 61±4.6 |
| 4 | 0.5 | 65.5±1.8 | 33±2.6 | 45.8±1.4 | 41±1.5 | 56.8±2.5 | 42±3.4 | 53.6±3.2 | 46±3.6 |

---

*Note.* The discrepancy between the percentage of copper in solution and sediment is due to the partial deposition of pure metal on the cathode.

## *Conclusions*

A discharge of more than 20 minutes is not profitable, both in terms of energy consumption and as well as increasing the output of copper. Further lowering the pH below 0.5 does not increase the yield of copper in the solution. The optimal conditions for the extraction of copper into solution are the duration of discharge HPD for 20 minutes at pH = 1, in the presence of silicate and phosphate ions. All interfering ions of other metals remain in the sediment, since copper is to the right of other metals in the galvanic series, and the reagents in the pulp contribute to their conversion into insoluble sediments. The mechanism of action of HPD in an acidic medium formed by a mixture of reagents is not completely clear and requires further research.

## References

1 Сейдалы А.С. Современное состояние угольной, горнодобывающей и металлургической промышленности Казахстана: аналит. обзор / А.С. Сейдалы, Е.А. Лазарева, И.А. Семилетова. — Алматы: КазгосИНТИ, 2000. — 24 с.

2 Куркаев И.С. Особенности процессов инвестирования минерально-сырьевого комплекса Республики Казахстан / И.С. Куркаев // Транзитная экономика. — 2002. — № 4–5. — С. 77–82.

3 Чернегов Ю.А. Научно-технический прогресс и эффективность минерально-сырьевого комплекса / Ю.А. Чернегов // Горный журнал. — 2009. — № 1. — С. 43.

4 Государственная программа индустриально-инновационного развития Республики Казахстан на 2015–2019 годы. — Астана, 2014. — 135 с.

5 Юткин Л.А. Электрогидравлический эффект и его применение в промышленности / Л.А. Юткин. — Л.: Машиностроение, 1986. — 253 с.

6 Аблесимов В.Е. Измерения характеристик электрического разряда в растворе NaCl / В.Е. Аблесимов, В.М. Карюк, А.Н. Павлов, А.А. Кирпичев, А.А. Симчук // Журнал техн. физики. — 2015. — Т. 85, Вып. 3. — С. 42–44.

7 Наугольных К.А. Электрические разряды в воде / К.А. Наугольных, Н.А. Рой. — М.: Наука, 1971. — 155 с.

8 Кусаинов К.К. Разрушение материалов подводным электрическим взрывом / К.К. Кусаинов, Б.Р. Нусупбеков. — Караганда: ТОО «Издатсервис», 2010. — 250 с.

А.М. Пудов, Е.С. Мустафин, Д. Хавличек,
Х.Б. Омаров, А.С. Борсынбаев, Д.А. Кайкенов

# Ұяшықтағы орта pH тәуелді электр гидроимпульстік разряд нәтижесінде Қарағайлы кең байыту фабрикасы қалдықтарынан мысты алу

Қалдықтардың (қалдық + су 1:1) қоспасы ұяшыққа құйылды, содан кейін реагенттер қоспасы арқылы қышқыл орта pH = 1,0–3,0 жеткізілді; (реагенттер әр жағдайда жеке таңдап алынады), бұл жағдайда электрхимиялық импульстің әсерінен импульстік электролиз процесі бір мезгілде жүреді. Содан кейін қақпақ тығыз жабылып, 5–20 мин бойы гидроимпульстік разряд жүргізілді. Разряд беру кезінде қоспа құрамындағы мыстан басқа барлық металдар ерітіндіге өтеді және бір мезгілде тұнады. Ерітіндіде қалған металдар жартылай катодта тұнады. Нәтижесінде қоспаны ГИР-мен өңдеуден кейін тұнбасы бар 20 ерітінді алынды. Барлық ерітінділер мен тұнбалардағы мыстың құрамы атомдық-абсорбциялық спектрометрімен зерттелді. Мысты ертіндіге шығару кезіндегі ең жақсы шарттар силикат және фосфат иондарының қатысуымен pH = 1, ГИР разрядының ұзақтығы 20 мин болды. Барлық кедергі жасаушы металл иондары тұнбада қалады, себебі химиялық элементтер кернеу тізімінде мыс басқа металдардың оң жағында орналасқан. Қышқыл ортаға ГИР-дің әсер ету механизмі толығымен анықталмаған және әрі қарай зерттеуді қажет етеді.

*Кілт сөздер*: қалдықтар, мыс, гидроимпульстік разряд, pH орта, ұяшық, қоспа, ерітінді, тұнба.

А.М. Пудов, Е.С. Мустафин, Д. Хавличек,
Х.Б. Омаров, А.С. Борсынбаев, Д.А. Кайкенов

## Извлечение меди из отходов Карагайлинской обогатительной фабрики при действии электрического гидроимпульсного разряда в зависимости от pH среды в ячейке

В статье проведена обработка отходов Карагайлинской обогатительной фабрики на опытной лабораторной установке гидроимпульсного разряда (ГИР) с целью перевода, содержащейся в них меди (0,11–0,14 %) в раствор и затем частичное осаждение ее в процессе импульсного электролиза. В ячейку заливалась пульпа из отходов (отходы+вода 1:1), далее с помощью смеси реагентов формировалась кислая среда pH = 1,0–3,0 (реагенты подбираются для каждого вида индивидуально), в этом случае при действии электрогидроимпульса одновременно происходит процесс импульсного электролиза. Затем плотно закрывалась крышка, и производился гидроимпульсный разряд в течение 5–20 мин. При действии разряда все содержащиеся в пульпе металлы переходили в раствор и одновременно осаждались, кроме ионов меди, которые оставались в растворе и частично осаждались на катоде. В результате после обработки пульпы ГИР были получены 20 растворов с осадком. Все растворы и осадки исследовали на атомно-абсорбционном спектрометре на содержание меди. Оптимальные условия извлечения меди в раствор — продолжительность разряда ГИР 20 мин при pH = 1, в присутствии силикат и фосфат ионов. Все мешающие ионы других металлов остаются в осадке, так как в ряду напряжений химических элементов медь стоит правее других металлов.

*Ключевые слова:* отходы, медь, гидроимпульсный разряд, pH среды, ячейка, пульпа, раствор, осадок.

## References

1 Seidaly, A.S., Lazareva, E.A. & Semiletova, I.A. (2000). *Sovremennoe sostoianie uholnoi, hornodobyvaiushchei i metallurhicheskoi promyshlennosti Kazakhstana: analit. obzor [The current state of the coal, mining and metallurgical industries in Kazakhstan: Analit. Overview]*. Almaty: KazhosINTI [in Russian].

2 Kurkaev, I.S. (2002). Osobennosti protsessov investirovaniia mineralno-syrevoho kompleksa Respubliki Kazakhstan [Features of the investment processes of the mineral resource complex of the Republic of Kazakhstan]. *Tranzitnaia ekonomika — Transit Economy, 4–5*, 77–82 [in Russian].

3 Chernegov, Yu.A. (2009). Nauchno-tekhnicheskii prohress i effektivnost mineralno-syrevoho kompleksa [Scientific and technical progress and efficiency of the mineral and raw material complex]. *Hornyi zhurnal — Mining Journal, 1*, 43 [in Russian].

4 *Hosudarstvennaia prohramma industrialno-innovatsionnoho razvitiia Respubliki Kazakhstan [State program of industrial-innovative development of the Republic of Kazakhstan for 2015–2019]*. (2014). Astana [in Russian].

5 Yutkin, L.A. (1986). *Elektro-hidravlicheskii effect i eho primenenie v promyshlennosti [Electro-hydraulic effect and its application in industry]*. Leningrad: Mashinostroenie [in Russian].

6 Ablesimov, V.E., Kariuk, V.M., Pavlov, A.N., Kirpichev, A.A., & Simchuk, A.A. (2015). Izmereniia kharakteristik elektricheskoho razriada v rastvore NaCl [Measurement of the characteristics of an electrical discharge in a solution of NaCl] *Zhurnal tehnicheskoi fiziki — Journal of Technical Physics, 85, 3*, 42–44 [in Russian].

7 Naugolnyh, K.A., & Roy, N.A. (1971). *Elektricheskie razriady v vode [Electrical discharges in the water]*. Moscow: Nauka [in Russian].

8 Kusainov, K.K., & Nusupbekov, D.R. (2010). Razrushenie materialov podvodnym elektricheskim vzryvom [The destruction of materials underwater electric explosion]. Karaganda: LLP «Izdatservis» [in Russian].

# АВТОРЛАР ТУРАЛЫ МӘЛІМЕТТЕР
# СВЕДЕНИЯ ОБ АВТОРАХ
# INFORMATION ABOUT AUTHORS

**Abdurazova, P.A.** — PhD, Department of Chemical Technology of Inorganic Substances, M. Auezov South Kazakhstan State University, Shymkent, Kazakhstan.

**Agdarbek, A.A.** — 1st year Master Student, Ye.A. Buketov Karaganda State University, Kazakhstan.

**Aitbekova, D.Ye.** — MSc, Chemical Technology and Petrochemistry Department, Ye.A. Buketov Karaganda State University, Kazakhstan.

**Aldabergenova, S.K.** — Candidate of Chemical Sciences, Assistant professor of the Inorganic Chemistry and Technical Chemistry Department, Ye.A. Buketov Karaganda State University, Kazakhstan.

**Amanbaeva, K.B.** — Senior Lecturer, Department of Chemical Technology of Inorganic Substances, M. Auezov South Kazakhstan State University, Shymkent, Kazakhstan.

**Aukadieva, S.B.** — Master Student, Ye.A. Buketov Karaganda State University, Kazakhstan.

**Baikenov, M.I.** — Doctor of Chemical Sciences, Professor, Ye.A. Buketov Karaganda State University, Kazakhstan.

**Baikenova, G.G.** — Doctor of Chemical Sciences, Professor, Karaganda Economic University of Kazpotrebsoyuz, Kazakhstan.

**Bakibayev, A.A.** — Doctor of Chemical Sciences, Tomsk State University, Russia.

**Bayakhmetova, B.B.** — Candidate of Chemical Sciences, Associate Professor of Chemistry and Chemical Technology Department, Shakarim State University of Semey, Kazakhstan.

**Bekturganova, G.K.** — Chief expert, Kazhakstan Institute of Metrology, Nur-Sultan, Kazakhstan.

**Besterekov, U.** — Doctor of Technical Sciences, Professor, M. Auezov South Kazakhstan State University, Shymkent, Kazakhstan.

**Bolatbay, A.N.** — Master Student, Ye.A. Buketov Karaganda State University, Kazakhstan.

**Borsynbayev, A.S.** — Researcher, Laboratory of the engineering profile «Physical and chemical methods of research», Ye.A. Buketov Karaganda State University, Kazakhstan.

**Burakhta, V.A.** — Doctor of Chemical Sciences, Professor of the Department of Ecology and Biotechnology, West Kazakhstan Innovation-Technological University, Uralsk, Kazakhstan.

**Burkeev, M.Zh.** — Doctor of Chemical Sciences, Professor, the Director of Research Institute of Chemical Problems, Ye.A. Buketov Karaganda State University, Kazakhstan.

**Burkeyeva, G.K.** — Senior lecturer, Organic Chemistry and Polymers department, Ye.A. Buketov Karaganda State University, Kazakhstan.

**Donbayeva, V.A.** — Independent expert on measurement of uncertainty, Kazhakstan Institute of Metrology, Nur-Sultan, Kazakhstan.

**Fengyun Ma** — Professor, Xinjiang University, Urumqi, China.

**Fomin, V.N.** — Candidate of Chemical Sciences, Associate Professor of the Department of Inorganic and Technical Chemistry, Ye.A. Buketov Karaganda State University, Kazakhstan.

**Gaisina, B.S.** — Master of Chemistry, Senior lecturer of Chemistry and Chemical Technology Department, Shakarim State University of Semey, Kazakhstan.

**Guba, G.Ya.** — PhD, Assistant Professor of the School of Earth Sciences and Engineering, Tomsk Polytechnic University, Russia.

**Gusar, A.O.** — Engineer, PhD Student of the School of Earth Sciences and Engineering, Tomsk Polytechnic University, Russia.

**Havlicek, D.** — Associate Professor, Full Professor, Charles University, Prague, Czech Republic.

**Hranicek, J.** — Assistant Professor, Doctor of Chemical Science, Faculty of Science, Department of Analytical Chemistry, Charles University, Prague, Czech Republic.

**Jubanaliyeva, A.M.** — Master of Technical Sciences, Lecturer of the Department of Chemistry and Chemical Technology, Zhangir khan West Kazakhstan Agrarian-Technical University, Uralsk, Kazakhstan.

**Kaikenov, D.A.** — Researcher of the laboratory of the engineering profile «Physical and chemical methods of research», Ye.A. Buketov Karaganda State University, Kazakhstan.

**Kassenova, N.B.** — Master of Chemistry, Senior lecturer of Chemistry and Chemical Technology Department, Shakarim State University of Semey, Kazakhstan.

**Kassymova, Zh.S.** — Associate Professor, Candidate of Biological Sciences, Associate Professor of Chemistry and Chemical Technology Department; Shakarim State University of Semey, Kazakhstan.

**Kasymova, M.S.** — Candidate of Chemical Sciences, Assistant professor of the Department of Physical and Analytical Chemistry, Ye.A. Buketov Karaganda State University, Kazakhstan.

**Kopylov, N.I.** — Doctor of Technical Sciences, Professor, Institute of Solid State Chemistry and Mechanochemistry of the Siberian Branch of the Russian Academy of Sciences, Novosibirsk, Russia.

**Koshkarbaeva, Sh.T.** — PhD, Associate Professor, Department of Chemical Technology of Inorganic Substances, M. Auezov South Kazakhstan State University, Shymkent, Kazakhstan.

**Kudaibergen, G.K.** — PhD Student, Ye.A. Buketov Karaganda State University, Kazakhstan.

**Minayeva, Ye.V.** — Candidate of Chemical Sciences, Assistant Professor of the Organic Chemistry and Polymers Department, Ye.A. Buketov Karaganda State University, Kazakhstan.

**Mukhametzhanova, S.K.** — MSc, Department of Chemical Technology and Petrochemistry, Ye.A. Buketov Karaganda State University, Kazakhstan.

**Muratbekova, A.A.** — Candidate of Chemical Sciences, Assistant Professor of the Chemical Technology and Petrochemistry Department, Ye.A. Buketov Karaganda State University, Kazakhstan.

**Mustafin, E.S.** — Doctor of Chemical Sciences, Professor, Head of the laboratory of the engineering profile «Physical and chemical methods of research», Ye.A. Buketov Karaganda State University, Kazakhstan.

**Omarov, Kh.B.** — Doctor of Chemical Sciences, Pro-rector on scientific work, Ye.A. Buketov Karaganda State University, Kazakhstan.

**Omasheva, A.V.** — Candidate of Chemical Sciences, Associate Professor of the Organic Chemistry and Polymers department, Ye.A. Buketov Karaganda State University, Kazakhstan.

**Orazzhanova, L.K.** — Candidate of Chemical Sciences, Associate Professor of Chemistry and Chemical Technology Department, Shakarim State University of Semey, Kazakhstan.

**Petropavlovskiy, I.A.** — Doctor of Technical Sciences, Professor, D. Mendeleyev University of Chemical Technology of Russia, Moscow, Russia.

**Pudov, A.M.** — Candidate of Biological Sciences, Researcher of the laboratory of the engineering profile «Physical and chemical methods of research», Ye.A. Buketov Karaganda State University, Kazakhstan.

**Raiymbekov, Ye.B.** — MSc, Department of Chemical Technology of Inorganic Substances, M. Auezov South Kazakhstan State University, Shymkent, Kazakhstan.

**Rustembekov, K.T.** — Doctor of Chemical Sciences, Professor of Inorganic and Technical Chemistry, Ye.A. Buketov Karaganda State University, Kazakhstan.

**Sadykov, K.I.** — Doctor of Medical Sciences, Professor, Head of the Department of Basic Military Training, Ye.A. Buketov Karaganda State University, Kazakhstan.

**Salkeyeva, A.K.** — Lecturer of Physics Department, Candidate of Physical-Mathematical Sciences, Karaganda State Technical University, Kazakhstan.

**Salkeyeva, L.K.** — Doctor of Chemical Sciences, Professor, Head of the Organic Chemistry and Polymers Department, Ye.A. Buketov Karaganda State University, Kazakhstan.

**Sarsenbekova, A.Zh.** — PhD, Senior Lecturer of the Department of Physical and Analytical Chemistry, Ye.A. Buketov Karaganda State University, Kazakhstan.

**Sataev, M.S.** — Doctor of Technical Sciences, Professor, Department of Chemical Technology of Inorganic Substances, M. Auezov South Kazakhstan State University, Shymkent, Kazakhstan.

**Satayeva, S.S.** — PhD, Lecturer of the Department of Chemistry and Chemical Technology, Zhangir khan West Kazakhstan Agrarian-Technical University, Uralsk, Kazakhstan.

**Sugralina, L.M.** — Candidate of Chemical Sciences, Professor of Organic Chemistry and Polymers Department, Associate Professor, Ye.A. Buketov Karaganda State University, Kazakhstan.

**Tateyeva, A.B.** — Candidate of Chemical Sciences, Associate Professor, Ye.A. Buketov Karaganda State University, Kazakhstan.

**Tazhbayev, Ye.M.** — Doctor of Chemical Sciences, Professor, the Dean of Chemical Faculty, Ye.A. Buketov Karaganda State University, Kazakhstan.

**Toybek, A.A.** — Master student, Ye.A. Buketov Karaganda State University, Kazakhstan.

**Vojtíšek, P.** — Associate Professor, RNDr., CSc., Department of Inorganic Chemistry, Faculty of Science, Charles University, Prague, Czech Republic.

**Xintai Su** — Doctor of Chemical Sciences, Professor, Head of laboratory, Xinjiang University, Urumqi, China.

**Yelemessova, G.T.** — Master Student, Shakarim State University of Semey, Kazakhstan.

**Yermekov, S.R.** — MSc, PhD Student, M. Auezov South Kazakhstan State University, Shymkent, Kazakhstan.

**Yesentayeva, N.A.** — Master Student, Ye.A. Buketov Karaganda State University, Kazakhstan.

**Zhanasbayeva, B.K.** — Leading expert of «Kazhakstan Institute of Metrology», Nur-Sultan, Kazakhstan.

**Zhaparova, L.Zh.** — PhD, Assistant Professor of the Organic Chemistry and Polymers Department, Ye.A. Buketov Karaganda State University, Kazakhstan.

**Zhumagaliyeva, T.S.** — Candidate of Chemical Sciences, Associate Professor of the Organic Chemistry and Polymers Department, Ye.A. Buketov Karaganda State University, Kazakhstan.